Development of Biofunctional and Biocompatible Surfaces for Biodiagnostic Applications Utilising Plasma Enhanced Chemical Vapour Deposition

A thesis for the degree of

PHILOSOPHIAE DOCTOR

Presented to:

DUBLIN CITY UNIVERSITY

By

Ruairí Monaghan

B.Eng (Hons)

M.Sc (Hons)

Research Supervisor

Dr. Stephen Daniels

Declaration

I hereby certify that this material, which I now submit for assessment on the programme of study leading to the award of Doctor of Philosophy, Ph.D, is entirely my own work, that I have exercised reasonable care to ensure that the work is original, and does not to the best of my knowledge breach any law of copyright, and has not been taken from the work of others save and to the extent that such work has been cited and acknowledged within the text of my work.

Signed: _____

ID No.: **_____**

Date: _____

Preface

The work contained in this thesis is entirely my own work; however I wish to acknowledgethe contribution from a number of collaborators and groups.

- Michael Toney and Christopher J. Tassone for their help and time performing XRR and XPS experiments in SLAC
- Paul Leonard and Valerie Fitzgerald for supplying fluorescent IgG and providing me with experimental plans and procedures

A number of research groups kindly allowed access to their equipment during this thesis work.

- National Centre for Plasma Science and Technology (NCPST) - PECVD chamber, mass spectrometers, ellipsometerand consumables.
- Biomedical Diagnostics Institute (BDI) –Perkin Elmer ScanArray,Tecan Scanarray, consumables and materials.
- Dr. A. Cafolla of Surfaces and Interfaces Research Laboratory – AFM
- National Centre for Sensor Research (NCSR) – FTIR, contact angle goniometer and consumables.

Acknowledgements

I would like to express my sincere gratitude to the following people;

Abstract

Plasma enhanced chemical vapour deposition was investigated for the deposition of biofunctional thin films onto surfaces in the fabrication of biomedical diagnostic devices. Two major aspects of the deposited films were assessed for their applicability in new diagnostic systems.

The first relates to the functionality of the surface. The functionality of the surface relates to the ability of specific surface functional groups to be deposited stably and in a manner that will allow for biomolecular adhesion. Biomolecular adhesion is an important feature of surfaces requiring immobilisation of a detection agent, especially in liquid throughput devices. A comprehensive characterisation of the films developed herein was carried out. Following on from work previously undertaken by members of our research group, the films developed have shown a high degree of stability of the density of surface functional groups after exposure to aqueous conditions similar to those employed by liquid throughput devices. I found that the densities of these surface groups are superior to films created through liquid chemical deposition. Processes developed as part of this work were tailored for optimal manufacturability, e.g. the removal of heating apparatus required by the aminopropyltriethoxysilane monomer by installing a complimentary tetraethyl orthosilicate and allylamine process.

Secondly, I investigated surface wettability and developed a novel process for surface wettability control using atetraethyl orthosilicate and acrylic acid film stack. The plasma polymerised acrylic acid film was employed to react with the underlying organosilicon matrix, causing a shift in the surface characteristics. The polymeric acrylic acid network was shown to have a wearing effect on the organosilicon, catalysed by environmental water vapour. This process was subsequently controlled for the purpose of wettability control of the surface. As the underlying organosilicon layer is reduced, the increasingly oxygen rich interface becomes more hydrophilic, giving specific and stable control over the surfaces' water contact angle. As the fluidic interaction with a surface is generally of high importance in microfluidics, control of this provides a method of improving the workability of novel fluidic systems with materials that previously showed unfavourable characteristics.

Publications

Ram P. Gandhiraman, N.C.H. Le, C.K. Dixit, C. Doyle, V. Gubala, **R. Monaghan**, B. James, R.O Kennedy, S. Daniels, D.E. William, "Multi-layered Plasma Polymerized Chips for SPR Based Biomolecular Detection", *ACS Appl. Mater. Interfaces*, vol. 3, no. 12, pp. 4640-4648, Dec. 2011

V. Gubala, J. Siegrist, **R. Monaghan**, B. O'Reilly, R. P. Gandhiraman, S. Daniels, D. E. Williams, and J. Ducrée, "Simple approach to study biomolecule adsorption in polymeric microfluidic channels.," *Anal. Chim. Acta*, vol. 760, no. 1, pp. 75–82, Jan. 2013.

C. E. Nwankire, G. G. Donohoe, X. Zhang, J. Siegrist, M. Somers, D. Kurzbuch, **R. Monaghan**, M. Kitsara, R. Burger, S. Hearty, J. Murrell, C. Martin, M. Rook, L. Barrett, S. Daniels, C. McDonagh, R. O'Kennedy, and J. Ducrée, "At-line bioprocess monitoring by immunoassay with rotationally controlled serial siphoning and integrated supercritical angle fluorescence optics.," *Anal. Chim. Acta*, vol. 781, pp. 54–62, Jun. 2013.

A. Cowley, Rajani KV, **R. Monaghan**, P. McNally,"Extremely bright excitonic luminescence from intermixed CuBr/KBr micropillars", Under Review

F. Soberon, **R. Monaghan***(Joint first author), Conor Byrne, Greg Hughes, S. Daniels, "A dual-layer approach to PECVD surface functionalisation of polymer substrates for biomedical applications", Under Review

R. Monaghan, F. Soberon, S. Kelleher, A. Cowley, S. Daniels, "Plasma enhanced chemical vapour deposition of a dual organosilicon/carboxylic acid film and the subsequent post process curing for tailoring of surface wettability", Under Review

Conference Publications / Proceedings

Oral presentation in Plasma Nanoscience Conference 2014 – PECVD of Organically Functionalised Thin Films foe Biosensor Development, at the Helix in DCU, Ireland

Oral Presentation at NanoSMAT-8 2013 in Thin Films and Surface Coatings - Plasma Enhanced Chemical Vapour Deposition of Functionalised Surfaces for Bioassay Development, at the Conference Centre in Granada, Spain

Poster Presentation at the Lab-on-a-Chip European Congress 2013 - Plasma Enhanced Chemical Vapour Deposition of Functionalised Surfaces for Bioassay Development, at the Hesperia Tower in Barcelona, Spain

Poster Presentation at the Smart Surfaces 2012 conference – Plasma Enhanced Chemical Vapour Deposition of Functionalised Surfaces for Biomedical Applications, at the Alexander Hotel in Dublin, Ireland

Contents

List of Figures

List of Abbreviations

PECVD – Plasma Enhanced Chemical Vapour Deposition

CVD – Chemical Vapour Deposition

TEOS – Tetraethyl Orthosilicate

ppTEOS – Plasma Polymerised Tetraethyl Orthosilicate

CLD – Chemical Liquid Deposition

AA – Acrylic Acid

ppAA – Plasma Polymerised Acrylic Acid

CW – Continuous Wave

XPS – X-Ray Photoelectron Spectroscopy

eV – Electron Volt

CA – Contact Angle

LBL – Layer-by-Layer

AL – Allylamine

ppAL – Plasma Polymerised Allylamine

PA – Propylamine

PGA – Propargylamine

APTES – Aminopropyltriethoxysilane

APTMS – Aminopropyltrimethoxysilane

COP – Cyclo Olefin Polymer

AFM – Atomic Force Microscopy

GOPS – (3-glycidoxypropyl)triemethoxysilane

BSA – Bovine Serum Albumin

DDS – Dichlordimethylsilane

HMDSO – Hexamethyldisiloxane

VP – Vapour Pressure

SE – Surface Energy

XRR – X-Ray Reflectivity

DI – Deionised

UV-Vis – Ultraviolet-Visible

DNA – Deoxyribonucleic Acid

IgG – Immunoglobin G

hIgG – Human Immunoglobin G

α-hIgG – anti-Human Immunoglobin G

EDC – 1-Ethyl-3-(3-dimethylaminopropyl)carbodiimide

NHS – N-hydroxysuccinimide

PBS – Phosphate Buffered Saline

MES – 2-(N-morpholino)ethanesulfonic Acid

Cy3 – Cyanine 3

Cy5 – Cyanine 5

RF – Radio Frequency

MFC – Mass Flow Controller

NMR – Nuclear Magnetic Resonance

amu – Atomic Mass Unit

ssDNA – Single Strand Deoxyribonucleic Acid

PEG – Polyethylene Glycol

FLISA – Flourescent Linked Immunosorbent Assay

EDA – Ethylenediamine

MTES – Methyltriethoxysilane

TMCTS – Tetramethylcyclotetrasiloxane

DME - Dimethoxyethane

DEGDME – Diethylene Glycol Dimethyl Ether

LoD – Limit of Detection

LoB – Limit of Blank

LoQ – Limit of Quantification

PDMS – Polydimethylsiloxane

SPR – Surface Plasmon Resonance

SEM – Scanning Electron Microscope

GPTES – 3 - (Glycidyloxypropyl) triethoxysilane

AGE – Allyl Glycidyl Ether

PSA – Pressure-Sensitive Adhesive

Chapter 1

Introduction and Literature Review

1.1 – Biosensors Introduction

A sensor is a device which detects and responds to inputs originating from a targeted physical environment. Biosensors, as a subdivision, are defined as devices that utilise organisms or biological molecules to detect specific target analytes, with the ability to generate an output through the use of a physicochemical detector. Typically, a biological recognition element will interact with a target compound, after which a transducer will convert the biological reaction into a detectable signal.

Biosensors find application in a broad range of sectors, including the pharmaceutical industry, food processing, medicine, and environmental monitoring. The largest singular market however is the biomedical diagnostic industry, which includes diabetes monitoring and pregnancy tests. A review by Turner [1] classifies contemporary biosensors into two distinct categories;

- **Type A** - Sophisticated, high-throughput laboratory based systems capable of processing multiple samples rapidly and accurately
- **Type B** - Point-of-Care (POC) portable devices which can be used by non-specialised individuals in non-clinical environments

A broad range of biological recognition elements are used in both type A and B biosensors. This encompasses enzymes[2]–[6], antibodies[7–9], DNA (Aptamers)[10]–[13], whole cells[14]–[16], and microorganisms [17], [18]. These different molecules can be designed to specifically identify an extensive range of target analytes including pathogens, proteins, cells, DNA and microorganisms. Enzymes are the most broadly used recognition elements, due to their high specificity and sensitivity, although they present significant difficulties in purification due to cost and time constraint [19], [20].

Type A biosensors are often based on complete bioassays, or thephysiochemical detection of by-products generated by enzymatic reactions. For example, the enzyme-linked immunosorbent assay (ELISA) has been employed for years in the detection of analytes present in patient samples. The ELISA is a sandwich assay, which employs

specific antibodies to extract analytes from a solution, before using a secondary antibody phase to signal the extracted analytes presence. This process involves several main steps;

1. Immobilisation of primary capture antibodies on a surface (typically through physisorption) – Settling time of several hours
2. Blocking of the surface to ensure target analytes cannot also adhere – Settling time of several hours
3. Mixing of patient samples (here is where the primary antibody reacts and captures the target analyte) – Settling time of several hours
4. Mixing of an enzyme-linked secondary antibody (typically peroxidise enzymes) – Settling time of several hours
5. Addition of a chromogenic substance that will react with the enzymes, producing an obvious colour discrepancy where analytes are present – Settling time of up to half an hour

Between each step there is also a washing phase to ensure no contaminants remain that may affect the overall outcome. Although a simplified description of a full ELISA procedure, it shows the amount of time and dedication required to perform this relatively routine procedure.

The apparatus in Type A biosensors are typically very expensive, and rely on operator competency and training as much as system reliability and robustness. Type B biosensors however are designed to be easily used by individuals who require little to no in-depth knowledge of the science behind the operation. Therefore Type B biosensors need to be designed robustly and allow for minimal user input to function correctly. Biosensor operation in general often involves the mixing of a number of solutions, ranging from target samples to pre-prepared stock solutions with varying properties and functions. For Type B biosensors, this process must be streamlined and simplified.

Lateral flow and microfluidic based devices allow for complex experiments to be carried out by less skilled individuals. Preferably only the addition of a patient sample is required before the experiment conducts itself. An example of a well-designedlateral flow biosensor is the standard pregnancy test. Pregnancy tests are simple lateral flow devices which use a simplified assay design. The initial sample area is populated withanti-human chorionic gonadotropin (hCG) specific monoclonal antibodies. As the

urine sample is applied, the lateral flow design will allow the urine to flow along the length of the test strip, bringing the anti-hCG antibodies and hCG molecules (in the urine) to the detection area, allowing for a result to be displayed. Typically this is a colorimetric reaction caused by the mixing of reactive agents linked to the initial anti-hCG antibodies, and surface adhered dyes in the detection zone[21].

Lateral flow and microfluidic devices can work off a variety of driving forces, such as capillary action, direct sample pumping, and centrifugal force on a spin stand [22]–[26].

In all instances however the surface plays three key rolls;

- Wettability – the wettability of the surface (a measure of how hydrophobic/hydrophilic a surface is) plays a key role in allowing for appropriate flow of solutions across the sensor surface when capillary action is the main driving force. It also heavily affects flow and coverage issues in physically driven sample devices. [9], [27]

- Functionality – The ability to robustly adhere the functional recognition elements to the surface. The adhesion must be stable enough to resist the forces applied by the flowing samples.

- Resistance to non-specific adsorption – By reducing the ability of random proteins present in patient samples from adhering to the surfaces, especially in the test area, false results can be avoided and laborious blocking phases can be removed from the procedure.

Although substrates can be manufactured to produce a wide range of surface characteristics, it is often expensive to do so. By creating different specific chemical coatings, cheaper off-the-shelf plastics could be used in highly specific biosensor systems. Chemical liquid deposition (CLD) offers a viable method of transferring specific surface characteristics to substrates [9], [28]–[30], but these methods can suffer from a variety of setbacks, from non-uniformity to solvents dissolving or damaging softer plastic substrates [31], [32].

Another method of surface manipulation is plasma enhanced chemical vapour deposition (PECVD). PECVD is used to grow specific chemical films on substrates, allowing for controlled manipulation of a materials interface characteristics. PECVD processes can be used on a broad range of substrates, due to the low processing temperature. This allows for transference of positive surface characteristics to materials

that display dissimilar properties. The combination of positive material characteristics can greatly increase the efficacy of the chosen material. Therefore, to negate the negative issue associated with CLD processes, films developed within this work shall be carried out using PECVD.

1.2– Plasma Enhanced Chemical Vapour Deposition – PECVD

The improvement of microprocessor fabrication technologies over the previous few decades has helped develop the knowledge base of plasma processing. Applications of plasma based research in fields such as polymer deposition [33]–[35], surface activation [36]–[38], and sterilisation [39], [40] have grown as a direct result of this. The versatility of the plasma system processes, coupled with the ability for custom designed chambers to be constructed 'in-house' has created an entire subsector of physics research. The specific aim of this is the control of specific processes, and subsequent control of the high quality surface manipulation. Plasma processing provides a relatively cost effective process for surface manipulation, and its high throughput manufacturing capabilities provide an excellent alternative to traditional wet chemistry surface coating.

Plasma, the fourth state of matter, consists of a mixture of electrons, ions and neutral molecules and atoms which is considered as a whole to be electrically neutral (quasi-neutrality), although individual charged regions are possible on a smaller scale. Plasma processes are used in a broad range of manufacturing industries, including the semiconductor manufacturing industry, where they are employed in the manufacture of microprocessors. These processes enable the formation of surfaces with specific characteristics on a range of materials that are unobtainable by other means [41]–[43].

The electrical breakdown of a gas is a complex process, involving controlled management of a range of possible system variables, i.e. gaseous pressure, gaseous input, distance between electrodes etc. An example of a simple capacitive discharge is shown below;
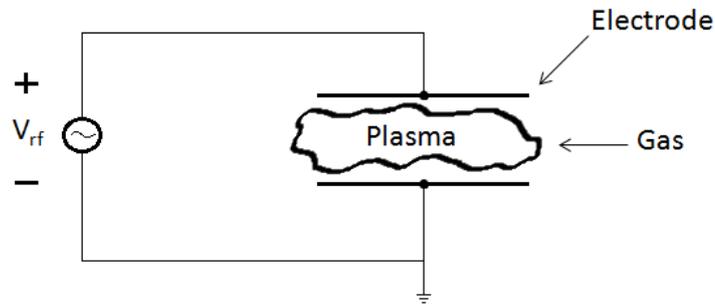
Figure 1.1: Basic plasma discharge model[42]

In Fig 1.1, two electrodes are separated by a certain distance, while being supplied by a radio frequency (RF) voltage V. In this model, a volume of an ideal gas is contained between the two opposing electrodes. Once a sufficient threshold voltage is applied between the cathode and anode, a current is driven through the gas causing it to break down giving rise to plasma. In this type of setup the plasma is usually considered to be weakly ionised, implying the plasma density (free electron and ionised gas density) is only a fraction of that of the neutral gas density [41], [43].

Electrons, present in the gas, are accelerated under the effect of the applied external electric field. The motion of the electrons depends on more than just the electric field, as collisions with gaseous molecules will impact their mobility.

An accelerated electron has a finite amount of time before a collision occurs, due to the presence of neutral gas atoms and molecules. This is known as the mean free path of the electron. An idealised example dealing only with simple elastic collisions is shown in Fig 1.2, where atoms are represented as solid spheres and only momentum is exchanged upon collision (no ionisation events occur). This is visualised by taking an area of gas, of volume *xyz*, within which several atoms are present[42], [43].
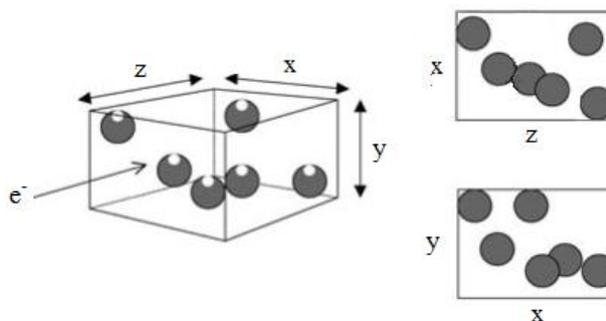
Figure1.2: Mean free path of electrons through gas populated medium [43]

When the z axis stretches as far as the mean free path, virtually all of the face xy will be impenetrable and a collision would be inevitable.

In a typical plasma system, elastic collisions will not be the only type of interaction between electrons and atoms. Often if the kinetic energy of the electron is large enough it may cause the atom to enter an excited electronic state. If the energy is great enough this process may lead to ionisation of the atom, where a secondary electron is released. Excitation and ionisation of atoms are examples of the outcome of an inelastic collision. The secondary electron may then be accelerated by the external electric field generating further ionising collisions, leading to an increase in the quantity of electrons, which undergo further ionising collisions. This phenomenon is termed an electron avalanche. Inelastic collisions are the most important form of collision in a plasma system, as they help sustain the discharge [42], [43].

Plasma enhanced chemical vapour deposition (PECVD) is an offshoot of the traditional chemical vapour deposition process (CVD). CVD typically depends upon substrate heating ranging from 200°C to above 1000°C [44]. As chemicals diffuse to the substrate surface, the heat enables chemical reactions which generate film development, while unwanted by-products diffuse away from the surface. In contrast to this, PECVD systems can be used with sub200^{o}C substrate temperatures, using ionic plasma constituents and electrons as catalysts for the dissociation of chemicals. This allows for a broader range of substrate materials to be treated. As the medical diagnostic market moves towards the use of cheaper plastic materials, PECVD has offered a manufacture worthy avenue for surface modification [41], [45].

Fig 1.3 shows the main processes involved in PECVD. The plasma sheath is an area displaying an overall positive charge due to the lack of electrons. The sheath develops around the substrate as a result of the primarily negative charge present on the substrate surface. This negative charge (relative to the bulk plasma) is caused by electrons accelerating and impacting the substrate surface. Due to the presence of the sheath, and the difference in potential between the sheath edge and a surface, positive ionic species in the plasma are accelerated towards the surface. It is this migration of ionic monomer vapour that is a major component of the growth of chemical films in PECVD systems. The levels of ionic bombardment of chemicals adhering to the surface, and subsequent sputtering of elemental groups, gives rise to the controllability of the surfaces elemental

composition. This allows for layers to be generated which can match the purity of those created by CVD methods [42], [43].
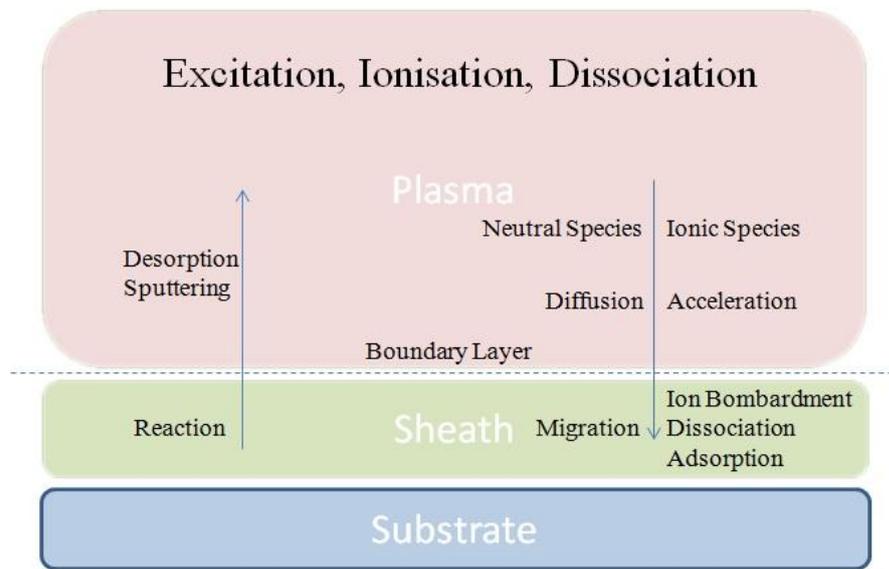
Figure1.3: PECVD process showing the movement of plasma constituents

1.3 - Tetraethyl Orthosilicate - TEOS

Silane (SiH_4) is a chemical compound used as a source of silicon in a variety of plasma deposition systems, including PECVD. Its use in research has been stunted in recent years due to the chemicals dangerousproperties. The main problem with silane, a toxic colourless gas, is that it is naturally pyrophoric, meaning it can spontaneously ignite when in the presence of air. A number of fatal industrial based accidents have occurred because of leaked silane gas, which can become even more volatile in air when mixed with inert gases such as argon [46]–[48]. This is one of the foremost reasons that the use of tetraethyl orthosilicate (TEOS), aka tetraethoxysilane, has become popular in the research community as a source of silicon for PECVD systems, especially in the case of SiO_x thin film depositions[49].

TEOS (Si $(OC_2H_5)_4$) is a chemically-stable organosilicon, making it more suitable for laboratory usage. It is also a liquid at room temperature, making handling of the chemical much easier than with silane. As the chemical structure contains a SiO_4 unit at its centre, the creation of a SiO_x layer is made simpler than when using silane, which would require the inclusion of high levels of oxygen during deposition of SiO_x layers. TEOS has been investigated as a silicon source for a range of products, such as micro-electronics [50]–[52], nano-particle shell coatings [53], sensor development [54], [55], organic light emitting diodes [56] etc.

TEOS has been used in plasma deposition systems since the 1970's. In a paper by Mukherjee & Evans [57], TEOS is described as enabling the deposition of both SiO_x and organo-silicon films (depending heavily on the process gas used).Coatings created using TEOS were attributed with being smooth, pin-hole free, and strongly adhered to the substrate surfaces (both metal and non-metal).

Like any PECVD based deposition process, the individual system parameters are of great importance to the process outcome. A variety of process parameters are available for control during any one deposition phase, these include chamber pressure[58], electrode spacing[59], RF Power[49], [60], substrate temperature[51], [58], deposition time [61], and mass flow rates [51], [56], [58], [62]. One of the most important, and easily adjustable of these parameters, is the RF power supplied to the system. Papers by both Voulgaris et al [60], and Mahajan et al[49]describe how varying the input power can lead to changes in the film deposition rate. Fig 4 displays the changes in deposition rate observed in both papers;
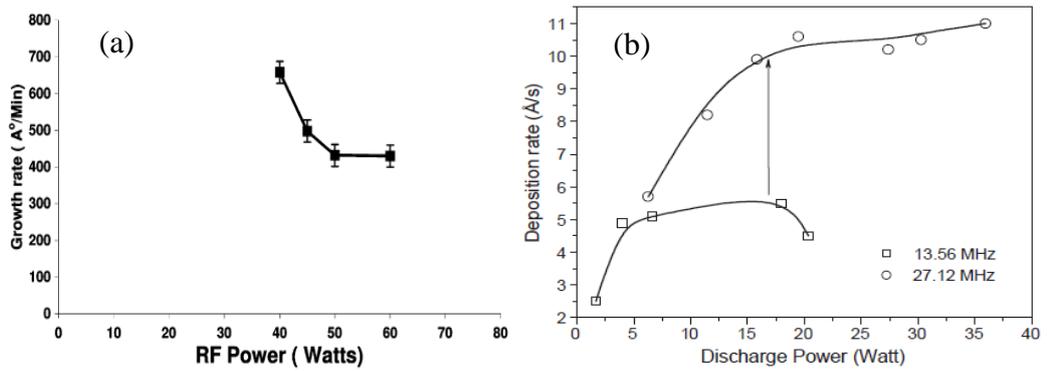
Figure1.4: TEOS deposition rates as a function of input power, (a) [49]**and (b)**[60]

In Fig 1.4, power settings are shown to influence the deposition rate. Increasingpower shows a corresponding increase in deposition rate. Both graphs however show how higher power levels cause a decrease in the growth rate of the films compared to lower power modes. Mahajan et al [49] attribute this change in deposition rate to an increase in surface bombardment (surface etching) on the growing film as a result of the increased power. Both sets of research are carried out using capacitively coupled discharges.

A contrast also exists between the two RF frequency settings, with the 27.12 MHz setup showing increased deposition rates. Voulgaris et al [60]relates these results to the change in the production of radicals created through increased electron impacts on the gas phase molecules. These radicals are in turn responsible for film growth, which explains the difference in deposition rates. The graph also shows how deposition rates tend to increase with rising input powers before levelling off, or as shown above eventually dropping. This results in a range of different RF powers which may be utilised with little change to the final film thickness [60].

During low power plasma deposition of TEOS however, there is the possibility of greater numbers of hydrogen atoms becoming incorporated into the thin film and reacting with oxygen atoms, leading to an increase in the concentration of Si-OH (silanol) terminals. Due to this increase in silanol terminals, the films can become increasingly porous, as every Si-OH terminal that forms will hinder the possible formation of -Si-O-Si- (or similar) bonds. This leads to an overall decrease in the deposited films density. Reports by both Mahajan et al [49] and Zeng et al[61] make reference to this phenomenon, stating the film becomes inherently weaker as a result of excessive silanol formations. Fig 1.5 shows how the increase in intensity of silanol groups corresponds to changes in the films hardness [61];

9
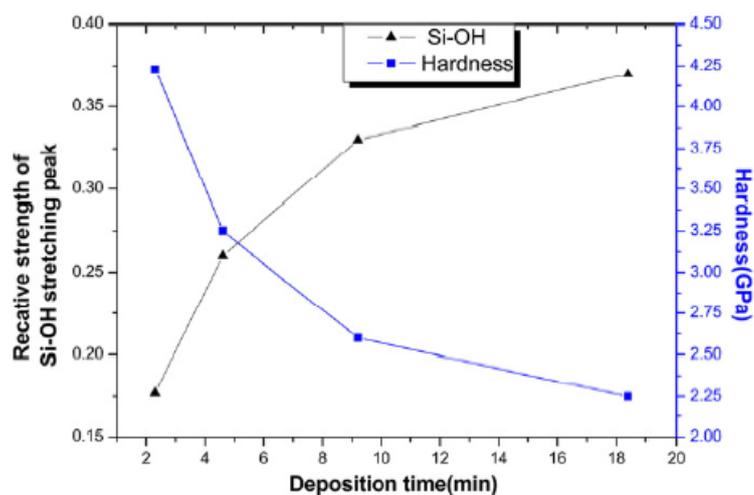
Figure1.5: Si-OH Prevalence Compared to Film Hardness [61]

As can be seen from Fig 1.5, in these experiments the process deposition duration is responsible for the higher population of silanol groups. Aside from uptake of free hydrogen atoms produced during monomer breakdown, the deposition method itself is also attributed with causing the changes. Using an atmospheric plasma jet allows for the formation of aggregated monomer in the gaseous phase before surface attachment occurs, leading to the build-up of a bead like surface with a lower density than would be present in a mostly polymerised matrix[61]. Although this data is gathered from research aimed at atmospheric pressure deposited silicon oxide films, the physical principals behind the changes in film properties relate to any deposition method, as silanol groups represent the hydrogen uptake of the film[49].

A higher abundance of silanol and $SiO_xC_yH_z$ groups in the thin film are indicative of an organosilicon layer as opposed to an inorganic silicon oxide matrix. However as with the previously described silanol rich films, the density of the films are lowered due to a decreased prevalence of -Si-O-Si- bonds. A report by Vallée et al [63] details how by shifting the TEOS:O_2 ratio the presence of $SiO_xC_yH_z$ groups becomes altered. A decrease in the overall density of the films is observed when lower oxygen concentrations are used, due to the increased carbon presence. This data is shown in Fig 1.6, alongside data showing the results from a thermally deposited silicon oxide film;
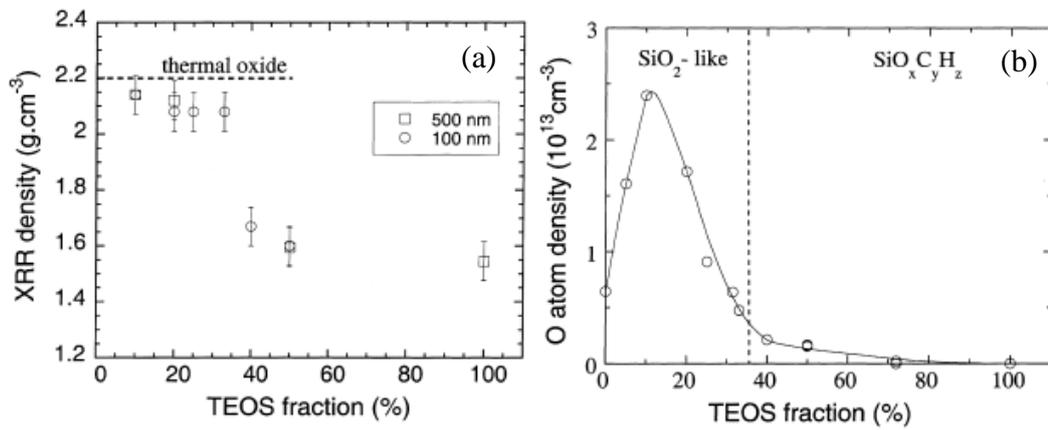
Figure1.6: (a) Physical Density of TEOS/O$_2$ Films and (b) Density of Oxygen Atoms in Films[63]

Fig 1.6 clearly shows the decreased film density caused by the removal of oxygen from the gaseous phase. Lower film densities are indicative of a more organosilicon like film containing higher carbon-hydrogen concentrations, whereas high densities are indicative of tightly packed SiOx rich matrices. This is matched by changing oxygen densities, another indicator of the shift from inorganic to organic films [63].

A report by Nicolazo et al [62]goes on to reinforce the idea that the development of purer SiOx films, using TEOS as the monomer, is dependent on the availability of oxygen. As is stated in the report, the deposition of SiOx films is a two-step process consisting of adhesion and subsequent ionic bombardment. This second phase relies on the reaction of oxygen species with the surface to remove the greater quantity of remaining ethyl and ethoxy groups of the fragmented TEOS monomer. This relates to previous results shown by Vallée et al [63], and also results presented by Sano et al [51] where it is outlined that oxygen radicals are required to remove intermediate products of the plasma (mainly hydrocarbons) before surface attachment can occur.

Although the presence of large quantities of silanol groups makes for softer layers, this is not necessarily a negative property, and is completely dependent on the intended usage of the films. A range of film characteristics can be altered to fit specific film needs, and these changes can be controlled through manipulation of the processing parameters. Another report by Mahajan et al [58] goes into detail on how varying process parameters (such as temperature, flow rate, and chamber pressure) allows for the tailoring of specific SiO based layers that fit a range of requirements. Film properties such as refractive index, film stress and film thickness can be altered through the variation of these process parameters. Fig 1.7 shows some of these results;

11
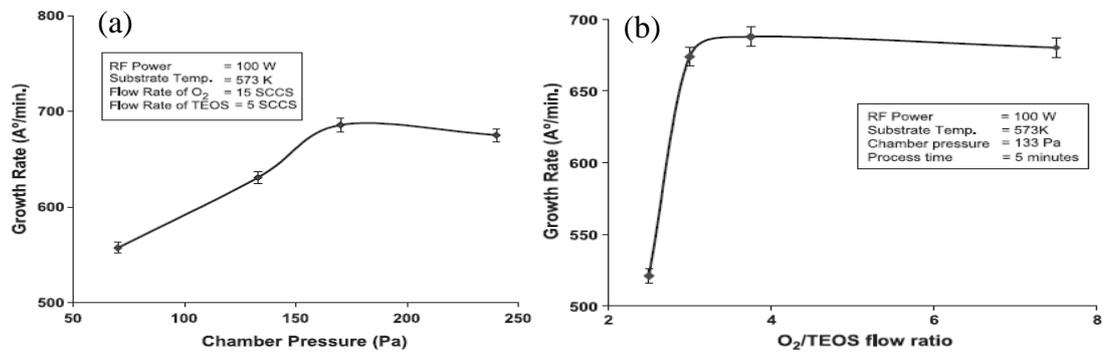
Figure1.7:SiOx Growth rate as a function of (a) Pressure and (b) TEOS/O2 ratio [58]

In Fig 1.7, an increase in chamber pressure allows for a larger monomer density within the chamber, leading to increased dissociation and build-up. This increasing growth rate begins to drop off however as the pressure is further increased. This is likely due to quenching of the plasma, as increased pressure and neutral density serves to reduce the electron mean free path, which in turn has an electron cooling effect due to the decrease in number of electrons with sufficient energy to participate in inelastic collisions. This cooling affect will decrease the overall electron density also.

The flow ratio also serves to influence the growth of the film, and requires that a threshold balance of oxygen and TEOS be reached to encourage faster growth rates. The figure shows that when the O_2/TEOS ratio favours higher TEOS levels the growth rate is stunted. This data relates closely to that shown by Vallée et al [63] previously. This phenomenon is again likely due to a quenching effect as the larger TEOS monomer levels increase while oxygen levels decrease, depriving the system of an electron cascade source while simultaneously increasing the electron mean free path. The growth rate of the film is seen to reach a sloping plateau (gradually declining) for both parameters tested, showing how an equilibrium of procedures for fast depositions must be applied [58].

The report also goes on to explain the importance of substrate temperature on the deposition rate, but states that during their process the most controllable and influential of the parameters listed related to chamber pressure and gaseous input [58].

Although the sequential, or paired, deposition of distinctive monomers (like the research undertaken in this Thesis) is not a focus of a great deal of research, TEOS can be used in conjunction with other gases to develop specific surface chemistries. Lee et al [56] have detailed a method in which TEOS was incorporated in a plasma chamber alongside

ammonia (NH$_3$), nitrogen (N$_2$), and oxygen. Through the use of plasma deposition with this mixture of gases, high quality siliconoxynitride (SiOxN$_y$) can be deposited.

During experimentation the mixture of gases was altered to study the impact on the growth rate of the film. Assuming that an increased presence of nitrogen in the recipe would result in greater nitrogen content in the film, both the ammonia and nitrogen gas input flows were varied and the subsequent growth rate of the films were monitored [56].

Increased nitrogen content appeared to cause little increase in film based nitrogen, but caused a large decrease in film growth rate. This nitrogen content however was attributed with helping to remove excess hydrogen and carbon from the film, making a purer (less carbon contamination) and more transparent film. The nitrogen gas at higher concentrations would therefore appear to primarily act as a bombarding agent in the deposition, as opposed to a deposition monomer, allowing for surface etching of unwanted elements [56].

The ammonia concentration had little effect on the growth rate in comparison, but the introduction of small percentages of ammonia lead to increased nitrogen in the film. However higher ammonia concentrations in the gas phase lead to the build-up of nitrogen impurities in the film (NH group build-up). Fig 1.8 shows the growth rates of the films deposited by varying the nitrogen, ammonia and TEOS flow rates [56];
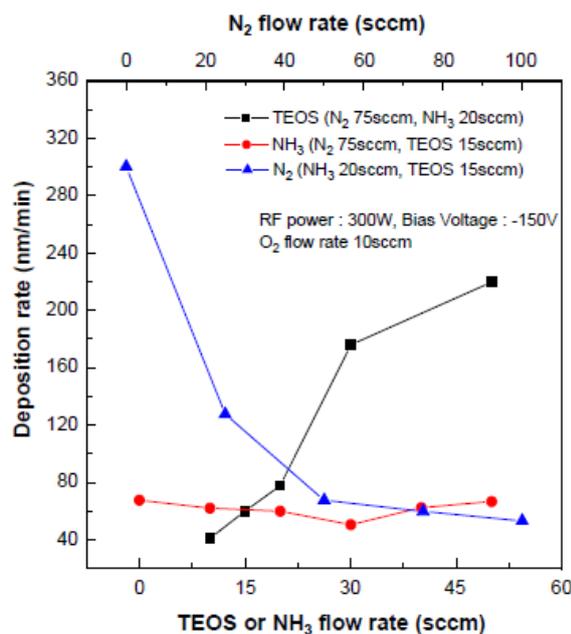
Figure1.8: Growth Rate of SiO$_x$N$_y$ Films with Alterations to Input Flow[56]

13

As a comparative method of deposition we can assess the efficacy of PECVD based TEOS films against chemical liquid deposition (CLD) of TEOS through a silanisation processes. Silanisation is a CLD process that involves self-assembly of a silane-based chemical. Although a range of solvents can be used in conjunction with TEOS to achieve silanisation [28], some solvents may prove too damaging to the substrates. Water, for this reason, is often employed as a solvent, or as a catalysing agent in a solution. The silanisation of TEOS (using H_2O) firstly involves the hydrolysis of the alkoxy groups [54];

$$Si(OC_2H_5)_4 + 4H_2O \rightarrow Si(OH)_4 + 4C_2H_5OH$$
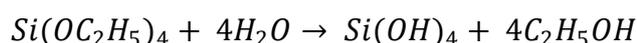
Adhesion occurs as covalent reattachment of the silanol groups react with a surface or other hydroxyl groups (assuming appropriate pH environment [53]);

$$Si(OH)_4 + 4OH \; (Bound \; to \; surface) \rightarrow SiOSi \; (Matrix/Polymer) + 4H_2O$$
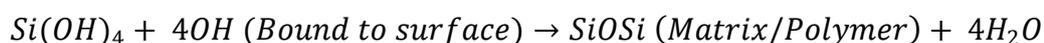
Although films of a high quality may be developed using silanisation, the process suffers from unavoidable shortcomings, such as the deposition time which can stretch up to 24 hours depending on the process [28], [54], [64]. Film characteristics are also difficult to alter if the need arises. The ratio of TEOS to the other chemicals in solution (i.e. H_2O and ethanol) is the main contributing factor in the control over thickness, as alluded to by Park et al [65]. Other film properties are however much less controllable in a CLD process, an issue less applicable to PECVD processes.

1.4 - Acrylic Acid - AA

Acrylic acid (AA) is an organic compound, consisting of a carboxylic acid terminus and a vinyl group (CH_2=CHCOOH). AA has been used for years in the production of a range of compounds, such as polyacrylates and acrylic esters. For example, polyacrylates can be used to created superabsorbent polymers[66]. Superabsorbent polymers are cross-linked polyacrylate structures that retain large quantities of liquids relative to their own mass. These materials are important for industries such as personal disposable hygienic products (i.e. U.S. Patent 5,026,596).

Carboxylic acid groups have been shownto have an affinity for strong cell and protein attachment, aided through the use of a chemical linker such as a carbodiimide (i.e.1-Ethyl-3-(3-dimethylaminopropyl)carbodiimide, EDC) [67], [68]. This functional

property of carboxylic groups has led to polymerised AA films becoming an important area of research in the medical device development industry, where immobilisation of biological detection components forms the key mechanism for molecular analysis of patient samples [69], [70].

AA is a suitable monomer for deposition in PECVD systems, and this method of creating carboxylated surfaces is well documented[35], [69], [71]. Although process dependent, research has shownthat films can be deposited while retaining high levels of reactive carboxyl groups [72]. The specific aim of plasma polymerised AA (ppAA) in the research performed in this Thesis is to create a layer of carboxyl groups (-COOH) which can be activated to interact with specific biomolecules. Retention of carboxyl groups' functionality is therefore a necessity.

An important characteristic of ppAA is the ability to form films which retainstability in solution. Biomedical devices often operate by testing aqueous patient sample solutions, and these devices will therefore encounter various liquid-surface interactions that may adversely affect the stability or functionality of a film. Therefore a surface which degrades in an aqueous environment is impractical, whether used with H_2O or other solutions/solvents. A report by Detomaso et al[69] describes how different AA coatings react to interactions with H_2O. In this work two different power modes were compared, continuous wave (CW) and modulated/pulsed.

Using X-Ray photoelectron spectroscopy (XPS), Detomaso et al [69] identified that the CW mode yielded 4% carboxyl coverage, whereas the modulated mode yielded 16%coverage. By assessing the robustness of these films, this research showed how the CW mode deposition retained its carboxyl groups after 30 days of water treatment, whereas the modulated mode dropped by 38% after only 24 hours. The data details a film that is wearing away in aqueous solution. As put forth by Detomaso et al, the main processes applicable in this instance for this delamination of film relate to loosely bound polymerised AA leaching away due tohydrolysis, hydrogen bonding with H_2O and swelling-contraction of the coating during wetting and drying phases. This data was backed up by adhesion studies of a biological agent (3T3 murine fibroblast cells) on the films. This experiment showed a higher affinity of cell adhesion on the CW deposited film. This difference is attributed to the lack of stability of the film produced by the modulated process, which in turn hinders surface immobilisation as the film delaminates [69].

15

In this set of experiments, the continuous deposition mode is considered advantageous when considering the intended purpose of said films. By maintaining a continuous RF deposition cycle, particle dissociation of monomers and surface bombardment is kept almost constant, which leads to a more robust matrix formation, with denser cross linking of the polymer and a more homogenous surface chemistry. Although the power setting of 100 watts may also seem high, possibly causing excess breakdown of the COOH group itself, this is not necessarily the case during all AA depositions as other parameters also influence this[69], [70].

A similar set of studies were performed by Alexander et al [72]. Herein ppAA films were tested for their dependence on plasma power. In this work the power was varied between 2 and 20 Watts, with 66% and 12% carboxyl group surface coverage recorded respectively. XPS data of these films showed that the low powered deposition created layers comparable to those of synthesised CLD poly-AA films, retaining high levels of intact carboxyl groups on the surface. The higher power depositions in contrast experienced an increased presence of ester functional groups and were denser and more heavily cross-linked. The report also details that the ppAA layers also take up more, or less, moisture from the atmosphere depending on plasma power chosen, as the more highly cross-linked films are less absorbent/porous [72]. This is an important feature of the ppAA films, as the wettability of polymeric films can relate to the adhesion performance[73].

A follow up report by Alexander [74] details the robustness of ppAA films on aluminium and the solubility in a range of solvents. Films deposited at lower powers were seen to be more susceptible to degradation when rinsed with water, as much larger reductions of thickness were recorded, similar to the results witnessed by Detomaso et al [69]. When rinsed with ethanol, all films displayed a thickness similar to that of the low powered (<5 Watts) films washed with water, indicating the ppAA films are covalently bound to the aluminium surface, but the bond strength and adhesion of the molecules throughout the polymerised layer is not as robust in the lower power deposition range due to the decrease in the level of cross-linking.

Through the addition of a 1, 7-octadiene (a hydrocarbon) monomer during deposition in conjunction with the AA, more robust functional layers were shown to be grown. With the new combination of monomers, the film displayed decreases in the acid/ester functionality, but retained much of the carboxylic group functionality. These results

show how although ppAA retains a certain level of robustness during a solvent wash phase (process dependant), the addition of a secondary monomer (acting to produce a stronger networked co-polymer layer) can make for more robust functional films without negatively impacting the reactivity [74]. It is also noted that the change to the surfaces wettability (increase in hydrophobicity) caused by the introduction of the hydrocarbon may also contribute to the increased robustness when rinsed with water.

In a report by Vilani et al[75], ppAA coatings were tested to show how differences appear when deposited on both silicon and polyurethane substrates using a range of RF power inputs. In this research, a comparative study was performed focussing on the XPS C1s core spectra peaks of several chosen films. The XPS data shows a large difference in the presence of carboxyl group (Fig 1.9) related peaks (289.2 eV region) between the 5 Watt and 30 Watt plasma depositions, and a further difference between these and the CLD synthesised poly-AA. The 30 Watt deposition process produced the lowest peaks relating to carboxyl groups, with the 5 Watt process creating films populated with a carboxyl density much closer to that of the synthesised poly-AA, much like the results experienced by Alexander et al [72], [74].

Further study of AA films deposited at higher powers (50-100 Watts) highlighted that films contained more intense peaks relating to carboxyl groups than that of the 30 Watt and 5 Watt processes[75].
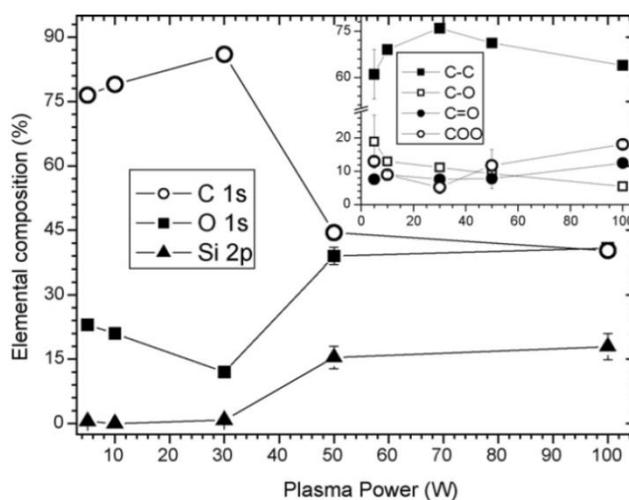
Figure 1.9:Shift of surface composition reacting to changes to input power[75]

Fig 1.9 shows the elemental changes undergone by the ppAA film as a result of the input power. As can be seen from the inlay, the carboxyl group signal (COO peak) increases at high powers. The process change also introduces higher levels of etching of

the substrate and film, leading to the films developing characteristics unlike those of the synthesised poly-AA, such as changes to water contact angle (CA). This is shown by the increase of silicon present in the film (Si 2p peaks), as silicon is sputtered and assimilated back into the surface during plasma phase.

Another XPS based analysis of ppAA surfaces was conducted by Morent et al [76], and the results therein reflect those referred to previously [72], [75], with reference to the effect on the primary carboxyl group density. In this work an increase in the plasma power causes increased dissociation of the monomer, leading to a decrease in carboxylic/ester groups, as the film as a whole contains more individual hydroxyl terminals.

A report by Cho et al [71]details the polymerisation process in a more in-depth manner. It is stated that the AA monomers vinyl group, a carbon double bond (C=C), has a specific energy of 2.74 eV required to become dissociated (becoming a C-C bond), whereas single bonded carbons (C-C) require 3.61 eV of energy to become fully dissociated. As energy that is transferred to the AA monomer in the plasma phase comes primarily from inelastic electron impacts, the increase of the discharge power is shown to increase polymerisation by fragmentation. This change to the polymerisation process is altered by the inherent increase in bombardment of the surface due to the increase in energetic species.

The report goes on to detail how changes in chamber pressure are used to assess the increase in monomer dissociation, with a 5 W process recording pressures from 17-18 mTorr, and a 20 W process experiencing pressures of 25-26 mTorr. As the pressure of the system is dependent on the amount of individual free gaseous materials, it is apparent that the monomers are being dissociated to a much higher degree with increases in input power. Much like the previously mentioned reports [72], [75], [76], it is again seen that a softer polymer film is deposited under low power techniques, whereas highly cross-linked layers form at higher powered cycles.

It is also worth mentioning that a report by Hutton et al [77]details how the dissociation energy required for a carbon-oxygen single bond (C-O) is 3.64 eV, and the carbon-oxygen double bond (C=O) requires 7.55 eV for dissociation. Matching this to the data from Cho et al [71] we can see how the C-O and C-C bond dissociation energies are very similar, showing that once a specific energy threshold has been surpassed there is a

likelihood of larger percentages of cross-linking and surface esters, essentially increasing the likelihood of removing some of the functionality of the carboxylated layers, i.e. loss of OH group.

As previously mentioned, the wettability of a plasma polymerised surface can be used to assess the outcome of a ppAA depositions general composition. Various papers have related the resulting surface water CA to the power used during deposition, such as a report by Ricciardi et al [78]. In this report, a graph is presented showing the changes inwater CArecorded when the input Power passes a certain threshold. These results are shown in Fig 1.10;
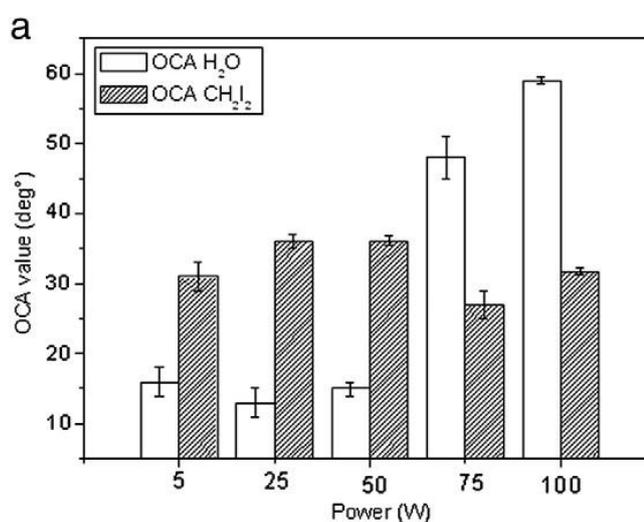
Figure 1.10:Water and diiodomethane contact angles on ppAA films[78]

Fig 1.10 shows how the water CA remains low when used at lower power functions, but once the power input is increased past 50 W a large water CA shift is observed. This is mostly due (as previously mentioned) to the increased dissociation of the gas phase AA monomer, and the constituents becoming polymerised and cross-linked on the surface. Other factors such as etched materials incorporating into the films due to increased sputtering of the substrate may also play a role in the changes. Individual plasma systems will of course create ppAA of varying degrees of similarity, but the principles behind the changes in the film characteristics remain the same and match those of the predescribed literature [72], [76], [77].

A report by Aizawa et al [79] goes into detail on ppAA films characterised by water CA, and shows how over time the water CA of ppAA can stabilise to a specific value regardless of the plasma processes used. Although initially the higher powered

processes yield CAs much higher than the lower power depositions (which show CAs similar to synthesised poly-AA layers), over 90 days all samples display a similar water CA ($\approx 28^{\circ}$). This was attributed mainly to the change in the presence of polar groups on the ppAA surfaces as opposed to external pollution (samples stored in vacuum).

Although the papers presented previously have primarily dealt with what is referred to as Continuous Wave (CW) plasma polymerisation processes, a wealth of research has gone into pulsed/modulated plasma deposition of AA films, with the intension to retain even greater functionality on the substrate surface[70], [77], [80]–[82]. The report by Hutton et al [77] details how by pulsing the plasma during deposition the films are given time to polymerise on the surface through conventional reaction pathways without constant bombardment. It was shown in the paper that the pulsed method yielded higher carboxylate group concentrations than with the CW method, similar to the results found by Detomaso et al [70]. This was attributed in part to the more conventional polymerisation reactions occurring during the 'off-period', but also to the removal of other by-products of the CW process, such as chemical etching and possibly detrimental Vacuum UV (VUV) interactions.

In a paper by Spanos et al [80] pulsed plasma deposition of a highly functionalised layer for gas barrier purposes is performed. Although carbon-carbon bond formations arising from alkene group opening is envisaged to be one of the primary growth mechanics of the film, the natural acid-base interactions between the AA carboxylic groups and the secondary functional group being deposited (amine, NH_2 groups) is hailed as one of the primary cross-linking processes that make the film so impermeable to gas. For this to occur however, the functional groups must be preserved throughout the plasma process, and when comparing CW to pulsed modes, it is clear from the results that the latter retains the highest level of functionality, and by extension shows the lowest gas permeability. This data relates closely to that of the report by Hutton et al [77]. It is apparent that under the right conditions the pulsed plasma deposition of AA can lead to the deposition of surface dense in carboxylic acids.

Typically the benchmark for depositing organically functionalised films comes from a CLD process. AA being a corrosive chemical by nature presents a difficulty when performing a CLD, as it can damage certain substrates or materials. A report by Kasputis et al [29] details a CLD approach to depositing polyAA (a chain polymerised AA) onto a silicon surface. In this process, the surface is oxidised by oxygen plasma

before being spin coated with an 'anchoring layer' containing poly(glycidyl methacrylate). Once annealing of this initial film is completed (@ 110°C under vacuum), polyAA is dissolved in ethanol, forming a 1% solution which is then spin coated onto the anchoring layer. Another annealing phase is applied under vacuum (@ 80°C) to chemically react the 2 layers. Loosely bound particles are finally rinsed away using ethanol. The temperature requirements of this process however rules out an adaptation to polymers such as COPs, which inherently have low melting points.

1.5 - Allylamine - AL

Allylamine (AL) is an organic compound, consisting of an allyl group and an amine terminus ($C_3H_5NH_2$). The typical AL chemical is considered a mono-allylamine (single allyl group), whereas a variety of AL based chemicals exist referred to more broadly as allylamines. Apart from the use of AL in chemical synthesis, synthetic allylamines have been used as anti-fungal chemicals for human use in both creams and pill form, i.e. Naftifine [(2*E*)-*N*-methyl-*N*-(1-naphthylmethyl)-3-phenylprop-2-en-1-amine] and Terbinafine hydrochloride [{(2*E*)-6,6-dimethylhept-2-en-4-yn-1-yl}(methyl)(naphthalen-1-ylmethyl)amine]. The mono-AL variant, which is the subject of the research in this Thesis, is toxic however, and direct contact may cause severe irritation and possible death in extreme cases due to overexposure.

AL has found extensive use in combination with PECVD systems for creating amine functionalised coatings for a range of materials, such as silicon [34], [83]–[85], gold [85], quartz [83], [86], polysiloxane [87], [88], aluminium [89], glass[79], [80], [90] and stainless steel [91]–[93]. The PECVD process allows for high retention of amine functional groups, while allowing for chemical cross linking, most likely through the breaking of the chemicals vinyl group, similar to the process of AA deposition mentioned previously[71].

Amine films are capable of attracting biomolecules (i.e. proteins) through simple differences in respective charge, known as electrostatic attraction. These electrostatic bonds can be robust in nature and provide strong adhesion of molecules to a surface. Amine films can also be chemically activated, similar to AA, to generate covalent attachments of biomolecules. Chemicals such as gluteraldehyde can be used to covalently immobilise biomolecules to amine films[34], although not in a zero length reaction like that created using a carbodiimide with a carboxylic group [68].

21

Glutaraldehyde linkage may be benefitted by the addition of sodium cyanoborohydride (NaCNBH$_2$), making the overall bond more robust [34].

Amine films may be deposited in a CLD process, but often the coatings are not robustly adhered to the surfaces and instead depend on charge based adhesion. Yoshida et al [30] describes a layer-by-layer (LBL) deposition of poly(allylamine hydrochloride) (PAH), a chain polymerised alteration of the allylamine chemical, on a gold surface. The film is held in place by the charge difference between the amine groups (positive) and the gold surface (negative) at physiological pH. Due to the orientation of the anchoring layer, subsequent layers of PAH contain the bulk of available amine functional regions. The surface is designed so that breakdown occurs at certain PH levels, which is the primary function in this case as it is used to slowly release the molecules contained. This method of deposition is similar in some respects to the AA depositions described previously by Spanos et al [80], where the layer growth is initially dependant on the function groups anchoring to attractive surface constituents.

This LBL process can also be performed using spin coating techniques, as described by Cranston et al [94]. Fig 1.11 shows a representation of how the LBL films are robustly adhered to the surface while retaining a viable level of amine groups available for biomolecular interaction. In this situation, Chen and McCarthy [95] use a poly(ethylene terephthalate) surface, and must therefore activate the surface using NaOH to create a PET-CO$_2$ film. The build-up of the film, with the amine anchors and subsequent free amines is similar to the methods described previously [30], [94];
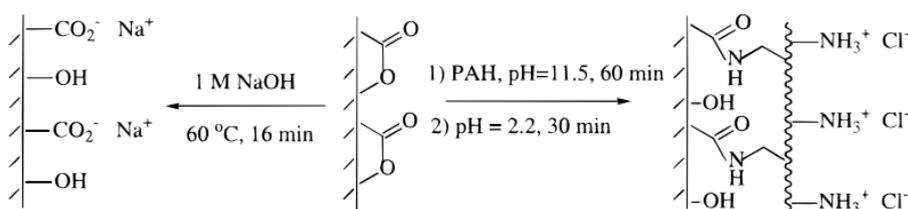
Figure 1.11: Layer-by-layer deposition of PAH[95]

CLD depositions of amines on carbon nanotubes have also been described in a report by M. Olek et al [96]. In this instance the coating takes place in solution, as the tubes are placed in an aqueous salt solution containing 0.5% PAH. After 4 hours of sonication the samples are stirred overnight before a secondary sonication step was performed. After washing of any excess build up the tubes were coated in amine films. This deposition

method is based around physical wrapping of the polymer layer however, and is therefore not applicable to geometries other than that of the nanotubes [96].

Plasma deposition of AL allows full covalent attachment of the AL monomer as opposed to charge based immobilisation. Plasma deposition of AL, much like the previously described ppAA, has been investigated for alterations in the primary amine (NH_2) concentration due to the deposition method used. CW and pulsed modes are compared in a paper by Choukourov et al [97]. Choukourov et al details how the mode of deposition in this instance does not appear to influence the primary amine concentration. Instead the pulsed mode allows for the generation of higher levels of secondary amines (NH), which are of negligible importance for biomolecular adhesion. The power level of the system is put forth as having the greatest influence on primary amine retention, with the higher 20 Watt (compared to 2 Watt) deposition power for both modes displaying much lower concentrations of primary and secondary amines. This shift in amine functionality caused by higher power levels is to be expected, as the increased level of surface-ion bombardment will play a detrimental role in the growth of the film[97].

Surface wettability is a characteristic encompassing both surface topography and surface chemistry (described mathematically in section 2.2.2). The importance of wettability cannot be overlooked when assessing a surface intended for use with biological agents, as alluded to by various authors [98]–[100]. The difference in surface wettability may encourage or diminish the ability for cells and proteins to adhere regardless of the presence of linkers etc. A report by Punzón-Quijorna et al[84] shows the AL films water CA to be roughly 60° immediately after deposition, but over the course of time this single droplet spreads and drops to a water CA of $\approx 46^o$. The drop-off trend follows closely the decrease in water CA experience by plain silicon (undoped Si (100) with removed native oxide layer), so the assumption is that the environmental effects influence the changes and not surface swelling or removal of material. Aizawa et al [79] also make reference to the ppAL films stabilising nature, showing how water CA may range from $\approx 47^o$ to $\approx 70^o$ initially. Over 90 days however, the ppAL films follow the trend of the previously referenced ppAA films in this work by reaching an equilibrium water CA of roughly 67°.

A report by Massey et al [88] details how that after 14 days of contact with water, the ppAL surface remained stable and XPS analysis showed no significant change in

surface composition, despite the drop in water CA. The change in water CA in this instance was resulting from the reorientation of hydrophilic groups present on the surface. The report goes on to detail how heating of the film causes a slight recovery in water CA, and this is attributed to thermal polymerisation effects essentially decreasing the mobility of the surface.

Although not present in the AL monomer, increased oxygen levels are often found in ppAL films, which are picked up by the film to form amide bonds. This integration of oxygen in the film matrix was recorded by various groups [34], [91], [97], [101], but it does not appear to be an artefact of the CLDs process (this data ignores underlying C-O groups present from substrate surface activation) [30], [94], [95]. Although it is assumed that oxygen may come from the chamber walls during deposition, the bulk of the oxygen is predicted to come from air [101]. This occurs during the period directly after deposition where the surface retains a certain energetic/unstable nature and elemental reformations are commonplace, i.e. polar group realignment.

As a functional group, amides are inferior in some respects to amines as the double bound oxygen segment allows for strong hydrogen bonding. This is due to the structure of the chemicals, specifically the functional difference. Carboxyl groups for example have a larger dipole moment than primary amine groups, as oxygen is more electronegative than nitrogen. This means the presence of oxygen on the carboxyl group will form stronger hydrogen bonds than the nitrogen found on amines. Primary amines in general allow for certain levels of hydrogen binding (tertiary amines do not form hydrogen bonds), but if specific adhesion of amines (i.e. glutaraldehyde binding) is the intended usage of a film amides are problematic. This is because they allow a secondary pathway for particles to become adhered through hydrogen bonding, reducing the specificity of the surface.

Similar chemicals to AL in composition, namely propylamine (PA) and propargylamine (PGA), offer interesting alternatives for PECVD deposition. As mentioned previously, the AL vinyl group is where most polymerisation and cross linkage is intended to form, due to breaking of the carbon double bond. PA removes this polymerisation pathway as the terminal carbon-to-carbon bond is saturated, leaving a more stable carbon chain. PGA however has an unsaturated carbon triple bond, making the chemical more unstable. Triple bonds require less energy to become open than double bonds, and therefore the chemical is more likely to be available for cross linkage and

polymerisation than its counterparts. In Fig 1.12, Mangindaan et al [83] shows how the chemicals display changes in deposition rates relating to power changes. The data in Fig 1.12 also relates to the difference in the dissociating and polymer building nature of the unsaturated and saturated carbon bonds.
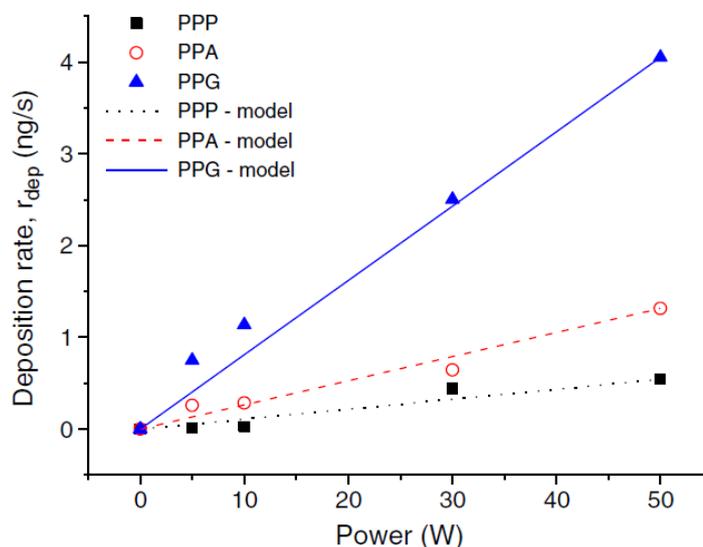
Figure 1.12: Graph detailing the difference in growth rate experience by AL at different power settings[83]

PGA (*PPG*) shows growth rates higher than that of both AL (*PPA*) and PA (*PPP*), proving the method of film growth stems from the ease at which the terminal carbon-carbon bond is broken. Of these chemicals however, AL was found to retain the highest levels of primary amines. PGA and PA showed primary amine densities of 62% and 86% respectively in comparison with AL, with secondary amine concentrations dropping to 36% and 60% respectively [83]. Cost also factors into the choice of chemicals used, as although the growth rate of PGA may be advantageous for certain applications, the cost of PGA at time of writing PGA is €161 per 30mL, whereas AL is €33.50 per 250mL (~€4 per 30mL)[*prices correct as of 26/03/2014 via Sigma Aldrich*].

1.6 - Aminopropyltriethoxysilane - APTES

Aminopropyltriethoxysilane (APTES) is a chemically stable organosilane, which has been widely adopted in the creation of amino functionalised surfaces for use in biological environments, i.e. the coating of implants. APTES is not typically used in PECVD systems, aside from ongoing internal research [9], [102]–[107], due to the difficulty in vaporisation of the liquid. However it is easily chemically deposited to prepare surfaces through silanisation.A typical silanisation process involves the

hydroxyl groups present on an oxidised substratesurface interacting with the alkoxy (ethoxy) groups of the APTES, creating covalently bound –Si-O-Si- matrices, creating H_2O and ethyl alcohol by-products. The most commonly used surfaces for this covalently immobilisation of the molecules are glass substrates and metal oxides, but generally any oxidised surface may be used [108], [109].
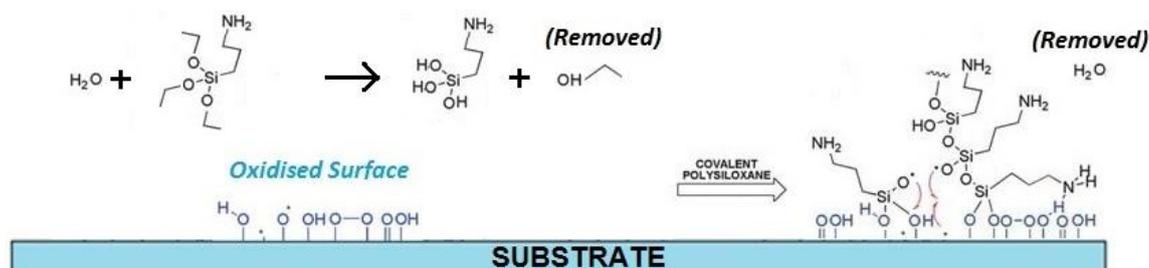
Figure 1.13: Diagram showing the silanisation of APTES onto an oxidised polymer

APTES has been used in conjunction with PECVD deposited films to create functionalised surfaces. In a paper by Szili et al[109], PECVD deposited SiO_2 films (using TEOS) are deposited on a titanium implantable device, and APTES is subsequently adhered to the thin film via organic silanisation methods. Organic silanisation involves direct conjugation of the APTES chemical to the surface without prior catalytic influence [32], [110], i.e. acetic acid and water are catalysts for polymerisation of silanes [31], [32], [111]. Organic silanisation may be improved through an open air curing phase, where environment water vapour helps the surface to polymerise to the fullest effect [112].

Szili et al [109] employed XPS analysis to show how, despite the difference in mode of silanisation, the nitrogen content of the CLD APTES films decreased by only 35% when incubated in aqueous physiological solution. This shows that the film is robust enough to survive in an organic environment.

Although non polar solvents, such as toluene, are often used to deposit APTES via silanisation (or aminopropyltrimethyloxysilane (APTMS), a similar chemical replacing the ethoxy groups with methoxy), polar solvents may also be used to this affect. Sharma and Asefa [113] detail the characteristics of depositions performed using toluene (non polar) and ethanol (polar) with APTMS at elevated temperatures (i.e. 78°C). Both modes lead to films with differing primary amine concentrations. Toluene depositions create high density amine films, whereas the ethanol based surfaces have a lower density and display an increased silanol density. The toluene films amine density is

higher still when deposited at an elevated temperature of 112°C, showing how temperature dependence is important for high amine density surfaces.

Sharma et al [114] perform further research on this, generating a set of data showing the nitrogen content of films deposited using the polar and non-polar solvent deposited films. In this work, all polar solvents generate aminopropyl-silane films with amine densities lower than all other non-polar solvents tested, with the exception of acetonitrile (a dipolar aprotic solvent) [114].

For softer polymer surfaces, such as cyclo olefin polymers (COPs), non-polar solvents are of no use, as the chemicals attack and dissolve the polymer. Therefore when considering CLD deposition techniques a milder method must be employed, such as the water catalysed silanisation mentioned previously [31], [32]. Raj et al [32] details how COPs can be coated with APTES using water and the polar solvent methanol in a 5:95 ratio (3% APTES mix). Oxygen plasma treatment is used to oxidise the surface before the solution is applied, and post CLD the samples are cured at 120°C. This is shown to generate a robust amine film, capable of employment in biological assay development.

Layers were often shown to grown to large thicknesses of >300nm. This is a by-product of the use of water in this silanisation process, as water is essentially recycled during the chemical interaction. When the chemicals hydroxyl groups (generated by ethoxy interactions with water) and the surface hydroxyl groups interact, water molecules are produced encouraging further reactions. Considering the information recorded by Sharma et al [114], isopropanol would serve as a more suitable solvent than methanol for the creation of amine rich films, possibly increasing the overall density by ~ 60%.

APTES may also be deposited purely using water, as is performed by G. Longo et al[115], wherein an atomic force microscopy (AFM) tip is coated using 0.2% APTES in water solution. As the tip is being completely coated in APTES there is no need for previous surface activation, allowing instead for the polymer chains to encapsulate the tip. This is similar in style to the deposition method described previously by Olek et al [96], where the polymer adhesion method is based around encapsulation rather than covalent bondage to an activated surface.

Although the amino functionalised surfaces can be used in conjunction with implants (as previously mentioned) for their ability to inhibit unwanted and hazardous immune reactions, other additional steps can be taken to ensure stability is retained once

27

implanted. A report by Nanci et al [108] details how the use of covalent protein immobilisation on an organically silanised APTES surface can improve the immunosuppressant features of the coating. Glutaraldehyde (as previously described in section 1.3) is an organic compound. When used in conjunction with amine surfaces, glutaraldehyde can covalently bind and immobilise proteins or other biological agents. This allows the APTES film to change from a protective layer to a reactive film which can have organic biomolecules strongly bound. By adhering active biomolecules the implant may appear biological in nature to the human immune system, and repress or control early biological reactions[108].

Another method widely used in the deposition of APTES films is vapour deposition. Vapour deposition allows for the monomer to evaporate, typically in a low pressure oven, and form self-assembled layers on a specific activated surface. Amrita et al [116] describe a process wherein APTES, among other chemicals, is deposited onto cleaned silicon surfaces. The surface is firstly oxidised using a plasma process, after which water and the silane chemicals were introduced to the chamber. The chemicals react with the surface through natural evaporation into the chamber environment. As with the CLD process, water is used to catalyse the reactions between the APTES molecules and substrate surface. A similar process described by Liang et al [117] references how he water and APTES vapour is introduced alongside a career gas into the heated chamber. This method of molecular layer deposition (MLD) was shown to also be highly stable in generating amine films.

Typically this method of deposition leads to extremely thin, often monolayer amine surfaces. And despite the varying advantages of this, i.e. uniformity and low surface roughness, there can be some disadvantages also. Liang et al [117] shows the need for the MLD deposition process to have a soaking after phase for several hours in de-ionised water, otherwise the films were found to be unstable. Whereas Amrita et al [116] found the films to have poor coalescence, and showed large amounts of desorption of the amine layer when soaked over a period of 21 hours, although the desorption is found to be lower than that of the CLD variants used in the experiment.

The bulk of the research focussing on APTES deals with the immobilisation of proteins/biomolecules to a substrate surface. A study by Awsiuk et al [118] details how APTES modified surfaces were compared to surfaces modified with (3-glycidoxypropyl) trimethoxysilane (GOPS), a silicon containing chemical with a

terminal epoxy functional group. These epoxy functional groups are highly reactive and are used much like the APTES amino group, i.e. in reactions aimed at immobilisation of proteins. In this study it was shown that APTES functionalised surfaces showed higher adsorption of the target IgG. Blocking with Bovine Serum Albumin (BSA) of the APTES film did not cause a change in protein adhesion unless low protein concentrations were used, showing good specificity. The GOPS layer however showed greater changes with blocking. Both layers contain a SiOx based anchoring matrix, but the amino group is considered to be more specific compared to the epoxy, as the near terminal oxygen present on the epoxy group is highly reactive. This reactivity makes the layer less specific and more able to react with molecules or chemicals that come in close proximity[118].

Specificity is important when considering APTES as an immobilisation film, and there are other phenomenon's inherent to films created using APTES that aid specificity. A paper by Mansur et al [119] makes reference to a characteristic of the APTES layers that aids the specificity of protein adhesion, specifically the steric repulsion of the propyl (3 chain carbons) group. Locatedbetween the amine functional group and silicon anchoring matrix, it acts in a manner that hinders protein adsorption on the film surface. Coupling this steric hindrance effect with the specificity of the amino groups (especially when linking using glutaraldehyde) makes APTES a good choice for functionalisation of surfaces for protein adsorption and immobilisation.

A report by Wang et al [120] also makes reference to another positive phenomenon of APTES which makes it a more viable choice than some other protein immobilising agents. In this report dichlordimethylsilane (DDS), an organosilicon compound which has found use in protein immobilisation [121], was compared to APTES with respect to the stability of the proteins once immobilised. With a layer comprised of DDS the proteins were found to suffer partial denaturation (loss of functionality) which often lead to the proteins leaching and washing off the surface. The amino groups allow for covalent attachment of the proteins, as referenced previously [108], and although partial denaturation still caused minor changes to the proteins reactivity, the overall resultant affect (i.e. leaching or removal) was decreased substantially and the surface binding was more stable than on the DDS.

This denaturation protective feature of the APTES film was again detailed in a report by Shah et al [122], where the rigidity of the SiOx underlying layer of the APTES is

attributed with helping retain the proteins structure. It was noted that the bound molecules (enzymes) were more stable to both pH and temperature fluctuations when compared to the enzymes' soluble counterpart. This was attributed to the rigid layer limiting *'the freedom of peptide-chain refolding of molecular motions'* which typically occurs during the denaturation process. Coupling this with previously mentioned highlights of the APTES layers, it becomes apparent that the use of this APTES chemical is generally more advantageous than many other functionalising agents, especially where protein immobilisation and functional retention is concerned.

1.7 - Primary Aim of Research

The primary aim of the research undertaken herein is to develop a portfolio of processes by which to generate films that translate desirable surface characteristics to specifically chosen substrates, i.e. Zeonor®. These characteristics are principally tailored to increase the applicability of the chosen substrates operation in the field of bio-analysis of biologic samples. Films deposited via PECVD must therefore be robust and functionally stable, while the process itself remains reproducible across a multitude of repeated experiments. The chemicals chosen studied are TEOS, AA, APTES and AL. Each chemical provides a different influential step in the development of this portfolio of thin films. Both functional and physical aspects (i.e. surface wettability) of the deposited films are the focus of the work carried out herein.

Chapter 2

Materials and Methods

2.1 –PECVD Chemicals and Substrates

2.1.1 – Precursor Chemicals

A variety of precursors can be used in conjunction with PECVD processes, as long as they fit certain workable criteria decided by the process parameters. The following precursors shown in Fig 2.1 are those that have been used during experimentation in this work;

3-Aminopropyltriethoxysilane	APTES - $C_9H_{23}NO_3Si$
Initial Boiling Point ($^\circ$C)	217 (@ 1,013 hPa)
Vapour Density	7.64
Vapour Pressure (hPa)	<13 @ 100°C, 133 @ 155°C
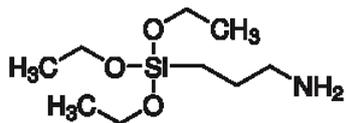
Tetraethyl Orthosilicate	TEOS - $C_8H_{20}O_4Si$
Initial Boiling Point ($^\circ$C)	168
Vapour Density	7.19
Vapour Pressure (hPa)	1.8 @ 20°C
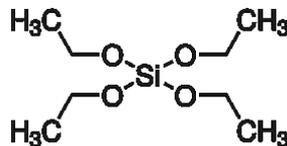
Acrylic Acid	AA - $C_3H_4O_2$
Initial Boiling Point ($^\circ$C)	139
Vapour Density	2.49
Vapour Pressure (hPa)	5 @ 20°C, 53 @ 60°C
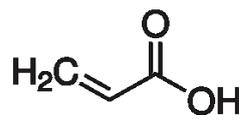
Hexamethyldisiloxane	HMDSO - $C_6H_{18}OSi_2$
Initial Boiling Point ($^\circ$C)	101
Vapour Density	5.61
Vapour Pressure (hPa)	44 @ 20°C, 175 @ 50°C
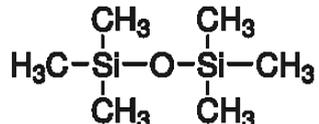
Allylamine	AL - C_3H_7N
Initial Boiling Point ($^\circ$C)	53
Vapour Density	1.97
Vapour Pressure (hPa)	282 @ 20°C, 1,127.6 @ 55°C
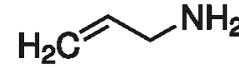
Figure 2.1: Chemical structures and information relating to processing parameters

One of the most important characteristic we look at when considering how to properly utilise these chemicals is the vapour pressure (VP). VP is a characteristic value directly related to the evaporation rate of a liquid, and is therefore an important piece of information when dealing with input vapours for low pressure processes. VP relates to the tendency of particles to escape from a liquid (or a solid). A substance with a high VP at normal temperatures is often referred to as volatile. As the VP of some of the chemicals employed herein appear quite low at room temperature, such as APTES (0.02hPa @ 20°C), experiments can include a heating apparatus to enhance evaporation rates, as the Clausius-Clapeyron relation states that the VP of any substance raises in a non-linear fashion with increases in temperature. This relationship is shown mathematically in the Clausius-Clapeyron equation;

$$ln\left(\frac{P}{P^o}\right) = \frac{\Delta H}{R}\left(\frac{1}{T^o} - \frac{1}{T}\right)$$
(Eq 2.1)

In equation 2.1 Prepresents vapour pressure, P^o represents vapour pressure at a known temperature T^o, ΔH is the enthalpy of vaporisation, R is the ideal gas constant, and T is the temperature. As the VP is equal to the pressure where vapour begins to condense, it is best (if heating is necessary) to maintain a temperature relating to a VP higher than that of the intended processing pressure[123], [124].

Assuming enough information is available for each chemical (temperature, pressure or enthalpy values), this equation can be incorporated to produce approximate VP graphs for any precursor. Although the enthalpy of vaporisation changes depending on the temperature of the liquid, it does not vary hugely once the chemicals state remains constant (i.e. stays liquid). A typical enthalpy range versus temperature/state of matter is shown in Fig 2.2. Typically a tabulated and unchanging enthalpy value can be used for the Clausius-Clapeyron pressure equations.
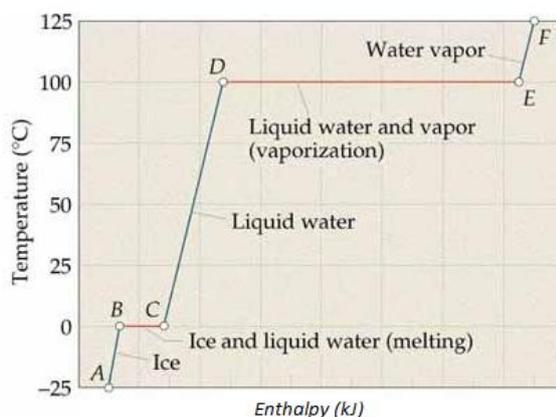
Figure 2.2: Enthalpy of water as temperature is increased [125]

Using the Clausius-Clapeyron equation, a set of data was created to display the VP curves of each chemical used in this work. This diagram allows us to assess the precursors required heating before depositions takes place. Data begins at 20°C as this is the ambient temperature of the canisters containing the precursors. The data stops at each chemicals respective boiling point at atmospheric temperature.
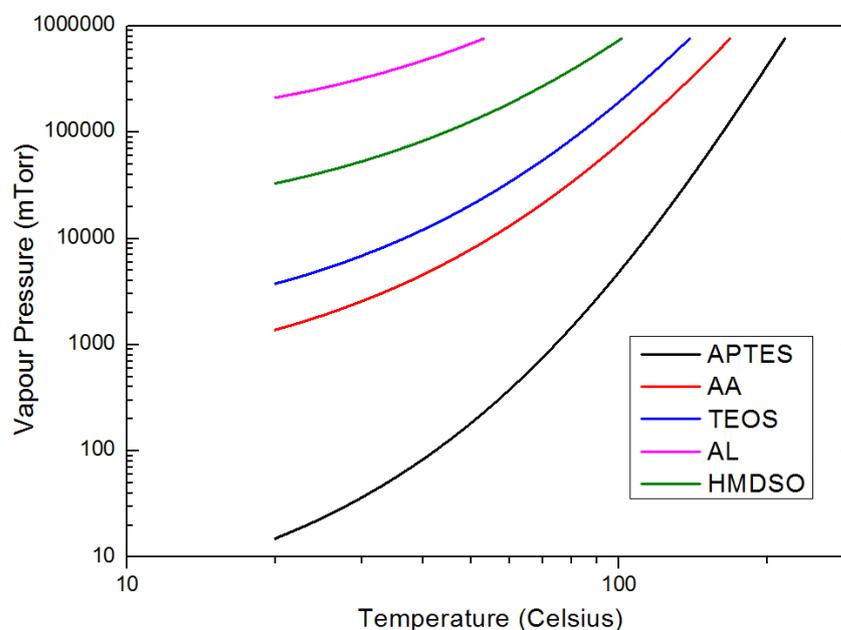
Figure 2.3:PECVD precursor VP curves from room temperature to atmospheric boiling point

A chemical is considered at its boiling point (point where molecules freely escape the liquid threshold) once its VP matches the ambient atmospheric pressure. As the plasma processes used in this work typically operate at 200mTorr of pressure, APTES appears to be the only chemical still below its boiling point. Therefore a temperature of no less than 52°C must be applied to encourage evaporation into the deposition chamber. All other chemicals display VPs that do not require further excitation for appropriate evaporation.

AA, although similar in mass to ALhas a lowerVP. This is due to the structure of the chemicals, specifically the functional difference. As stated in section 1.4, carboxyl groups have a larger dipole moment than amine groups. This added binding force acts to reduce VP as AA molecules attract each other, lessening their likelihood of escaping the liquid/vacuum interface. Similarly the APTES and TEOS chemicals can be compared. Although similar in mass, the added interaction between amine groups hydrogen bonding serves to hinder vaporisation in low pressure environments.

2.1.2 – Cyclo Olefin Polymer (Zeonor® 1060R)

Cyclo Olefin Polymers (COPs) are amorphous polymers used in a range of applications, such as lenses, optical storage media and medical devices. Zeon Chemicals is a company dedicated to development of innovative polymer development, and in 1983 developed a ring-opening polymerisation procedure to create COPs. Using this process Zeon Chemicals have developed 2 COP products; Zeonex® and Zeonor®. These COPs are attributed with characteristics such as low water absorbency, dimensional stability, excellent precision moulding capabilities, high transparency and low birefringence [126], [127].
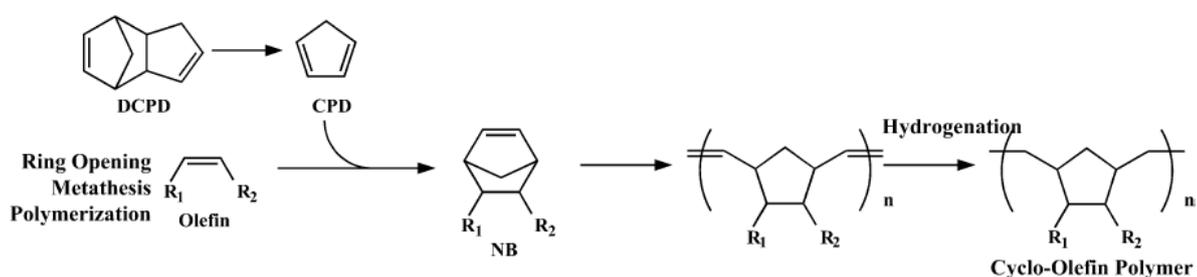
Figure 2.4:Ring opening polymerisation of cyclo olefin polymers[127]

Many medical experiments and diagnostic devices work on the principal of quantification of signal from fluorescently labelled detector molecules reacting with target analytes. Therefore the optical properties of the materials used are important in developing the most efficient device [32], [128]. COPs offer medical devices an easily manufacturable polymer surface with high quality optical features.

Zeonor® 1060R was chosen as the primary COP in this work on account of the optical properties and compatibility with plasma processing. The substrates are purchased from Sigolis AB as microscope slides, measuring 75x25x1 mm.

2.2 - Characterisation Methods

2.2.1 - Ellipsometry

Light has been employed in systems for thickness measurements since as early as the 1700's, where colours observed after passing through thin transparent layers were assumed to be caused by a quantifiable interference. D. Brewster relates to this in 1831 by pointing out that the observations "*may be regarded as presenting us with a micrometer for measuring thicknesses of transparent bodies by their colours, when all other methods would be inapplicable*"[129]. Ellipsometry is now a powerful and sensitive optical technique which has found use in a variety of different fields. This ranges from in situ analysis of thinly deposited layers on substrates, to dynamic exploration of film growth in organic layers. With a resolution of as low as 0.01nm, and the fact that a vacuum ambient is not required for general usage, ellipsometry has proven an invaluable characterisation tool for a range of experimental disciplines [129]–[131].

Ellipsometry is based around the polarisation changes of a polarised monochromatic light source reflecting off of a surface. Ellipsometry is an indirect technique, and the returning polarised light does not directly relay the relevant data. Insteaddata must be interpreted and analysed in optical models, and this fitting allows for assessment of surface characteristics, i.e. thickness or complex dielectric function. Ellipsometry may also be employed in multilayer analysis, where the collected polarisation shift can be broken down into different film combinations. In these cases the scattering matrix formalism is employed, featuring sets of matrices which represent each layer and interface of the coating. All values and parameters gained from these various methods can be plotted versus a library of pre-obtained values, allowing for extrapolation of the actual thicknesses [129].
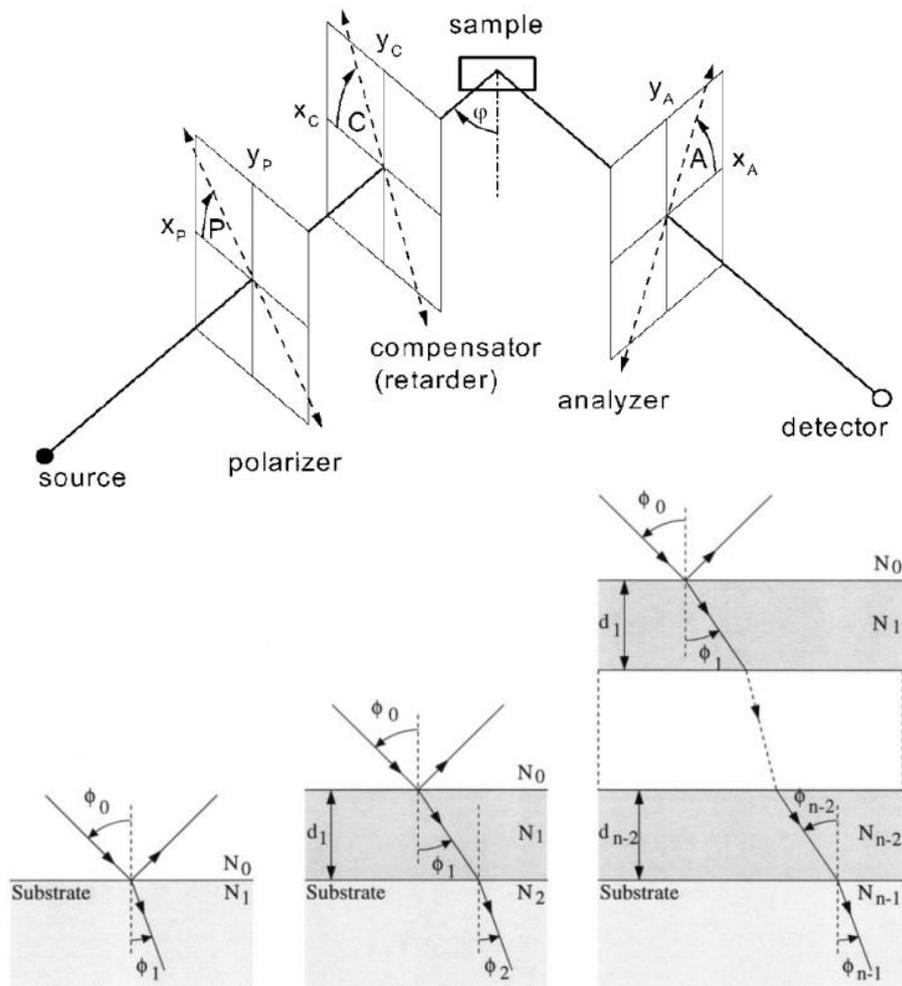
Figure 2.5:(Top) Typical ellipsometer setup [129] **and (bottom) refractive and reflective changes of incoming light to multi-layered surfaces** [131]

In the case of the experimentation conducted during this thesis, the ellipsometer was employed to assess the layer thickness of PECVD deposited coatings on undoped silicon (1 0 0) wafers.This is a necessity as polymer substrates, such as those used in this work, are transparent and are unable to reflect the input radiation. The data obtained from silicon pieces can be used to interpret the probable thickness of all other substrate slides included in the deposition cycle.

With the possibility of a resolution of 0.01nm the ellipsometer is a more than proficient system for examining all thin films created using the PECVD system. Differences in the functionality and specificity of similarly deposited coatings could then be compared using the original thickness of their respective coatings, forming a basis for any discrepancies [129]–[131].

Ellipsometry was carried out in open environment at room temperature on an M-2000UI ellipsometer (J.A. Woolam Co., Inc.). Multiple areas of each silicon sample are tested to

extrapolate an average film thickness. The ellipsometer used in experimentation is shown in Fig 2.6.
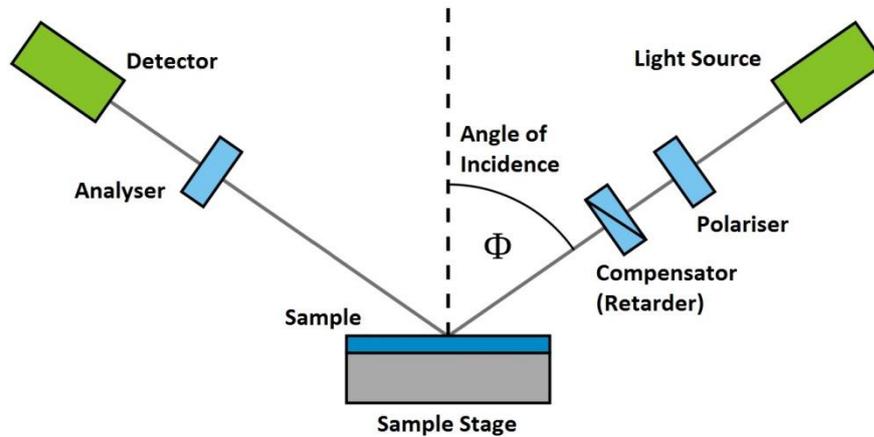
Figure 2.6:Diagram depicting the M-2000UI ellipsometer general setup

2.2.2 - Water Contact Angle Analysis

Water contact angle (CA) measurement of surfaces is an important characterisation technique when dealing with a thin film intended for use in biological experiments.Although a relatively simple characterisation method, the wettability of a surface influences a range of properties, such as the adhesive capabilities of the surface[99], [132], biological interactions[98], [100], [133], and fluidic flow capabilities[27]. CA is geometrically defined as the angle formed at the interface between a droplet of liquid, and the surface under examination. Some benefits of this characterisation technique are its non-destructive nature, as well as its rapid throughput and inexpensive setup costs.

The shape of a droplet at the interface of a surface is determined by various factors. The Young-Laplace equation incorporates these influencing factors to estimate unknowns (i.e. surface energy), with the CA value being utilised as a boundary condition for the equation. The theoretical explanation of CAs comes from looking at the thermodynamic equilibrium between the three states of matter: the droplet (Liquid Phase, L), the substrate (Solid Phase, S), and the ambient atmosphere (Gas/Vapour Phase, G) [134].
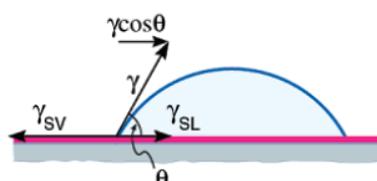
Figure 2.7:Contact angle constituents between a droplet and surface [134]

Young's equation assumes a perfectly flat and homogenous surface, with θ being used as the equilibrium CA;

$$\gamma_{SV} = \gamma_{SL} + \gamma_{LG} \cos \theta \qquad \text{(Eq 2.2)}$$

In this equation γ_{SV} represents the surface energy (SE) of the substrate, γ_{SL} represents the liquid-solid interface, and γ_{LG} represents the liquid surface tension. Although this idealised equation gives a good indication of a surfaces free energy, the actual value will likely vary as the surface CA is also dependant on a range of other interfering constituents, such as surface roughness and environmental/physical interference (pressure changes, vibrations etc.). A paper by Tadmor[134]shows how a theoretical value for θ_C can be calculated using the maximum and minimum angle values of a droplet, often referred to as the advancing angle (θ_A) and the receding angle (θ_R). As surfaces are often not perfectly uniform the droplet may 'pull' more towards the more attractive side, giving rise to these differing CA values. The following equation for θ_C can then be used to assess the actual CA of a surface [134], [135];

$$\theta_C = \arccos \frac{\Gamma_A \cos \theta_A + \Gamma_R \cos \theta_R}{\Gamma_A + \Gamma_R} \qquad \text{(Eq 2.3)}$$

Where,

$$\Gamma_A = \sqrt[3]{\frac{\sin^3 \theta_A}{2 - 3\cos \theta_A + \cos^3 \theta_A}} \qquad \text{(Eq 2.4)}$$

$$\Gamma_R = \sqrt[3]{\frac{\sin^3 \theta_R}{2 - 3\cos \theta_R + \cos^3 \theta_R}} \qquad \text{(Eq 2.5)}$$

The efficacy of this theoretical equation was proven in a paper by Chibowski et al., where the experimental and theoretical values were well correlated. In this set of experimentation, constant recording of CA values can provide us with a rapid and accurate method for testing our batch to batch PECVD process reproducibility [134], [135].

Figure 2.8: Example ofa hydrophobic surface with droplets used for water CA assessment positioned in linear patterns across the wafers diameter

Surfaces are considered hydrophilic once the water CA of the surface drops below 30°. Surfaces exhibiting a water CA greater than 90° are considered hydrophobic (e.g. Fig 2.8). Superhydrophobic surfaces exhibit water CAs of greater than 150°. For this work, surfaces will be considered hydrophilic if the water CA drops below 30°, but any value above this shall be referred to broadly as hydrophobic. Much of the research herein for water CA analysis was performed using an OCA 35 goniometer (Dataphysics). Experimentation employed 2μL and 4μL droplets of DI water for analysis, at a dose rate of 1μL/s. Diiodomethane droplets were used for SE measurements.

Surface wettability however is slightly different than the normally measured water CA. There are two equations that can be used to determine the wettability of a surface; the Wenzel equation (for homogenous surfaces), and the Cassie-Baxter equation (for heterogeneous surfaces). These equations are as follows;

$$\cos \theta^* = r \, \cos \theta \qquad \text{(Eq 2.6)}$$

This is the Wenzel equation, where r is the roughness ratio (ratio of the true surface area to the apparent area), θ is the contact angle predicted by the young's equation, and θ^* is the apparent contact angle on the rough surface [136].

$$\gamma_{LV} \cos \theta^* = \sum_1^N f_i \, (\gamma_{i,SV} - \gamma_{i,SL}) \qquad \text{(Eq 2.7)}$$

This is the Cassie-Baxter equation, where γ_{LV}, $\gamma_{SV,}$ and γ_{SL} represent the surface tension at the liquid/vapour, solid/vapour, and solid/liquid interfaces, and f_i is the fraction of surface area under the droplet [137].
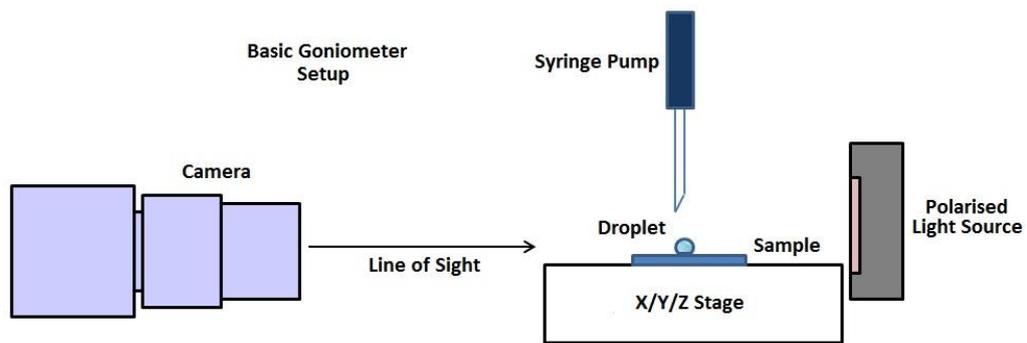
Figure 2.9:Diagram depicting the basic setup of the OCA 35 goniometer

2.2.3 - X-Ray Photoelectron Spectroscopy

X-Ray Photoelectron Spectroscopy (XPS) is a form of photoemission analysis used in surface composition investigations. XPS focuses on the analysis of electrons ejected from a materials core level by an incoming X-ray photon [138]. The energy of emitted electrons are analysed using an electron spectrometer, with the subsequent recorded data culminating in an X-Ray photoelectron spectrum. This is a graph of counts (or intensity) versus electron binding energy. XPS can analyse depths of between 1-10nm, which equates to several atomic layers, across an area of a few microns. By altering the orientation of the material with respect to the incoming X-Ray beam the spectrum collected can focus on different specific depths. The main limitation of the XPS however is the inability to measure hydrogen and helium elements, meaning the data collected is relative (not absolute) ratios of elements in a surface [138]. A basic XPS setup is shown in Fig 2.10;
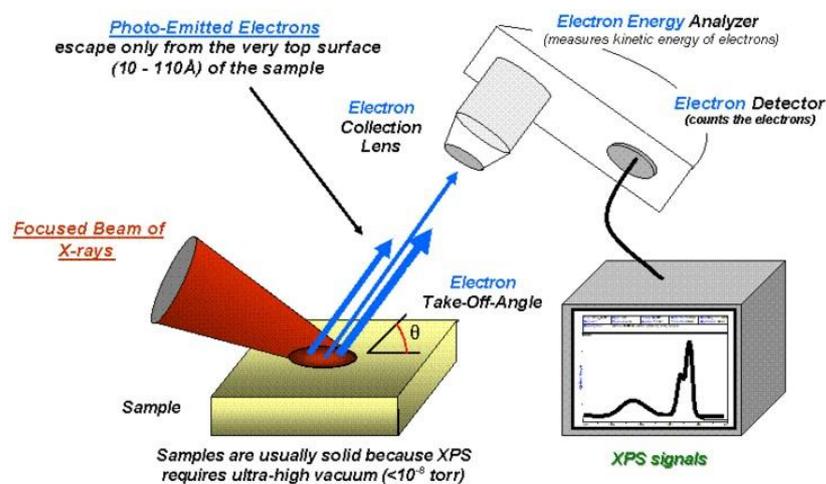
Figure 2.10: Typical XPS Setup [139]

40

The XPS system spectrometer measures the kinetic energy (E_K) of electrons being ejected from the surface under investigation, but this value is highly dependent on the input photonic energy of the X-Ray and therefore does not relate to direct material properties. The binding energy (E_B) of the electrons is the parameter which will need to be extrapolated, as this is the value that identifies the electron specifically with respect to the parent element it originated from [138]. Equation 2.6 is used to determine the binding energy of an electron;

$$E_B = h\nu - E_K - W \tag{Eq 2.8}$$

In this equation $h\nu$ represents the photon energy, E_K as previously stated is the kinetic energy of the ejected electron, and W refers to the work function. The work function refers to the minimum energy required by an electron to move from a solid to an area immediately outside of the solid (Fermi level to vacuum). This electron ejection mechanism is shown in Fig 2.11;
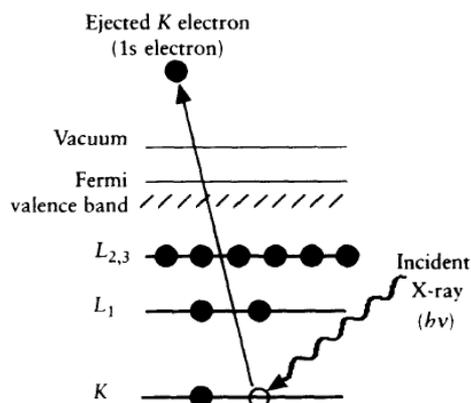
Figure 2.11: Diagram of the XPS electron ejection process, showing photoionisation of an atom [138]

XPS analysis was carried out using a VG Microtech electron spectrometer at a base pressure of 1×10^9 mbar. The photoelectrons were excited with a conventional Mg K ($h\nu = 1253.6\text{eV}$) x-ray source and an electron energy analyser operating at 20eV pass energy, yielding an overall resolution of 1.2eV.

2.2.4 - X-Ray Reflectivity

X-Ray Reflectivity (XRR) is a surface characterisation method, used to ascertain the morphology (thickness and roughness) and density of thin films. This method of analysis focuses on monitoring the intensity of the non-destructive X-ray beam as it is

reflected off of a sample substrate at grazing angles, with conditions aimed at generating total external reflection. A simplified XRR setup is shown in Fig 16;
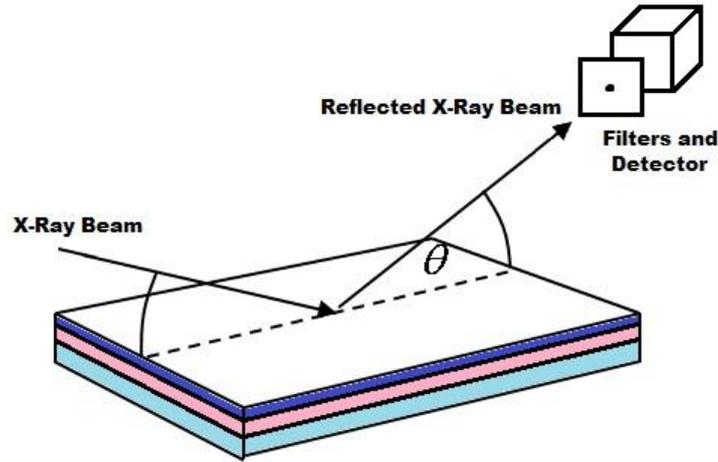
Figure 2.12: X-Ray input and output, simplified setup

For an XRR system to operate it must be ensured that the angle of incidence θ is sufficiently small enough to allow for total external reflection. For this to occur, the incident angle of the X-ray beam must therefore be below the critical angle of the material (θ_C) [140]. The following equation can be used to find the materials' critical angle;

$$\cos\theta_C = n \qquad\qquad \text{(Eq 2.9)}$$

For X-rays however, the refractive index (*n*) of the material is affected by both the scattering and absorption of the material, therefore n must first be extrapolated using the following equation;

$$n = 1 - \delta - i\beta \qquad\qquad \text{(Eq 2.10)}$$

In this equation δ accounts for the material scattering, and β for the material absorption of X-Rays. These values (both positive) respectively depend on the materials electron density ρ, and linear absorption coefficient μ. Keeping this in mind, the critical angle formula can now be written as;

$$\cos\theta_C = 1 - \delta \qquad\qquad \text{(Eq 2.11)}$$

Much like ellipsometry, the data collected from XRR analyses of a surface is indirect, and must be modelled against theoretical best fits for the materials in question. During

scanning, the sample holder will roll through a series of angles determined by the critical angle of the material. During these cycles there will be constructive and destructive interferences of the reflected X-rays caused by the surface topography, which leads to wave like intensity data being recorded [140]. Fig 2.13 shows a typical XRR plot, and a subsequently fitted model overlaid on the raw data;
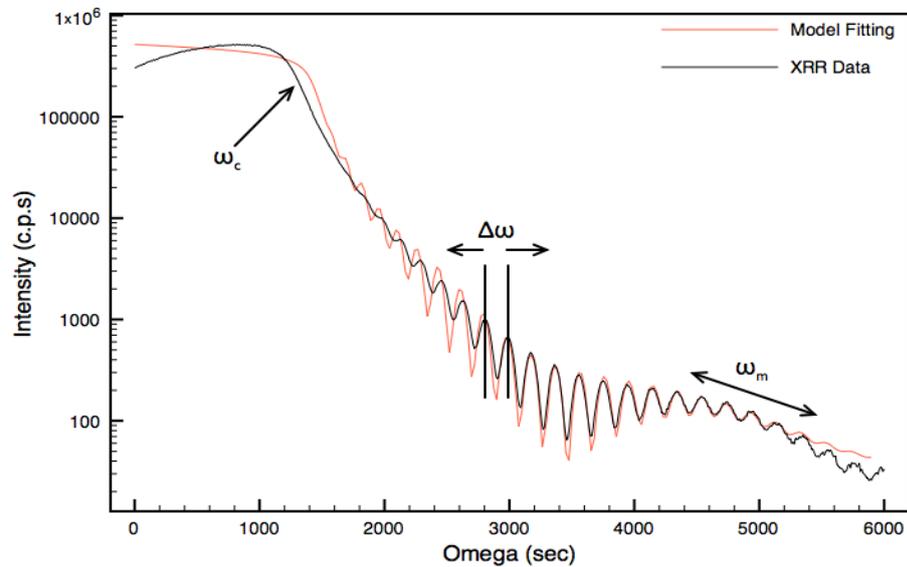
Figure 2.13: Typical XRR emission graph, showing both raw and model fit data

In the case of an XRR plot, ω_c represents the critical angle, which relates to the materials density. The $\Delta\omega$ symbol represents the distance between oscillations, and relates to the thickness of the films. The ω_m section of the plot, the slope of reflection, refers to the roughness profile of the material.

X-Ray reflectivity (XRR) was carried out using a Jordan Valley D1 Evolution XRD. Fitting of the XRR scans was carried out via generic algorithm fitting using the commercial BedeREFS program.

2.3 –Experimental

2.3.1 - COP Cleaning Protocol

A pre-process cleaning phase was introduced to remove unwanted surface contaminants that arise from storage and the manufacturing process of the COP substrates. It was found that cleaning of substrate slides prior to plasma deposition can help to improve the efficiency of flow through assays performed on integrated microfluidic devices. The protocol is as follows;

1) Sonicate the substrates in 2% Micro-90 cleaning solution (20mL Micro-90 added to 980mL deionised (DI) water) for 30 minutes at 50°C
2) Rinse substrates thoroughly with DI water and isopropanol
3) Sonicate the substrates in isopropanol for 30 minutes at 50°C
4) Remove substrates and rinse with DI water before drying with nitrogen

Once dried the substrates are kept stored in their respective holders, preferably in a desiccator, to prevent the build-up of interacting with the surface.

2.3.2 - Chemical Liquid Deposition of APTES onto COP

APTES is a chemical which can be chemically deposited onto a surface through a process of silanisation. The silanisation of APTES onto polymers is a well characterised process [32], [109], [111], [114], and the films created are both chemically stable and robust. Chemical liquid deposition of APTES allows for a comparison for PECVD deposited APTES films. The protocol for chemically depositing APTES is as follows;

1) Oxidise substrates (either through oxygen plasma treating or other methods like UV-ozone treatment)
2) Place the freshly oxidized substrates in the deposition solution (92:5:3 mixture of isopropanol (may be substituted with ethanol), DI water, and APTES)
3) Store the substrates for 2 hours at room temperature in solution
4) Sonicate substrates in isopropanol 15 minutes twice
5) Rinse the substrates with isopropanol
6) Bake the substrates in oven for 1 hour at 80°C (substrates may stick to holder during baking so care must be taken)
7) Cool the substrates for 30 minutes at room temperature

Coated slides can then be stored as needed.

2.3.3 - Spin Coating Zeonor® onto Silicon

Silicon is required for use in some characterisation techniques, such as XRR and ellipsometry. Although depositions on both COP and Silicon substrates are thought to be chemically similar, the intended substrate for biomedical applications in this work is COP. Therefore it is important to test silicon samples with spin coated COP in some instances for otherwise inaccessible information. The COP deposition protocol is as follows [141];

Preparation of Solution

1) COP dried by incubating @ 45°C overnight
2) Dissolve 0.125g of COP in 50mL of xylene
3) Sonicate for 10 minutes
4) Filter using a 0.45μm pore to filter out undissolved Zeonor®

Spin Stand

1) Cover silicon in polymer solution after placement
2) Spin recipe is as follows;
    a. RPM1 = 1000, Ramp1 = 2secs, Time1 = 10secs
    b. RPM2 = 2000, Ramp2 = 2secs, Time2 = 5secs
    c. RPM3 = 100 (Stopping Speed), Ramp3 = 2secs
3) Remove samples and allow to dry before use

Once spin coated samples are completed they can be used in plasma depositions, although depending on the thickness of the COP coating a shorter pre-deposition cleaning phase may be needed to ensure the layer is not completely etched away.

2.3.4 - Toluidine Blue Staining

Toluidine blue (tolonium chloride) is a cationic dye that shows a strong affinity for interaction with carboxylic acid groups under certain conditions. The procedure for toluidine blue staining of carboxylic surfaces is shown below [142];

1) Using a 0.1mM NaOH solution, create a 0.1mM dilution of toluidine blue (0.0305g per 1L)

2) Incubate substrates for 1 hour @ 40°C with 50mL of fresh toluidine blue solution

3) Rinse surfaces using fresh 0.1mM NaOH to remove excess dye

4) Incubate substrates in Acetic Acid:Water (50:50) solution for 30 minutes @ 40°C

5) Solution can be measured using ultraviolet-visible spectroscopy (UV-Vis) (absorbance 626nm – 635nm)

UV-Vis data is not definitive, so a calibration curve must be created to compare subsequent experiments. Fig 8 shows the chemical process of the toluidine blue experiment, with respect to its attraction to carboxyl groups:
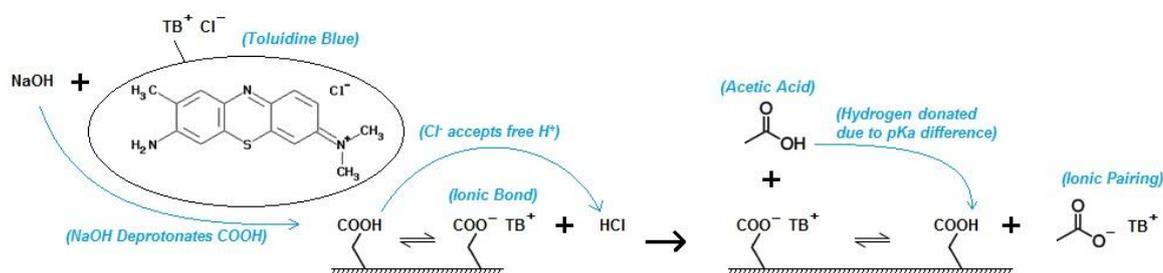
Figure 2.14: Toluidine blue carboxylic attachment and removal process

2.3.5 - EDC-NHS Linked Protein Immobilisation Experiments

Biological assays are investigative laboratory experiments used to quantitatively assess the presence and levels of specific biological targets, i.e. proteins, enzymes, DNA. In this work a sandwich assay was chosen to display the surfaces functional ability to immobilise proteins. The assay begins with the immobilisation of an anti-human immunoglobin (α-hIgG) antibody. This is immobilised through using a zero length linking reaction, which uses EDC and N-Hydroxysuccinimide (NHS) (see Fig 2.15). Human IgG (hIgG) in this experiment is then used as an analyte and is the target of the immobilised anti-hIgG. A secondary α-hIgG, linked with the cyanine 5 dye (Cy5), is then used as a labelling protein to assess the level of hIgG captured, therefore giving a signal relative to the efficacy of the surface for performing immobilisation assays. Cy5 dyes are chosen because of their bright emission strength, and good stokes shift between excitation and emission wavelength. The protocol used is as follows;

1) Prepare 2-(N-morpholino)ethanesulfonic acid(MES), phosphate buffered saline (PBS) and PBS Tween (1%) buffer solutions

2) Place substrates securely in gasket cells (holders representative of microwell plates)

3) Create EDC/NHS solution (10mg and 3mg respectively per 500μL MES)

4) Add 100μL of EDC/NHS solution to each well

5) Store at room temperature for 15 minutes

6) Rinse wells with PBS

7) Add 100μL of α-hIgG to each well (10μg/mL conc)

8) Place in oven at 37°C for 40 minutes (cover gasket to limit evaporation)

9) Wash surface with 3 x PBS Tween (1%), and 3 x PBS stages

10) Block surface using 100μL ethanolamine for 5 minutes (0.1M concentration)

11) Rinse wells with PBS

12) Add 100μL of hIgG to each well (varying concentrations for standard curve, i.e. 4μL, 1μL, 0.4μL… etc.)

13) Place in oven at 37°C for 1 hour (cover gasket to limit evaporation)

➔ Otherwise leave @ room temperature for 2 hours

14) Wash surface with 3 x PBS Tween (1%), and 3 x PBS rinses

15) Add 100μL of Cy5 labelled α-hIgG to each well (20μg/mL)

16) Place in oven at 37°C for 1 hour

➔ Otherwise leave at room temperature for 2 hours

17) Wash surface with 3 x PBS Tween (1%), and 3 x PBS rinses

18) Remove substrate from gasket and rinse once with PBS

19) Spin dry before scanning

By varying the concentration of the analyte hIgG molecules we can see how applicable our surface is at measuring different quantities of the target.
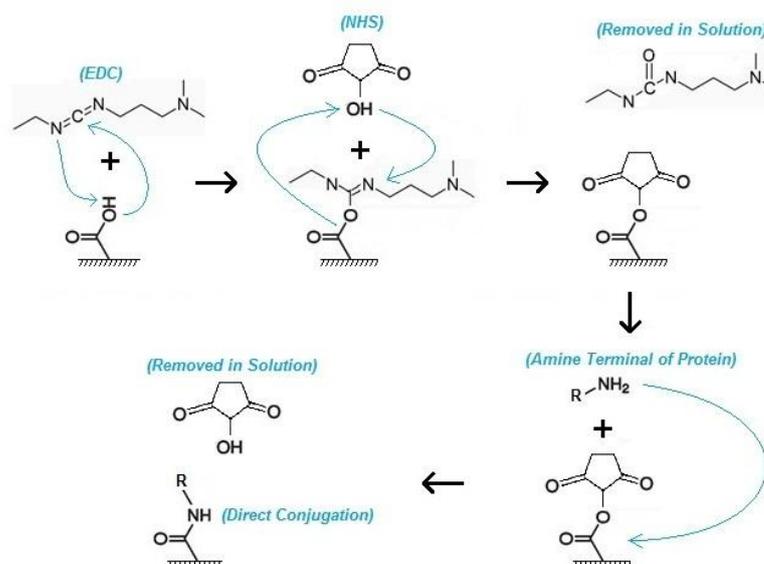
Figure 2.15: EDC/NHS coupling of a carboxylic acid group to an amine group

2.3.6 - Direct Protein Immobilisation through EDC/NHS Protocol

As described previously, biological assays are investigative laboratory experiments used in quantitative analysis. By copying the first stages of the full bioassay (e.g. section 2.3.5) a relatively fast experiment can be performed to assess the presence of stable carboxyl groups on a surface. The procedure is as follows;

1) Prepare MES, PBS and PBS Tween (1%) buffer solutions
2) Place substrates securely in gasket cells (holders representative of microwell plates)
3) Create EDC/NHS solution (10mg and 3mg respectively per 500µL MES)
4) Add 100µL of EDC/NHS solution to each well
5) Store at room temperature for 15 minutes
6) Rinse wells with PBS
7) Add 100µL of Cy5 labelled α-hIgG to each well (10ug/mL conc)
8) Place in oven at 37°C for 40 minutes (cover gasket to limit evaporation)
9) Wash surface with 3 x PBS Tween (1%), and 3 x PBS rinses
10) Remove substrate from gasket and rinse once with PBS
11) Spin dry before scanning

Experiments of this nature give a definitive answer to whether carboxyl groups are present on the surface, and whether they can withstand aqueous washing phases.

Chapter 3

3.1 - PECVD System Setup

Experiments were carried out on an Oxford Instruments Plasmalab System100 PECVD reactor. The chamber is connected to a Dressler 300W radio frequency (RF)generator with an operating frequency of 13.56 MHz, used in connection with an OIPT automatch unit. Gas and precursor vapours are distributed uniformly to the chamber through a combination of an electrically isolated gas spreader and RF powered shower head. The quartz substrate holder is mechanically loaded via a low pressure transfer chamber. The substrate holder is placed on an electrically grounded lower electrode, which has the capability to be heated to 400°c. Figs 3.1, 3.2 and 3.3 shows the PECVD chamber in both open and closed position.
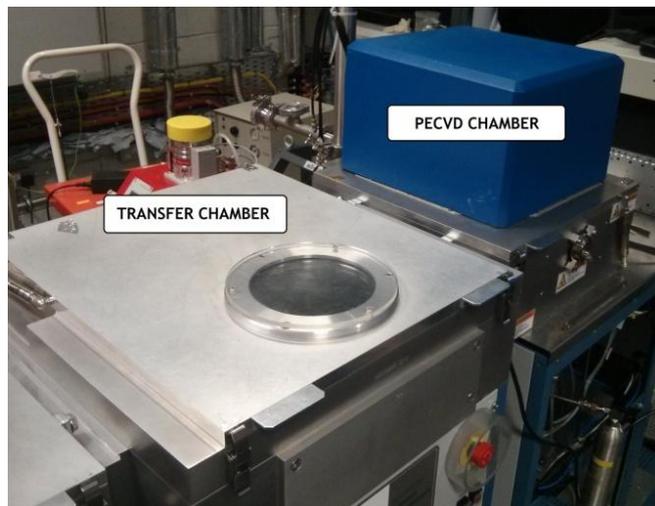
Figure 3.1: Oxford Instruments Plasmalab System100 PECVD reactor with transfer chamber
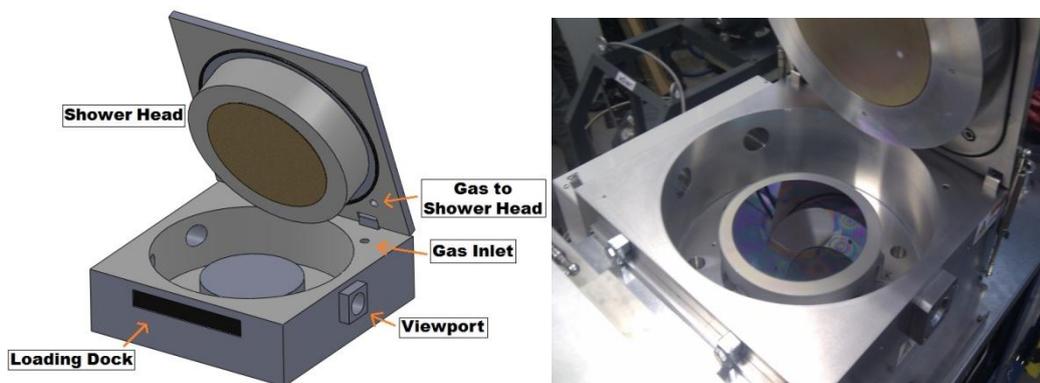
Figure 3.2: (Left) 3D model of Oxford System plasma chamber and (right) Photo of Oxford System plasma chamber
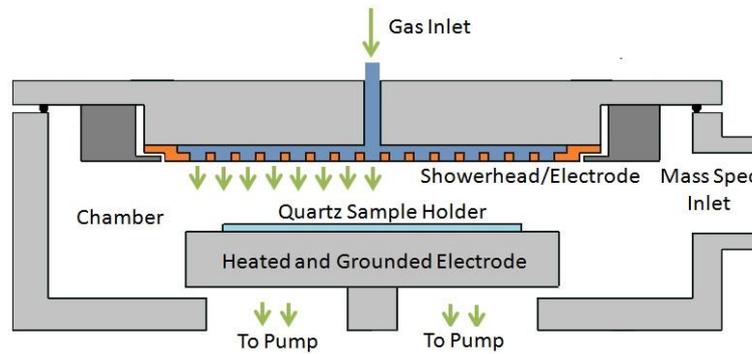
Figure 3.3: Diagram showing the layout of the PECVD chamber in the Oxford100 system

A mechanical arm located in the transfer chamber is used to load samples into the deposition chamber, ensuring the deposition chamber remains in a vacuum environment between depositions. This reduces the presence of contaminants such as water vapour from the processes. The substrates chosen for use in this work were microscope slides (75x25x1mm). For this reason a quartz holder was machined to allow for the inclusion of multiple substrates to be used per deposition. The design of this plate is shown in Fig 3.4. The quartz material provides a solid plate for loading and unloading samples via the mechanical arm located in the transfer chamber. Quartz was chosen as it is rigid and naturally resistant to plasma etching. The microscope sized grooves are machined into the quartz plate to ensure the samples undergoing processing remain in a consistent location within the chamber.
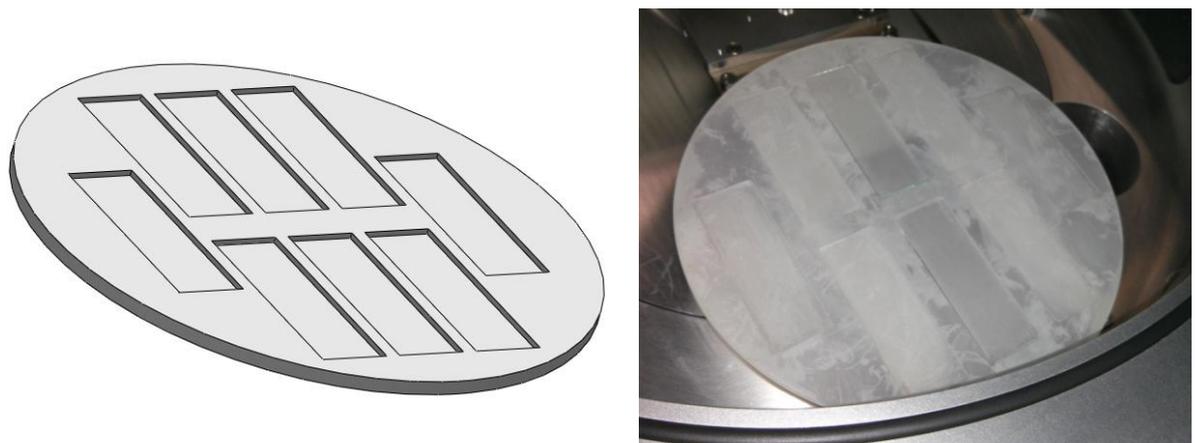
Figure 3.4: Quartz substrate holder (300mm in diameter) for PECVD system loading, designed to accommodate 8 x microscope slides

Gas enters the chamber through the back of the shower head and is dispersed evenly over the area of the sample holder. The gas and vapour lines feed into this inlet from

below the chamber, and this is where the precursor canisters are housed. The manually operated precursor canisters are shown in Fig 3.5, while the two mass flow controllers (MFCs) operating the two secondary precursor canisters are shown in Fig 3.6. Quarter inch diameter pipes are installed throughout the system for gaseous flow from both the MFCs (gas and vapour) and manual vapour canisters.
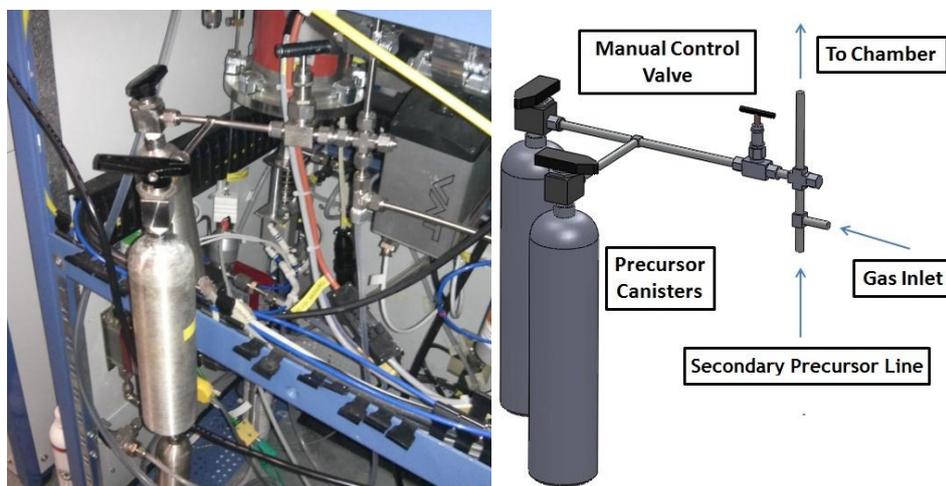
Figure 3.5:The two precursor canisters located below the deposition chamber with manual isolation valves installed on each canister and a manual control valve separating them from the gas line
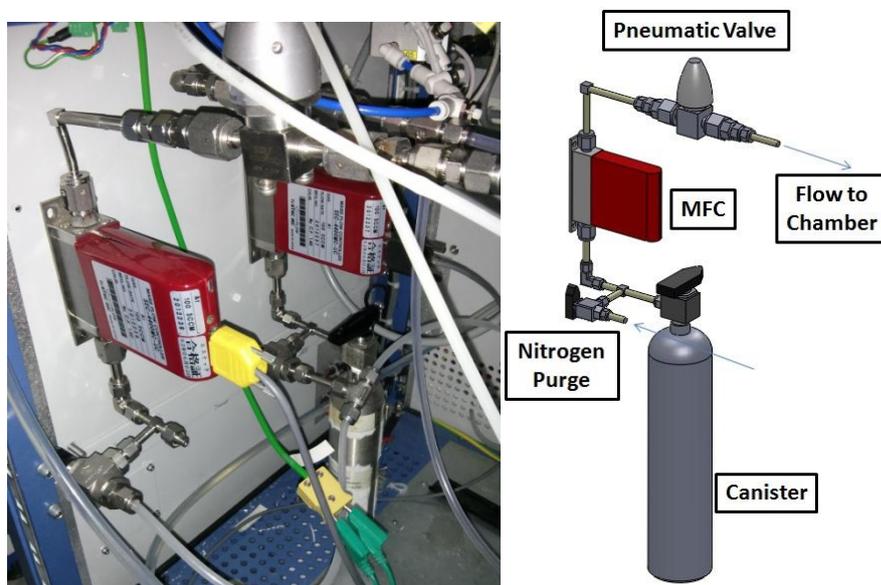
Figure 3.6:The two identical positions for MFC operated precursor canisters located below the manual precursor canisters, both are piped through the same chamber feed line

The MFC operated canisters (Fig 3.6) are used with precursors that exhibit a high VP to allow for sufficient control, as the MFCs require sufficient pressure from the canister

side to operate efficiently. Therefore in this work the only chemicals used in the MFC operated canistersare AL and hexamethyldisiloxane (HMDSO). The manually controlled canisters are then used with the lower VP chemicals, which are TEOS, AA and APTES.

3.2 – Process Control

As the MFCs installed are designed for gas applications the actual flow rate will differ from that registered by the system. Therefore an experiment was run to assess the actual flow rate of the precursors into the chamber.To achieve this argon was used to create a calibration baseline. Different flow rates of argon were chosen and timed to see how long it takes to reach a chamber pressure of 500mTorr. This created a linear plot with which to base our precursors flow rates. AL, TEOS, and AA were tested as they are the predominant precursors used in this work. As AL is controlled via a MFC, a rate of 100sccm was chosen (maximal system input). Canisters containingboth AA and TEOS were opened fully via manual valves. The time taken to reach the intended pressure with each precursor allowed for a simple estimation of the actual flow rates of each. The equation used to extrapolate the precursor flow rate is the equation of the line of the argon linear fit;

$$y = 1.728 + x(323.905) \hspace{2cm} \text{(Eq 3.1)}$$

where y is the control argon flow rate, and x is the inverse time taken to reach equilibrium pressure. Using this equation the flow of vapour from each precursor was calculated, and this data is shown in Fig 3.7. Note the estimation of APTES flow rate was ignored in this work due to the different in deposition process.

Input	Flow (sccm)	Time to reach 500 mTorr (secs)	1/Time (s^{-1})
Argon	10	41.5	0.02
	15	24	0.04
	20	17.3	0.06
	30	11.3	0.09
	35	9.9	0.1
TEOS	7.2	59	0.02
AA	52.3	6.4	0.16
AL	10.6	36.7	0.03
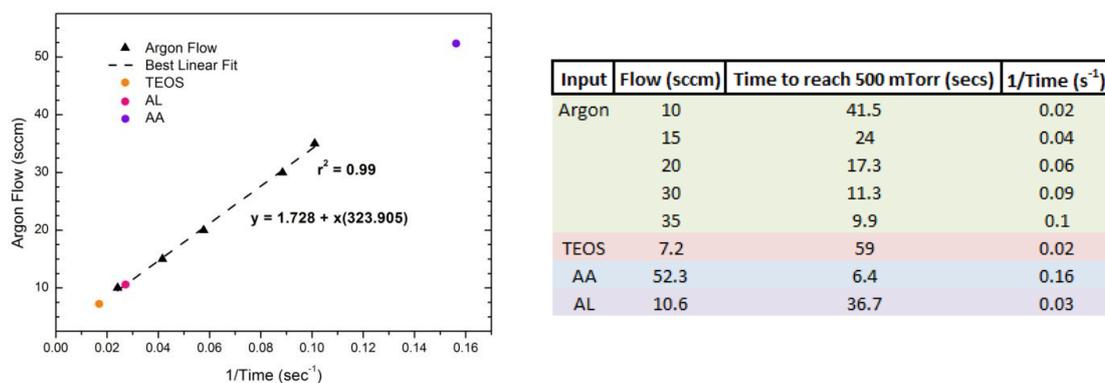
Figure 3.7: Graph showing the estimated flow rates of the precursor vapour with respect to the argon baseline equation

52

Dalton's law of partial pressures states that '*the total pressure exerted by a mixture of gases is equal to the sum of the partial pressures of individual gases*'. Therefore by mixing a vapour and an input gas the pressure in the chamber should reflect the combination. Upon further inspection however, it became apparent that the combination of gas and vapour often displayed a pressure relating to the presence of the gas only. In some instances increasing the gas flow gradually caused the vapour presence to become negligible within the chamber. An experiment was performed to assess the percentage contribution of each monomer to the overall chamber pressure. Data is generated by comparing the mixture of vapour and gas pressure against the singular gas pressure. Through this a percentage of the contribution the vapour makes to the chamber volume was calculated. This data is shown in Fig 3.8.
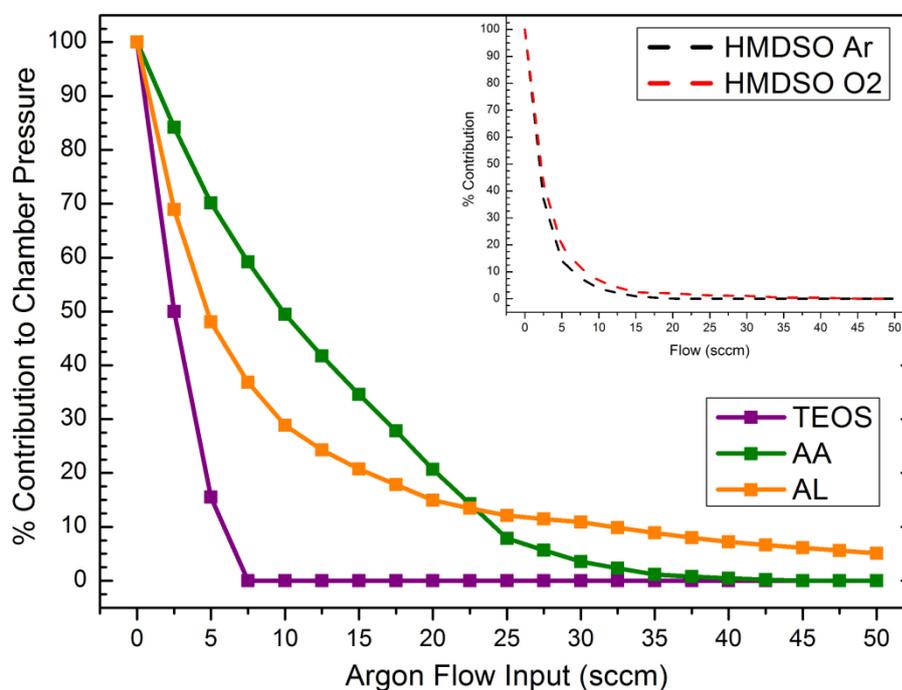
Figure 3.8: Contribution of vapour to overall chamber pressure versus increasing gas input

As shown by Fig 3.8, the vapour presence in the chamber is negatively impacted by increased levels of accompanying gas. TEOS is shown to be minimally present once the argon gas input is pushed above 5sccm, whereas as a result of the higher VP AA is present until argon flow is increased past 40sccm. AL retains a steady presence even at 50sccm argon (system maximal rate). On the inset graph, HMDSO showsreduced contribution when gas inputs (both oxygen and argon) reach 5sccm. This is due in part tothe difference in gas density (argon = 1.784g/L and O_2 = 1.429g/L). HMDSO retains a

presence in the chamber up to an accompanying oxygen flow of 42.5sccm, or 20sccm for argon. Processes will in future be adapted to this procedural drawback.

As mentioned the chemical precursors used for depositions are housed in stainless steel canisters (300mL volume). Chemicals are stored and transferred to these canisters in a nitrogen environment (Fig 3.9), and once installed in the system each is exposed to the vacuum. This serves to protect the chemicals from any contamination. Precursors can be stored in these canisters for weeks without replenishment due to the minute volume used per deposition. Therefore depositions can be continually run with no negative process issues.
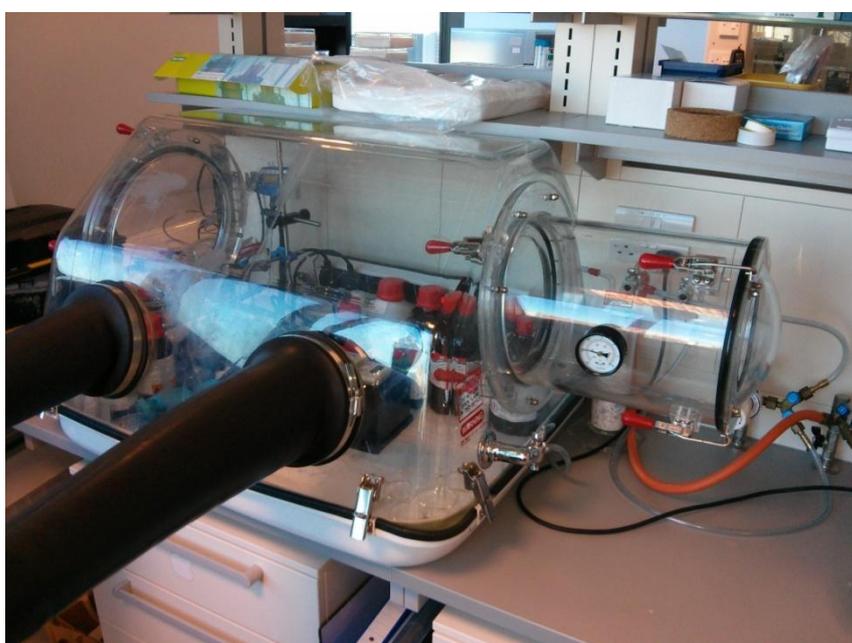
Figure 3.9: Nitrogen hood used for precursor storage and exchange

Over extended periods of time (>3 months) however there is a chance of some chemicals spoiling. APTES is the most obvious for this as the presence of water or water vapour causes a rapid silanisation reaction that leads to the formation of a thick white polymer. The same process of degradation applies to TEOS also. But the nitrogen chamber and vacuum storage remove any instance of this happening once installed on the system.

AA however has shown to develop a thick polymer like layer (polyAA) when stored for an extended period. Suspended polymer particles in solution are a clear sign of this. As this appears more pronounced with the AA precursor a set of experiments was run using nuclear magnetic resonance (NMR). The results are shown in Fig 3.10, 3.11 & 3.12.
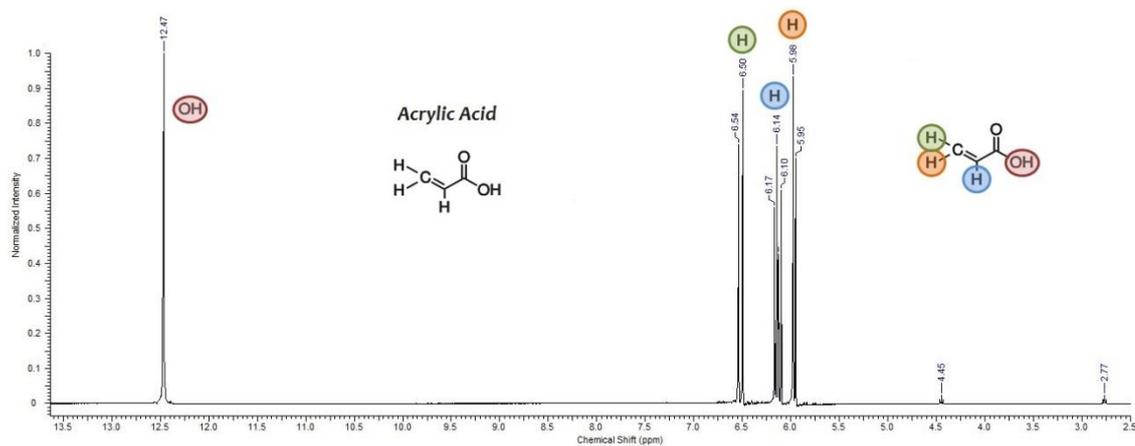
Figure 3.10: NMR of newly purchased AA (highlighting associated peaks to molecule hydrogen), showing negligible evidence of polymerisation
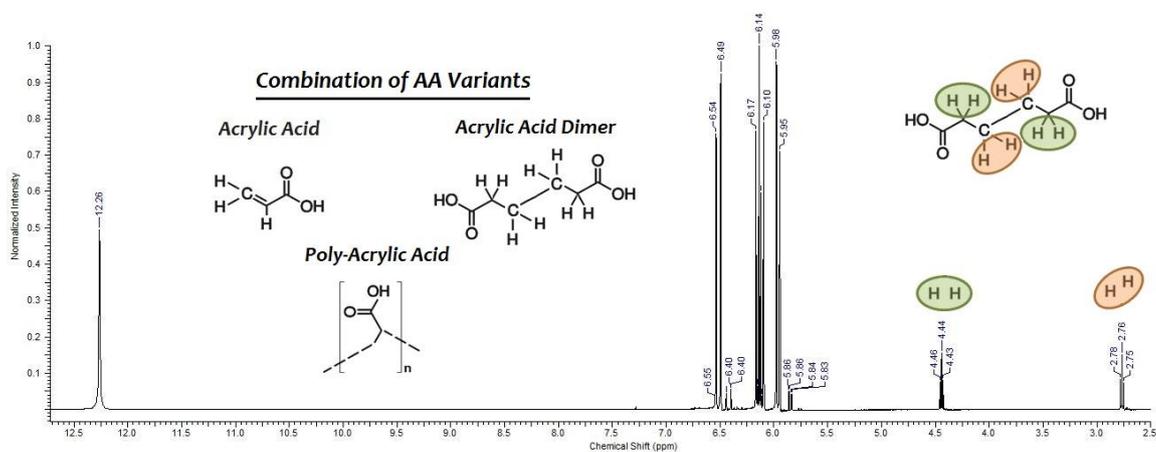
Figure 3.11: NMR of AA removed from PECVD canister after 1 month of usage (including heating of precursor canister)
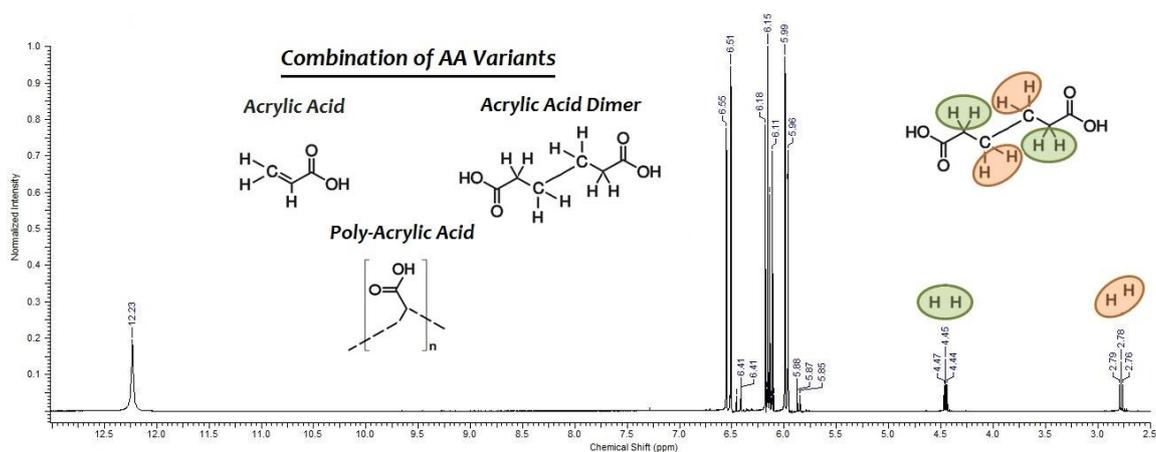
Figure 3.12: NMR of AA after storage for 1 year in nitrogen chamber

Figures 3.10 and 3.11 show how over time the AA precursor can begin to polymerise in the canister, despite being kept under constant vacuum. Heating of the containment

55

canister is in part responsible for speeding up this process. AA can experience polymerisation regardless of heating, as evident from Fig 3.12, but heating of the precursor appears to speed the chemical reactions responsible for the creation of polyAA variants. To measure the NMR of AA the chemical must first be dissolved in a deuterated solvent, such as deuterated chloroform. Long polyAA chains however do not dissolve and only small chains and dimers appear in the NMR results. Fig 3.13 shows visible polymerisation of the AA chemical.
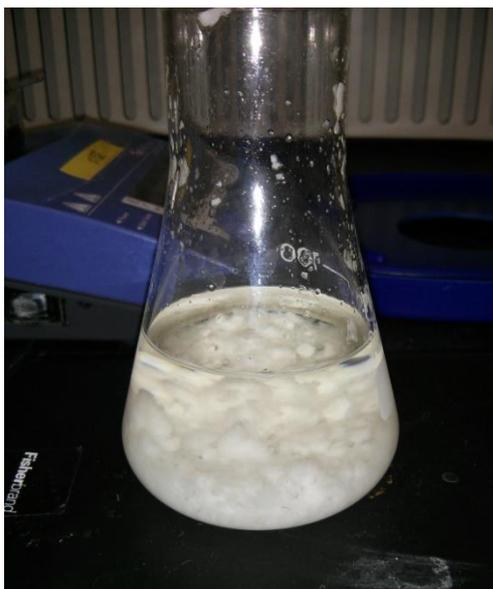
Figure 3.13: AA chemical showing large amounts of suspended polymeric formations

Visual inspection of the chemicals investigated in Fig 3.11& 3.12 yielded suspensions similar to that shown in Fig 3.13. The peaks associated with the altered AA appear more pronounced for the sample shown in Fig 3.11 than for Fig 3.12, showing a more prevalent presence of polymerisation. For this reason, and reasons that will be expressed in section 4.1, the heating of AA was discontinued.

All other chemicals used herein showed no visible signs of polymerisation, such as discolouration of the fluid or obvious signs of polymeric suspension. They were therefore presumed fit for extended periods of usage before replenishment.

Reproducibility of a plasma process depends on the consistency of the many variables influencing the discharge. One of the most important of these is the level of monomer vapour present in the chamber during deposition phases. To assess the level, a mass spectrometer was employed to gain a quantitative measure of ionic species synonymous to the monomer vapours used. A quadrupole mass spectrometer, Pfeiffer QME 200,

wasused to monitor the PECVD process in real time. As a proof of the reproducibility of the processes designed in this work, the TEOS and AA dual layer deposition was chosen as an example.

An atomic mass unit (amu) of 179 was chosen to represent the TEOS monomer, and an amu of 72 was chosen as the AA monomer marker. These values were chosen as they represented the highest signal when a broad scan was performed on each individual chemicals process. These relate to species of the chemical that have undergone mild dissociation or activation caused by the plasma. The composition of the species under investigation is shown in Fig 3.14. Due to the low power employed during depositions, dissociation is weak and large charged particles dominate the spectra. The graphs showing the consistent nature of the process are shown in Fig 3.15.
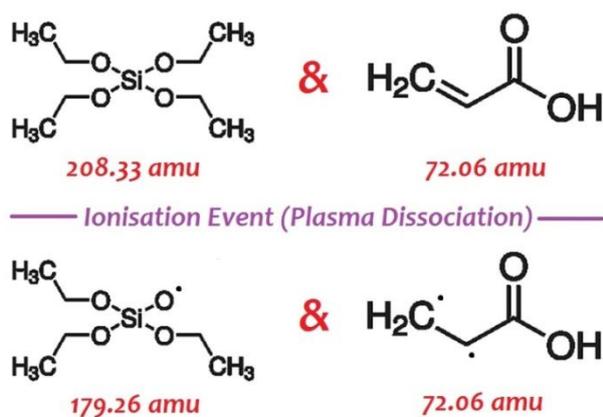
Figure 3.14: Complete monomers of TEOS (Left) and AA (Right) and the associated ionised monomer under investigation using Mass Spectrometry
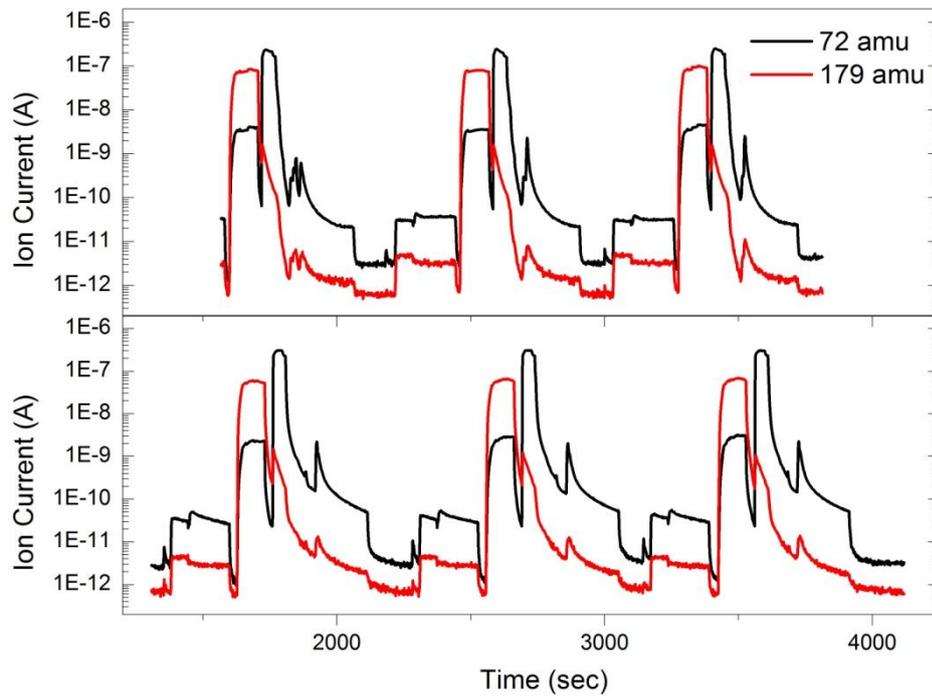
Figure 3.15: Mass spectrometer data on 2 separate days showing the reproducibility of the TEOS/AA process with respect to levels of specific fragments present in the chamber

As can be seen from Fig 3.11, both separate experiments produce similar profiles of both the 72amu and 179amu constituents of the plasma. To put the data in perspective, the TEOS is first run for 90 seconds, before a 10 second venting phase. Then the AA vapour is flown for 45 seconds before a secondary venting phase. Once the samples are removed from the chamber an oxygen plasma discharge is run for a period of 5 minutes to clean the chamber. The cleaning plasma is apparent on the graphs as a sharp jump of both TEOS and AA. This is likely just a combination of removal of leftover monomer from the chamber and noise created by the striking of higher power plasma. The phase before the influx of TEOS and AA is of the pre-treatment, showing that although the monomers are not present there is a little flux in the graphs relating to noise introduced by the presence of high powered plasma.

3.3 – Deposition Recipes

Deposition recipes were adapted from those used previously in work on a Europlasma CD300 plasma reactor deposition system[102], [104], [105], [143], [144]. Where possible, recipes were kept as in line with these early processes as possible, but this was not always possible as the argon influence (Fig 3.8) proved to hinder the precursor flow.

From here on in this work, the following recipes are considered the standard deposition recipe;

	Argon (sccm)	Oxygen (sccm)	TEOS	AA	Pressure (mTorr)	Time (sec)	Power (Watts)
Pretreatment 1	50				200	30	50
Pretreatment 2	50	50			200	150	150
Venting						10	
TEOS Stabilisation	0.1		Open		200	60	
TEOS Deposition	0.1		Open		200	30	25
Venting						10	
AA Stabilisation	0.1			Open	150	30	
AA Deposition	0.1			Open	150	15	15
Venting						10	

Figure 3.16: Sequential TEOS/AA deposition recipe as per Oxford system inputs

	Argon (sccm)	Oxygen (sccm)	TEOS	AL	Pressure (mTorr)	Time (sec)	Power (Watts)
Pretreatment 1	50				200	30	50
Pretreatment 2	50	50			200	150	150
Venting						10	
TEOS Stabilisation	0.1		Open		200	60	
TEOS Deposition	0.1		Open		200	30	25
Venting						10	
AL Stabilisation	0.1			Open	150	30	
AL Deposition	0.1			Open	150	15	25
Venting						10	

Figure 3.17: Sequential TEOS/AL deposition recipe as per Oxford system inputs

	Argon (sccm)	Oxygen (sccm)	APTES	Pressure (mTorr)	Time (sec)	Power (Watts)
Pretreatment 1	50			200	30	50
Pretreatment 2	50	50		200	150	150
Venting					10	
APTES Stabilisation	50		Open	200	60	
APTES Deposition	50		Open	200	120	10
Venting					10	

Figure 3.18: APTES deposition recipe as per Oxford system inputs

Considering the TEOS to be the only gas present, with negligible argon influence, the films shall be considered low in oxygen compared to SiO_2 pure films. These films will likely resemble the 100% TEOS fraction films detailed in the work by Valleé et al [63]. Taking into account the values shown in Fig 1.6, which detail similar depositions, these films will likely have a low oxygen composition and a density of approximately 1.5-1.6g/cm^3.

As with many plasma based processing systems, a phenomenon known as the 'first-wafer effect' can occur during the first complete deposition process. This causes coatings to display properties and characteristics unlike those of subsequent processes. Some factors that influence this problem are;

- The condition of the deposition chamber itself, i.e. chamber wall contamination and absorbance of radicals onto the chamber wall.

- The addition of elements sputtered from the substrates interacting with the plasma bulk

- Temperature of the system, i.e. chamber walls, substrate holder, electrodes etc.

By running several complete dummy processes, including vapour introduction, the first-wafer effect can be stymied. This allows for thesubsequent reproducibledeposition of characteristically homogeneous films.

Chapter 4

Results Section 1 – Development of Carboxylic Acid Thin Films and Subsequent Control of Surface Wettability using Post Process Curing

4.1 – Introduction

The aim of this research is to develop a robust film populated with a high density of carboxylic acid groups present on the surface interface. These carboxylic groups are chosen for their binding potential of biomolecules, as referenced in section 1.3. Creation of a stable carboxylated film will serve to improve the manufacturability (and subsequently the cost) of devices designed to take advantage of this specific mode of biomolecular immobilisation. In this work, TEOS and AA have been combined to create a film comprising of a stable organosilicon anchoring matrix with a carboxylic acid dense surface. A basic illustration of the outcome of the sequential deposition is shown in Fig 4.1. This idealised representation does not take into account the many layers of each individual chemical likely present in an actual deposition, but instead serves as an example of the general process and outcome.
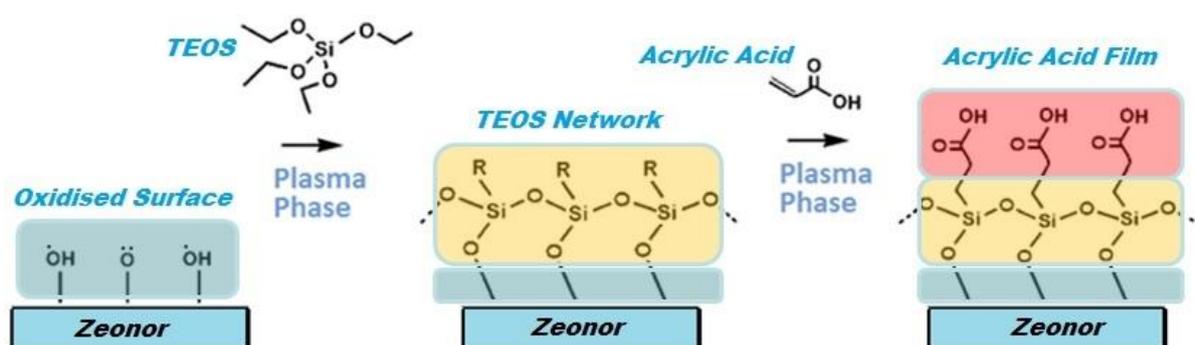
Figure 4.1: Sequential TEOS/AA deposition depicting the intended layered affect

The results presented in this chapter correspond to data currently under review in several publications. Specifically this research follows on from work detailed in previous publications from our research group[143]–[145]. The key scientific findings are as follows;

- Low power argon free deposition of TEOS/AA generates films which, if under certain conditions, allow for reformation of final surface wettability
- TEOS/AA hydrophilic films are robustly adherent and resistant to hydrophobic recovery
- TEOS/AA films are applicable for use in assay formats, and retain a high level of specificity and functionality

4.2 - Process Control and Development of Deposition Standards

During processing, regardless of intended chemical deposition, each recipe ran includedthe pre-deposition plasma phase to oxidise and clean the substrates. The function of this step is to promote surface adhesion of monomers through surface radicals whilst removing possible surface contaminants. The pre-processing phase however will cause both surface etching, leading to increased roughness, and a change in the surface density of the outer face of the material. As silicon is employed for thickness analysis throughout this work, it is important to address the effect this pre-processing has on the silicon substrates.

The silicon samples used (4 inch x 0.5mm thick boron doped silicon wafers) have a native oxide layer of roughly 2-3nm, measured after cleaning in solution (if necessary) and before plasma interaction. After the pre-processing however, changes can be observed using ellipsometry. This data is shown in Fig 4.2;
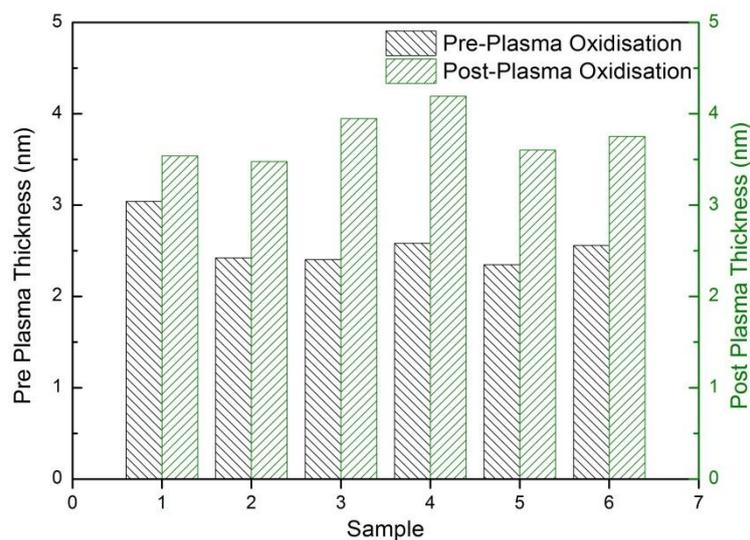
Figure 4.2: Native silicon oxide thickness as recorded by ellipsometry both before and after plasma treatment

This data shows the apparent increase in thickness of the native oxide layer of the silicon substrate. Although the data points to an increase in film thickness, the actual process is more likely an etching effect on the silicon surface, furtheroxidising the surface while lowering the density. This creates the apparent increase in oxide film thickness. As the models used during ellipsometric analysis of our silicon based films are the same as those used herein, an assumption is thus made moving forward that all films showing thicknesses of below 4nm are to be considered negligible/incomplete. However as the initial layer deposited by PECVD is typically silicon based, we assume the native oxide and organosilicon collectively form the anchoring organosilicon matrix. Therefore, all ellipsometric data shown in this work is inclusive of the combined baselayer.

To develop a silicon oxide based networking layer, a suitable chemical must be chosen. HMDSO and TEOS were compared for their individual properties to this affect. Both chemicals are elementally similar. TEOS is naturally more oxygen rich, with its central SiO_4group allowing for less complicated, higher purity SiOx film grown. HMDSO however naturally has a more favourable VP, making it a more suitable chemical for passive vaporisation in a low pressure system.
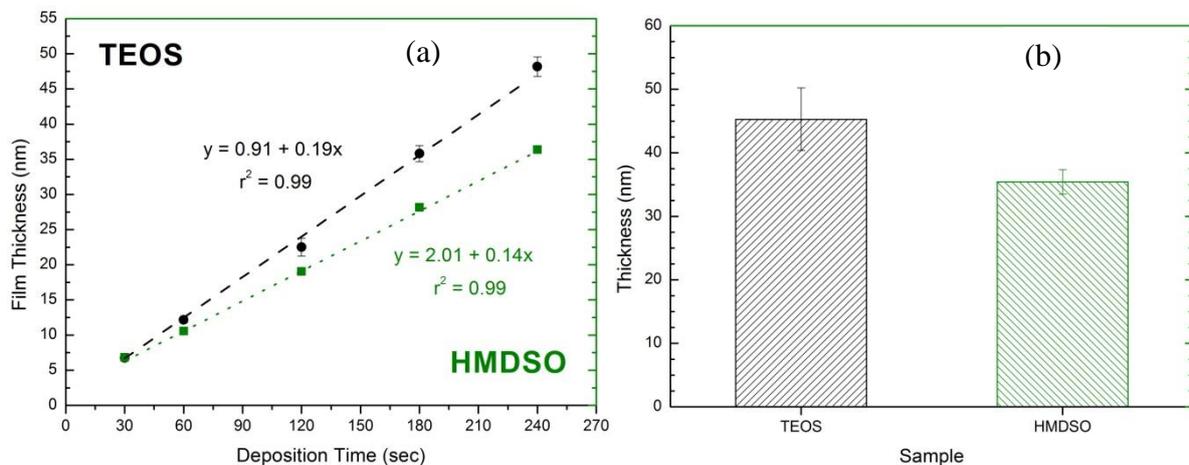
Figure 4.3: (a) Deposition rate of both TEOS and HMDSO and (b) thickness uniformity over area of a microscope slide (4 minute deposition)

As can be seen the HMDSO thickness uniformity over a full sample area is slightly better than that of the TEOS. This is attributed to the more volatile nature of the chemical, and the difference in the chemical vapour density. The vapour density has a direct effect on the chamber pressure. HMDSO displays a lower vapour density than that of TEOS, 5.61 and 7.19

respectively (Air = 1). Larger concentrations of HMDSO are thus present during processing (due to the constant operational pressure maintained), creating a more isotropic dispersion.

Despite the many operational improvements over TEOS, HMDSO deposited films were found to be unsuitable for a variety of reasons. Most importantly, the films created were more silicon rich compared to TEOS, and were prone to cracking due to the rigidity of the layer. The more ductile nature of the COP substrate also likely exacerbated the issue. This cracking effect is shown in Fig 4.4. Cracking on the surface allows for proteins and other biological molecules to become trapped on the surface, ruining any chance at surface selectivity or non-specific adhesion repulsion.
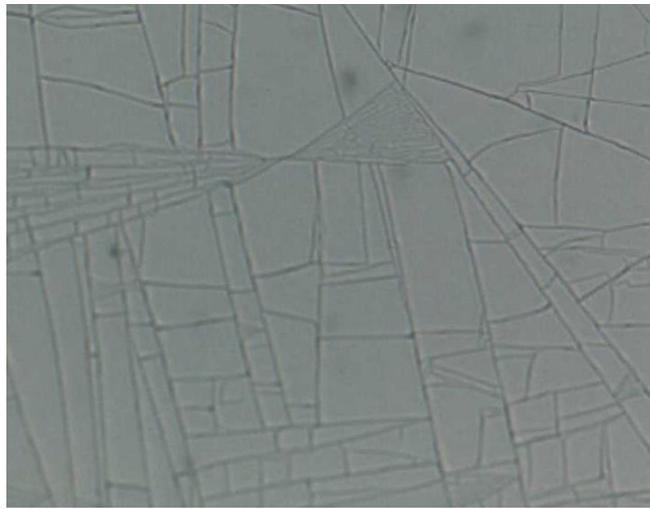
Figure 4.4: Microscope image of surface cracks developing on HMDSO derived organosilicon layer

A secondary issue with the use of HMDSO was the glass like build-up in the chamber. Due to this, several instances of intense plasma arching were observed as the showerhead pathways became occluded. For these reasons, the softer and more organic TEOS films were chosen for the remainder of the work.

By analysing the VP data shown in section 2.1.1 an assumption was made to attempt a deposition of TEOS and AA without heating of the precursor canister. As both precursors displayed VPs higher than that of 200mTorr (our typical processing pressure) heating was assumed to be unnecessary. Twosets of 5 minute depositions were run with both TEOS and AA separately. Unfortunately ellipsometrical analysis showed no film growth with either monomer. These depositions were run with an argon flow rate of 50sccm, akin to processes performed previously in the Europlasma deposition system [104], [105].

An assumption was made that within the gas/vapour line feeding the chamber the pressure was in excess of 200mTorr due to the argon presence (effect shown in Fig 3.8). To counteract this, both precursor canisters were heated to a temperature that allowed for both precursors to exhibit similar VPs. In this case 2 different approximate temperature sets were used;

Temp set 1 → TEOS at 50°C and AA at 30°C ≈ 8000mTorr VP

Temp set 2 → TEOS at60^{o}C and AA at 40°C ≈ 15000mTorr VP
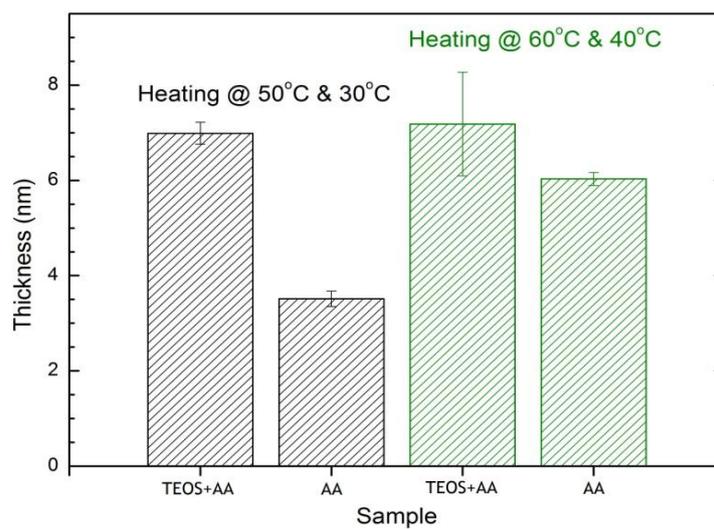
Figure 4.5: Differences observed during short 1 minute depositions of TEOS/AA films with AA films deposited singularly to display important discrepancies

Fig 4.5 shows that although thin films are being deposited, the lower temperature appear to provide sub-optimal conditions, as the AA acid film thicknesses are below those deemed acceptable (Fig 4.2). The higher temperature allows for appropriate levels of AA to enter the chamber for deposition. The similarities in TEOS/AA films despite increasing temperature are likely the result of erratic temperature control at time of deposition, as well as possible plasma quenching caused by increased levels of the large TEOS monomer, decreasing the initial growth rate.

Fluctuations in batch to batch deposition thickness due to insufficient temperature control led to the removal of the installed heating apparatus from the system. Instances of precursor condensation in the gas/vapour lines (high risk of valve and pipe occlusion), and polymerisation of the AA in the canister (see section 3.2) added to the need for removal of the heater. Therefore processes were developed using no precursor heaters, but with reduced or no argon to allow for appropriate monomer flow, as per Fig 3.8.

4.3–Characterisation of TEOS/AA Surface

4.3.1 – Formation of Soft PolyAA Layer and Subsequent Control over Surface Wettability through Novel Curing Technique

Having shown the ability of theprecursors to supply the chamber with appropriate monomer vapour without heating (Fig 3.8), it was decided that a minimal argon flow processes would be developed. Using the previous pressure experiments (Fig 3.8) and mass spectrometer outputs (Fig 3.15), it was found that gaseous flow of >5sccm caused TEOS vapour signals to disappear from the chamber. This lead to the application of a process using passively vaporised precursor (no heating) alongside a 0.1sccm (0.1 - 0.5sccm actual) argon carrier gas input. This, in theory, would have minimal influence on the discharge.

To test the new process a set of samples were run using TEOS and AA separately, not in a dual layer deposition. The films were measured for thickness atthe differing time steps, and were measured again after a mild 10 minute wash step in DI water. These results are shown in Fig 4.6.
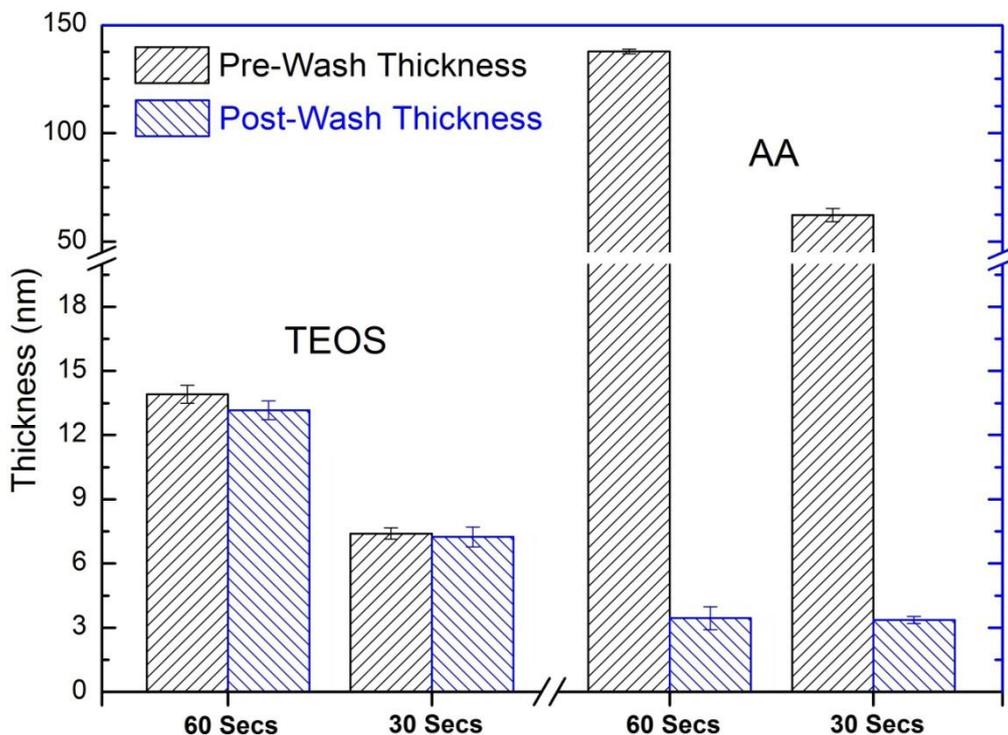
Figure 4.6: (Left) TEOS thickness stability over multiple processes and post wash thickness and (Right) AA process stability over multiple runs and subsequent changes due to washing

In Fig 4.6 it is shown that both processes deposit films that retain a standard thickness throughout numerous depositions, and that halving the deposition time essentially halves the thickness recorded. TEOS films also show stability and resilience when washed, varying negligibly after rinsing. AA however shows a complete loss of the film, as the thickness of various depositions drops to below the pre-declared negligible thickness standard. This highlights the weakly polymerised nature of the AA depositions generated using this process. This 'soft' polymer film is easily removed through rinsing, and shows visible degradation when in an open-air environment, further accentuating the instability of the layer.

The growth of a softly polymerised thick film of AA is a direct artefact of the argon-free deposition. Originally, AA depositions were run utilising argon. This required heating the AA precursor. Although processing issues were synonymous to heating the precursor, as shown to in section 3.2, the surfaces created showed signs of polymeric cross-linking, generating films that could resist extensive damaged from a H_2O rinse. This cross-linked carboxylic acid filmis referenced extensively in the literature, where the effect of power on the cross-linkage was typically assessed [69], [70], [72], [74], [75]. The cross-linkage of the AA surfaces however typically came at a cost of a reduced density of functional carboxylic acid groups. It was theorised that an appropriate anchoring matrix was required to grant efficient adhesion of the AA monomers.Thus the next phase was to employ the TEOS films as a network building matrix for the AA top layer. Fig 4.5 shows the thickness measurements associated with these experiments. The TEOS and AA films showed consistent thicknesses to previous experiments and the combined films (pre-wash) show a thickness equivalent to what was expected.
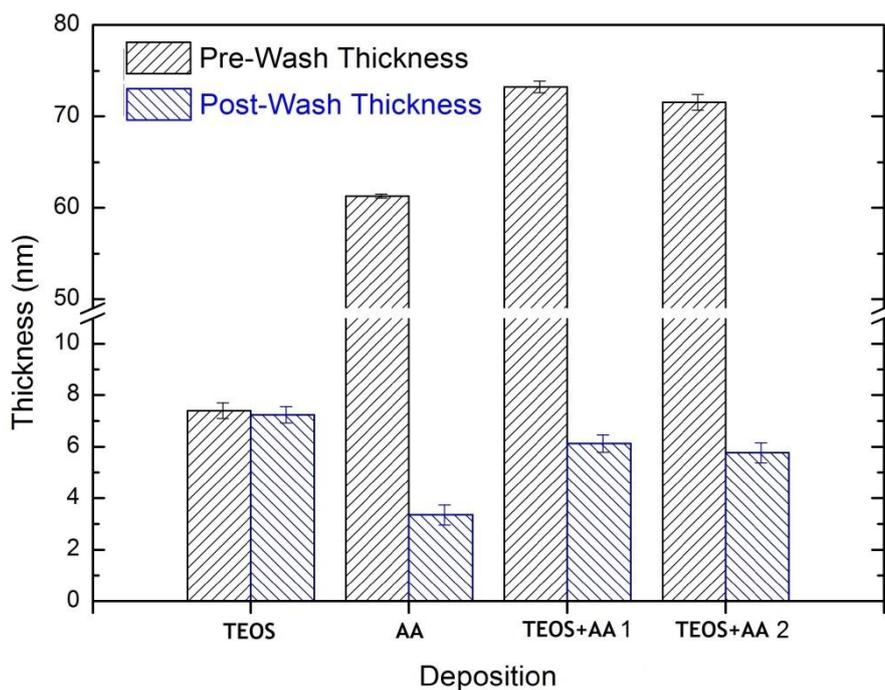
Figure 4.7: Data showing the pre and post wash thickness of TEOS, AA and dual TEOS/AA films

Fig 4.7 shows how the TEOS and TEOS/AA (although thinner) films are retained after washing, unlike the singular AA coating. The appearance of a slightly decreased thickness of the TEOS/AA films compared to the plain TEOS coating is assumed to be the influence of both a secondary plasma ion bombardment of the surface, and chemical wearing of the surface due to the corrosive nature of the AA monomer. The dual film is assumed to be comprised mainly of organosilicon with a thin, almost mono-layer, of AA on the outermost interface.

TEOS/AA surfaces created previously using the Europlasma system exhibited hydrophilic surface properties [144]. This was not the case however with the films developed in the Oxford100 system, where TEOS/AA films often showed a wide range of water CAs. This was interpreted to be storage related, as those with higher water CA tended to be stored in vacuum up until use. It was initially assumed that the uppermost layer of the soft polyAA (Fig 4.7) may serve as a protective layer for the covalently bound underlying carboxylic acid matrix, protecting if from external interaction until washed away. During investigation into the difference in water CA however, it was discovered that the soft layer had a curing effect on the underlying film. Given the appropriate stimuli this soft film allowed for alteration of the wettability of the surface.

An initial experiment was conducted comparing the changes in surface wettability in two contrasting environments to determine whether water vapour or oxygen presence, assumed the 2 most influential environmental factors, had the greatest impact. The first set of substrates was placed in a container partially filled with warm water, with a relative humidity (RH) range of 85-99%. The second set was placed in a dry air environment, showing a range of 5-10% RH. Both surfaces reacted differently to the external stimuli, and the data detailing this is shown in Fig 4.8.

Note: All samples are washed (mild rinse with DI water) before wettability assessment. Samples referred to as washed or unwashed relates to pre storage.
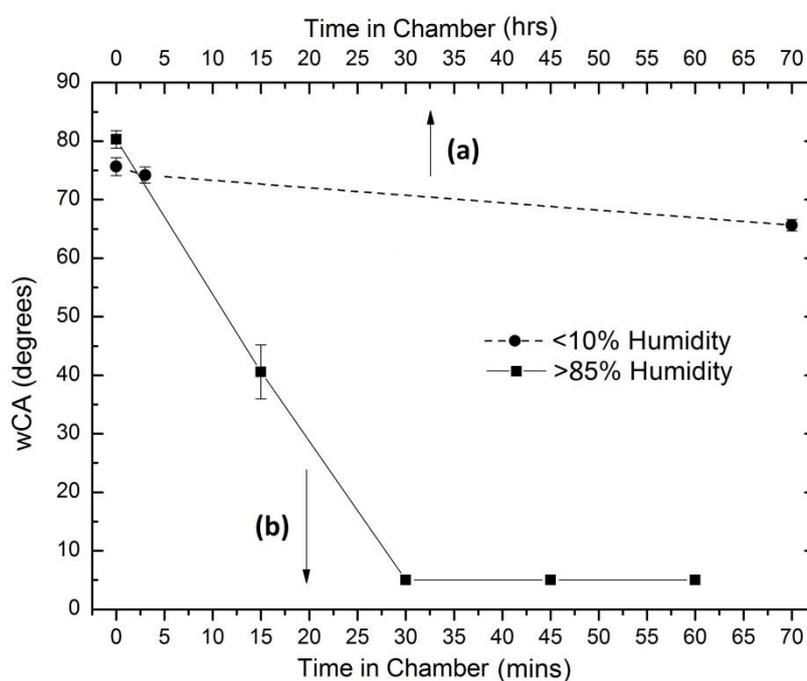
Figure 4.8: Wettability control of TEOS/AA surface using two separate environments

As can be seen from Fig 4.8, the process of wettability manipulation is highly dependent on the presence of water vapour. The rapid drop in water CA of the >85% RH sample shows the alteration of the properties of the filmswithin the space of 30 minutes, whereas the 'dry' experiments water CA remains almost unchanged after upwards of three days. Once the soft film is rinsed away, the water CA remains more resilient to change brought on through natural processes, showing different changes in water CA depending on environment. These changes are assumed to be primarily a product of mild hydrolysis and polar reformation on the surface [79], [101].

As Fig 4.8 alludes to the substantial influence water vapour has on the surfaces, a secondary experiment to this affect was performed. To gain an understanding of the controllability of the surface alteration, with respect to RH manipulation, a set of experiments were performed employing 3 specific RH values. These RHs were 80%, 60% and 40%, and water CA measurements were taken hourly. This data is shown in Fig 4.9.
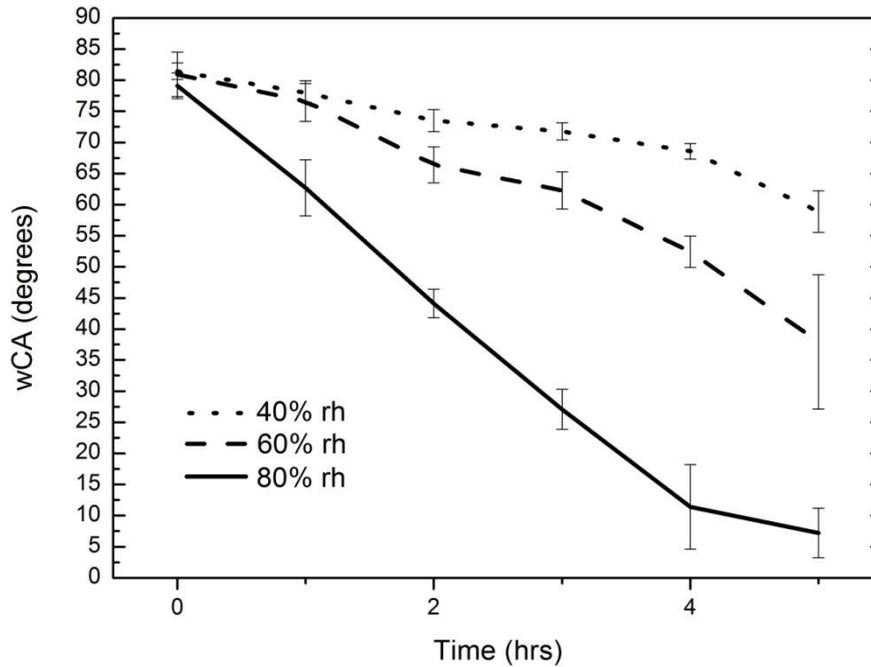
Figure 4.9: Wettability profile of surfaces stored under different humidity's

As can be seen once more, the higher humidity environments allow for more rapid changes on the surface, following the trend of the previous data. Unfortunately the turbulent nature of the airflow can be damaging to the surfaces, as the soft layer exhibits visible wearing under the gaseous turbulence due to its weakly bound nature. With this data however there is clear precedence that shows films can be manipulated to controllably exhibit a water CA range of roughly 80– 5 degrees.

A constantly shifting water CA is however counterproductive. Therefore a follow-up experiment was performed to assess the best environment to stored samples in, with the intension of retaining the water CA throughout the timeframe. The water CA stability of washed and unwashed films in different environments is shown in Fig 4.10.The 4 environments chosen are; Open bench (B), nitrogen (N), vacuum (V), and '*cured*' (C). The cured samples refer to heat curing films (at 70°C) for 24 hours before storing under vacuum for the remainder of the experiment. The washed samples are chosen to represent films that

have been cured previously by humidity interaction. Unwashed samples are used to contrast these results.
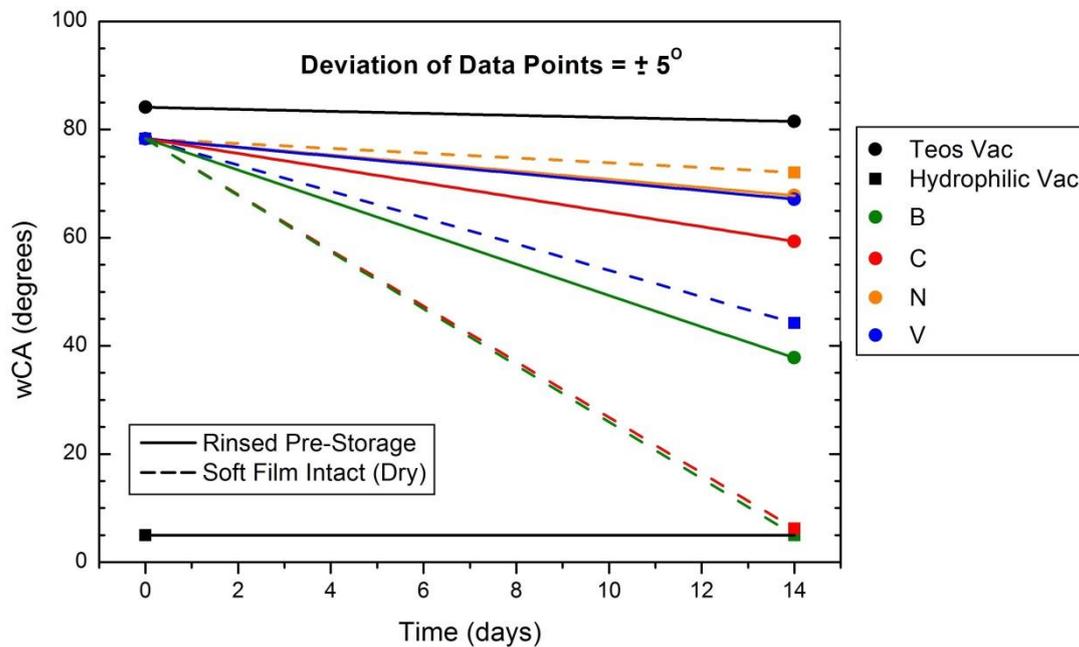
Figure 4.10: Water CA stability of surface (both washed and unwashed) stored in several environments over a period of two weeks

Fig 4.10 shows how the surfaces react to the different external stimuli of their respective environments. The most stable films, with respect to retention of original water CA (washed before storage), are the nitrogen and vacuum. This was expected due to the low water vapour presence. The nitrogen environment may be preferential in future iterations of the curing process, as passive evaporation of the water in a vacuum is likely a slower process than drying of the slide in an actively arid environment. Although the oven employed for curing was measured as retaining a RH percentage of less than 10%, the heat appears to speed up the process of water CA reformation. Samples stored on the bench show the largest drop of both washed and unwashed water CA, again as was expected due to the RH range in the lab varying between 38-50% over a 24 hour period.

The effect which increased temperature has on the films reformative properties was considered external to the primary experiments and was not investigated further in this work. It is worth noting however, that the heat-cured films present the largest water CA difference between washed and unwashed samples. It is assumed that the heat curing of the film does in fact stabilise the surface layer to a degree, hindering the surface reformations. The presence of air and water vapour during the initial incubating period ($\approx$1hr) is considered the

71

contributing catalysts to the drop in the unwashed films wettability. This method of storage is therefore considered flawed in its current state.

A duplicate experiment was performed using the V(washed, soft layer removed) process to show the reproducibility of the surface manipulation. This method of post deposition curing was chosen as there are fewer variables involved, i.e. nitrogen storage involves loading process and a longer time exposed to ambient air. The samples were washed immediately after deposition and stored in a desiccator directly after spin drying. The desiccator was unopened for the duration of the experiment ensuring no contaminants or water vapour is present. Other post processing methods suffer from excess environmental interactions compared to this method, and are thus less controlled. Although this effect is likely not drastic for some of the other methods, the rinse and vacuum seal process is chosen as the most controlled and manufacture worthy. The result of the two separate sets of experiments (performed on samples deposited several weeks apart) is shown in Fig 4.11.
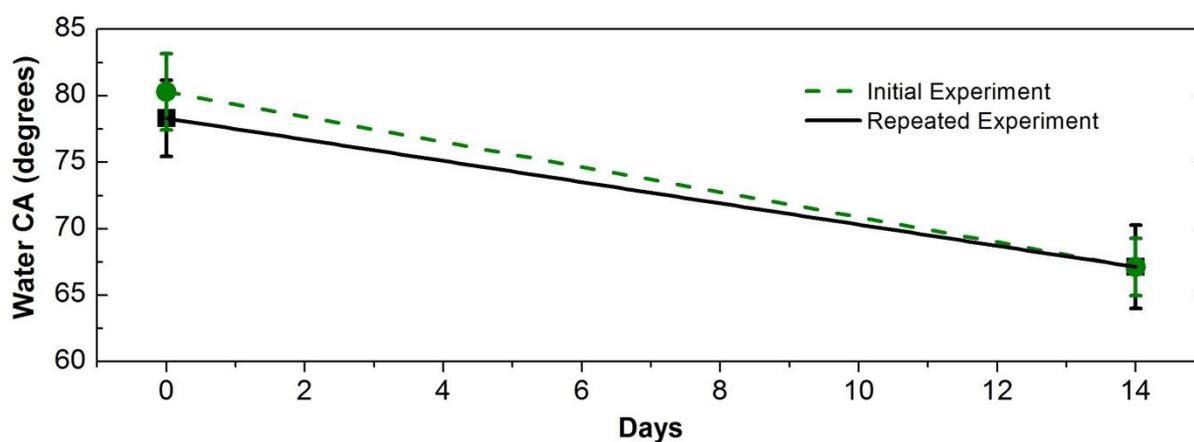
Figure 4.11: Longevity assessment of two TEOS/AA deposited films displaying matching final water CA

As can be seen from Fig 4.11, the post processing of the film can be tightly controlled if appropriate facilities are in place to closely control the affecting factors. To assess whether the water CA will also stabilise on the unwashed samples, as opposed to continuously drop until highly hydrophilic, another experiment was performed. This time the V (unwashed, soft layer intact)process was chosen. The reason for this being again that the vacuum represented the most stable environment experimentally speaking. Also the unwashed sample provided a larger wettability change than that of the washed sample in Fig 4.10, allowing for a potentially larger variance of final water CA. The results in Fig 4.12 show how the surface

appears to have reached equilibrium wettability as the 14 day sample shows a water CA range comparable to that of the samples stored for 41 and 43 days.
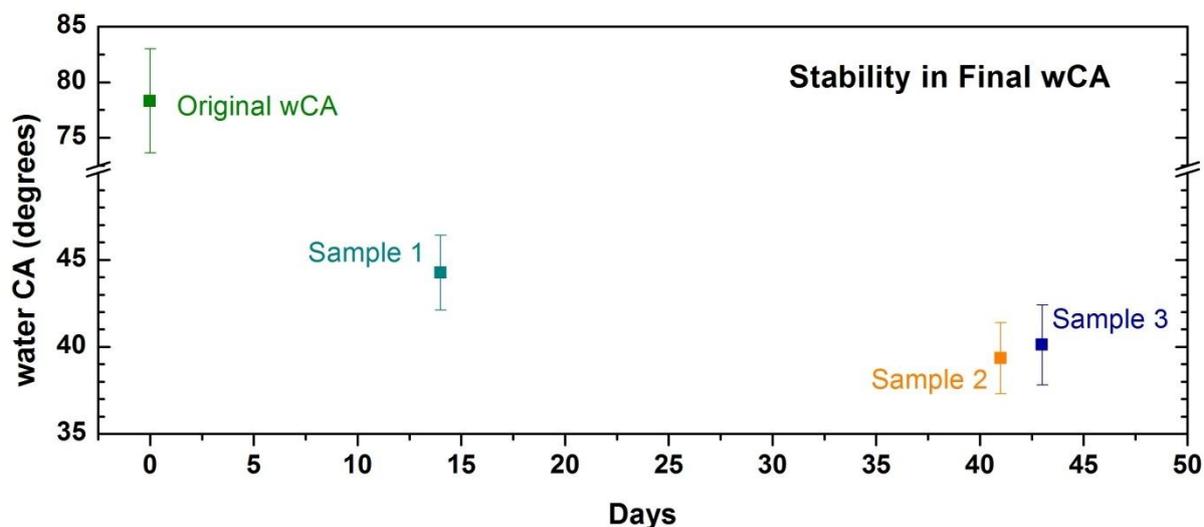
Figure 4.12: Water CA of unwashed TEOS/AA samples stored for an extended period in vacuum, showing the eventual stabilising of the wettability change

To better understand the wettability changes, a set of specific experiments was prepared. A wettability shift can be associated to a range of possible surface changes, the most likely changes in this instance being;

- surface roughness change due to chemical etching of the corrosive AA chemicals
- the polymerisation of AA molecules into a hydrophilic polyAA films
- A combination of both

To assess the validity of a surface roughness change taking place an AFM analysis was employed. By using the AFM in tapping mode (utilising a TESP AFM tip), the surfaces were scanned in several areas of 2µm x 2µm. Before this however, AFM was used to assess the roughness of the underlying TEOS film. TEOS was shown to provide a smooth under layer, with an average roughness of 0.235nm – 0.4nm, thus contributing negligible roughness to the dual process coating. The AFM images of the hydrophobic and hydrophilic surfaces are shown in Fig 4.13.

73
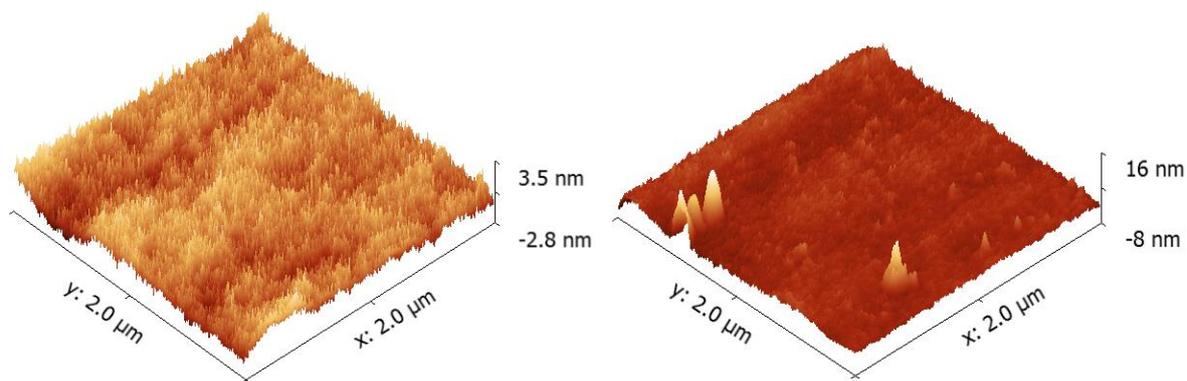
Figure 4.13: AFM image of (Left) hydrophilic TEOS/AA film and (Right) hydrophobic TEOS/AA film

By analysing the AFM data it is clear that the roughness of the surface plays no significant role in the changes to hydrophobicity. The hydrophilic sample shows an average roughness of 0.32nm - 0.4nm, while the hydrophobic sample shows 0.3nm – 0.45nm roughness. These roughness ranges are negligible and both surfaces are considered smooth.

The initial assumption for the wettability shift of the TEOS/AA surface was that the covalently bound carboxylic acid groups reacted with the weakly bound soft layer, causing polymerisation events similar to polyAA growth. The process of polyAA growth from AA chemicals is shown in Fig 4.14.
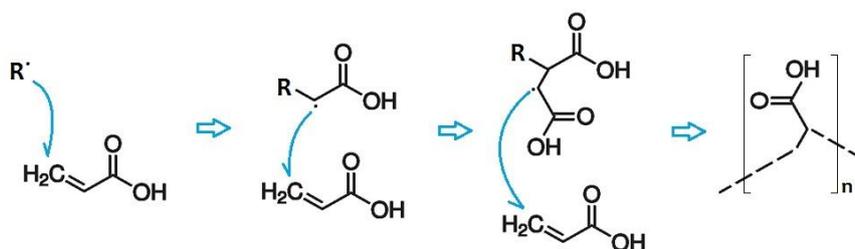
Figure 4.14: Diagram showing the polymerisation process of AA chemical, beginning with a radical interaction with the AAs methylene group causing a self-replicating cascade of further polymerisation

The soft layer is assumed to contain small chains of polyAA held together mainly by hydrogen bonding of the carboxylic acid groups. This is likely the same attraction anchoring the layer to the substrate surface, due to the large dipole moment present in the carboxylic acid. If this mode of surface alteration was accurate, it should be applicable to assess this through investigation of the individual layer thicknesses. As the 2 layers reacted with one another, the covalently bound carboxyl surface layer would increase in thickness as further

74

chains of polyAA were adopted. This polymerisation process is self-replicating, i.e. it causes a chain reaction encouraging the polymeric chain to continue growing. Therefore the thickness after an extended period of curing should provide thicker films (XRR data with water CA).

Due to the smoothness of the deposited films, XRR analysis can be employed to gain a clear data set. Assuming the film is allowed to develop the polyAA layer under curing conditions; a clear difference should be noticeable in the XRR spectra. For these experiments the TEOS deposition length was increased to 3 minutes (roughly $\approx$ 35nm) to ensure adequate peaks are present allowing a more accurate fitting. This data is shown in Fig 4.15 and 4.16.

	Hydrophobic (nm)
Acrylic Acid	1.7
TEOS	32.4
SiO$_2$	3.1
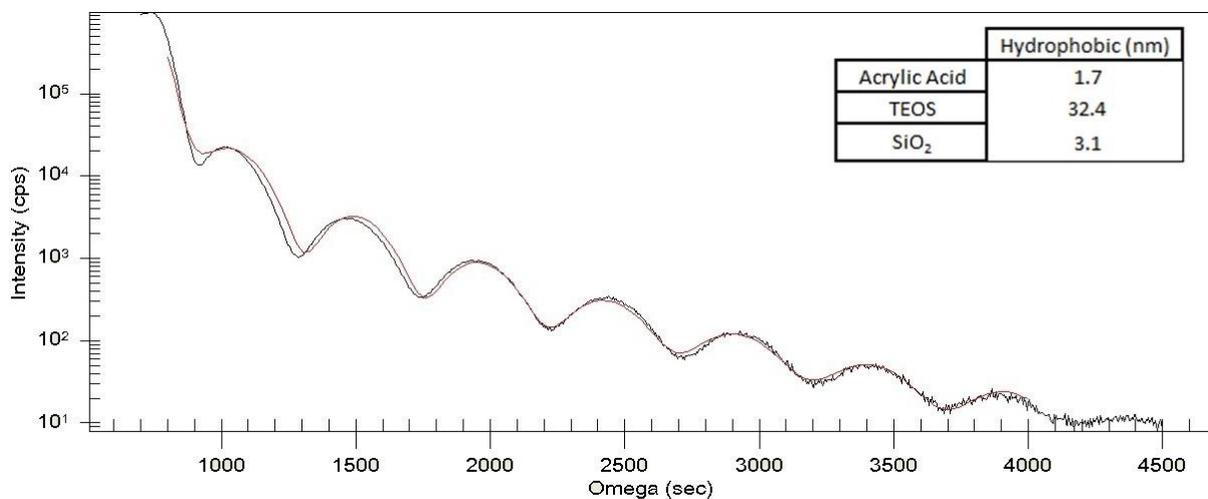
Figure 4.15: XRR fit of a Hydrophobic TEOS/AA film (water CA $\approx$ 80°)

	Hydrophilic (nm)
Acrylic Acid	2.4
TEOS	17.1
SiO$_2$	2.6
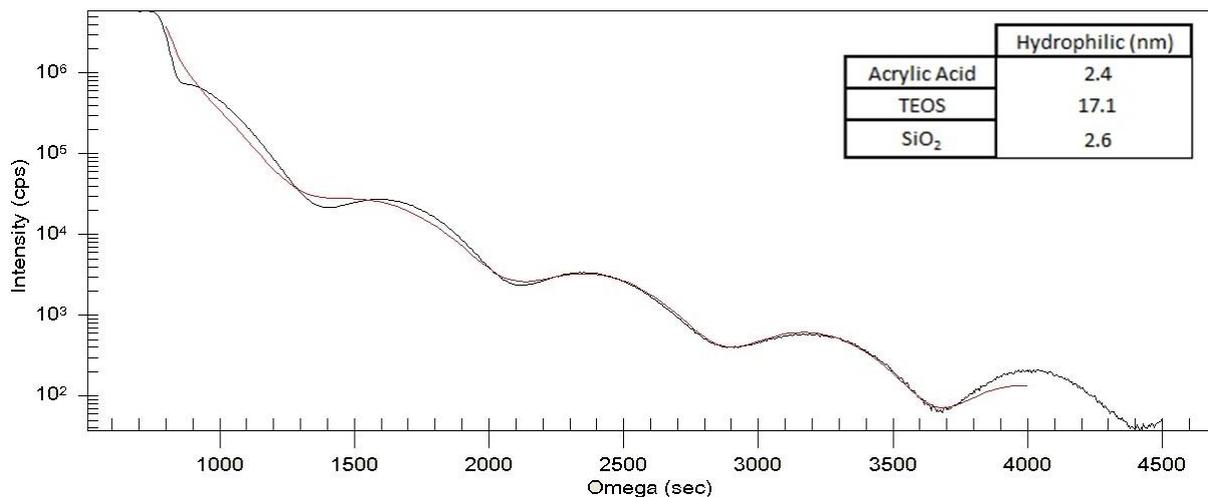
Figure 4.16: XRR fit of a Hydrophilic TEOS/AA film cured for 3 days in humidity>85° (water CA ~ 30°)

75

A clear difference can be seen in the distances between peaks of each sample, relaying to a contrast in the thickness of each film. Although the AA appears to be present and similar in thickness in both films, the underlying TEOS film appears to undergo sizeable wearing, decreasing by roughly 50%. This matches data extracted using ellipsometry (Fig 4.17 and Table 4.1). This thinning (although only moderate) is also apparent in earlier data, i.e. Fig 4.7. This shows the films left to cure undergo surface thinning, the degree of which appears subject to the thickness of the underlying film. This is likely due to the composition of the TEOS underlayer upon AA introduction, as shorted deposition cycles may serve to produce denser films with less silanol groups (similar to results shown by Zeng et al in Fig 1.5[61]).The less dense the TEOS underlayer becomes as the deposition continues, the more susceptible to corrosive wearing. TEOS samples show negligible surface wear due to washing. A small decrease is seen when stored in the wet environment, but is attributed to swelling and contracting of the polymer, which when washed removes the loose surface material.
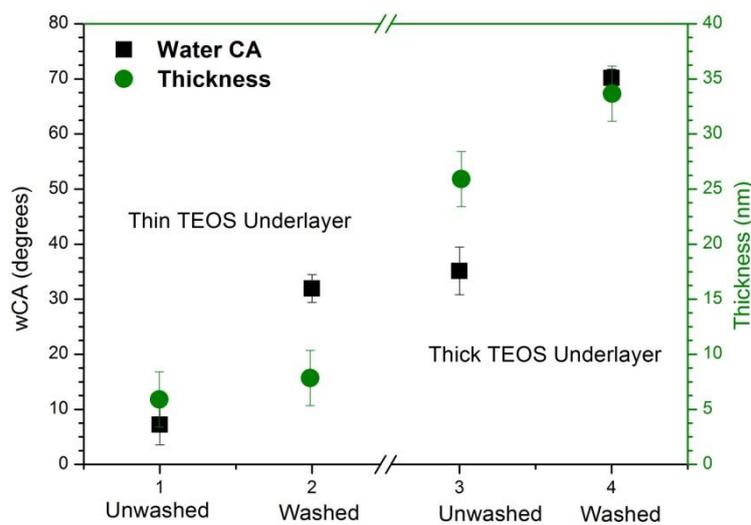
Figure 4.17: Thickness and water CA of thin and thick TEOS/AA surfaces before and after storage for 24 hours in a high humidity (wet) environment

	Original (nm)	Post Wash (nm)	Difference (nm)
TEOS (vac)	38.7	38.5	0.1
TEOS (wet)	39.5	37.3	2.2
TEOS/AA (vac)	35.5	33.6	1.7
TEOS/AA (wet)	35.3	25.9	9.4

Table 4.1: Thickness values (measured using ellipsometry) of TEOS and TEOS/AA samples pre and post storage for 24 hours in vacuum and high humidity (wet) environments

The secondary process (the growth of a thicker polyAA network) was therefore considered as having a weak effect on the surface change. The most obvious change herein is the reduced thickness of the entire film. Although the reduction is extensive in the thick TEOS/AA films, thin layers are not completely worn away (Fig 4.17). Therefore it is theorised that, as mentioned in the previous paragraph, the state of the underlying organosilicon matrix (impacted by the extended length of the deposition) is influential in the rate at which the surface wettability shifts.

It is hypothesised that the water in the environment reacts with the polyAA soft layer and the surface, causing a hydrolysing reaction that leaves the surface oxygen rich. This oxygen rich top layer, likely populated largely with carboxyl and hydroxyl groups, may appear in the XRR to be a separate layer as the density of this layer will be more like AA than organosilicon. As alluded to, the more porous and weaker organosilicon films created over longer deposition times are more susceptible to this wearing and oxidising process.

Fig 4.18 shows the influence of the underlying TEOS films, alongside a single TEOS deposition used as a reference. All samples were stored in a similar high humidity environment to show theeffect of the polyAA soft layer. Thin TEOS films develop lower water CAs than their thicker counterparts despite similar treatment. The final water CA of the plain TEOS films is closer in nature to that of pure silicon oxide than that of the original organosilicon, hinting at surface silanisation caused by the water presence.
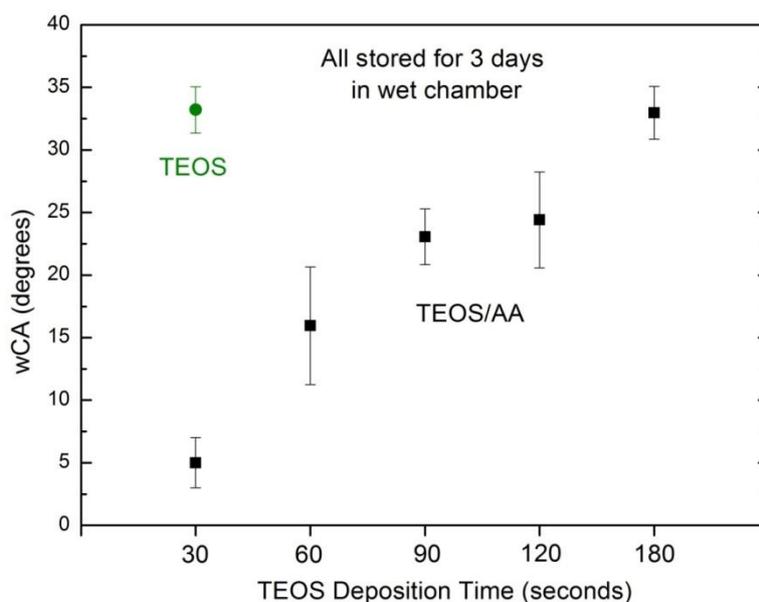
Figure 4.18: Influence of the underlying TEOS film on the final water CA of TEOS/AA samples (stored unwashed)

Further studies on the process of surface shift are required to understand the nature of the realignment. Regardless of the mechanics of the physical alteration, control has been shown. Secondary information gained from the XRR data, namely film density values, allowed for the validation of a previous assumption; that the TEOS film is primarily organosilicon in nature. The density of the plasma polymerised TEOS (ppTEOS), pure silicon dioxide and pure TEOS are shown below;

$$SiO_2 \rightarrow \quad 2.65 \text{ g/cm}^3$$

$$TEOS \rightarrow \quad 0.94 \text{ g/cm}^3$$

$$ppTEOS \rightarrow \quad \approx 1.8 \text{ g/cm}^3$$

The density of our plasma polymerised TEOS (ppTEOS) lies between the 2 extremes of the original TEOS molecule and a pure SiO_2 matrix. This density measurement is also in close proximity to that predicted in section 3.3 ($1.5 \sim 1.6 \text{g/cm}^3$) using the data extracted by Valleé et al [63]. Considering the low level of dissociation apparent in the standard deposition process, it is likely the organosilicon layers deposited herein retain more oxygen than those described by Valleé et al using similar recipes. This would account for the difference in density measurement, as due to the low power plasma the TEOS monomer fragments deposit while retaining the majority of the ethanol groups. Coupling the possibility of surface etching and silanisation events, the film appears rich in both carbon and silicon, creating a more ductile film (compared to high purity SiOx films) which should resist negative deformations seen in HMDSO based depositions (see Fig 4.4).

To attempt an elemental analysis of the surfaces, each sample was scanned on an FTIR spectrometer. Although the AA layers are thin it was hoped that some data could be gained from the FTIR system with regards to the surfaces elemental composition. This data is shown in Fig 4.19.
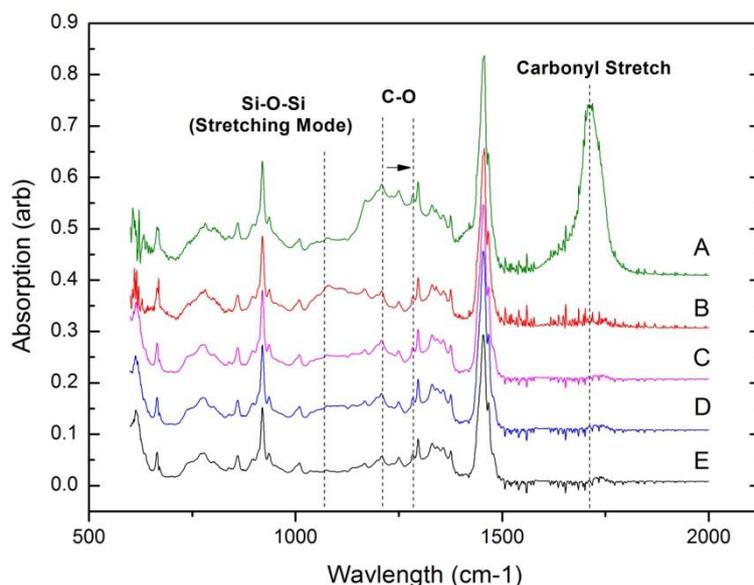
Figure 4.19: FTIR waterfall data showing 5 samples scanned in the range of 600 – 2000 cm⁻¹

Fig 4.19 shows data for 5 different samples which are as follows;

A – Standard TEOS/AA deposition unwashed (maintaining soft layer) ≈ 70nm

B – 1 minute TEOS deposition ≈ 12nm

C – Hydrophilic TEOS/AA deposition ≈ 7nm

D – Hydrophobic TEOS/AA deposition ≈ 7nm

E – Untreated Zeonor® Slide

Due to the thin nature of the hydrophilic and hydrophobic surfaces the peaks relating to carboxylic acid groups show little variation from the plain Zeonor®. However a slight increase in the Si-O-Si stretching mode appears in both samples, matching the same larger peak present on the plain TEOS deposition. Assuming the TEOS layer makes up the bulk of the film we can estimate that the AA layer, although present, is too thin to measure accurately. The unwashed deposition, retaining the softly bound layer, shows the presence of large amounts of carboxylic acid groups with the combination of peaks for both C-O and C=O. This shows a film comprising a thin carboxylic acid matrix at the surface interface, matching data put forth before these experiments.

XPS measurement of the coating was employed to generate a more detailed elemental analysis. After FTIR showed little differentiation between the hydrophobic and hydrophilic

surfaces (and system availability), it was considered unnecessary to scan both types of film. The uncured hydrophobic film (washed directly after deposition) was therefore chosen as the subject of the experiment. As no reasonable signal was gained through the FTIR scanning relating to carboxylic groups on the TEOS/AA films, a secondary TEOS/AA process was created. This process was based off the idea of increasing the deposition power of the AA cycle, with the aim to remove the soft layer development and instead create a more heavily crosslinked and covalently bound carboxylic matrix. In the first sample (a) the standard deposition was run (10 Watts AA cycle), and in the second (b) the power was increased (50 Watts).

A power of 50 W was chosen as a second set point due to similar works in AA deposition carried out by Vilani et al [75]. Therein, 50 W depositions were shown to increase the primary carboxylic acid group densities (shown in Fig1.9). Although deposition chemistries differ, it was predicted that a similar increase in carboxylic density would occur. This process alteration allowed for a layer formation retaining higher levels of the carboxylic acid film after washing due to a larger degree of crosslinking on the surface. Powers above this were ignored considering the data gathered by Ricciardi et al [78], wherein ppAA is shown to display large changes in surface characteristics when deposited at powers above 50 watts (see Fig 1.10). This was considered a by-product of extensive breakdown of the AA monomer.

The films deposited at 50 watts allow for a comparative assessment of the standard deposition. The new process exhibits a larger peak directly related to carboxylic acid groups on the surface. This data is shown in Fig 4.20.
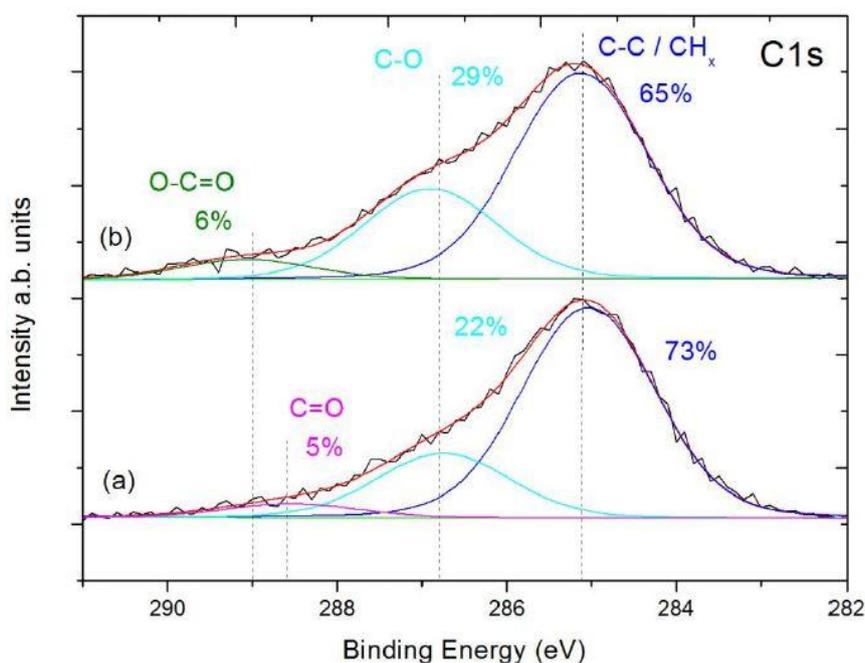
Figure 4.20: C1s spectra of samples (a) and (b) showing the various associated peaks (paper in preparation)

Both samples (a) and (b) were rinsed before scanning. As can be seen from the comparison between the two samples, the standard deposition (a) does not display a specific peak relating specifically to complete carboxylic acid groups. Instead the C=O peak encompasses the COOH (O-C=O) binding energy range, much like the way the COOH peak dominates the C=O peak in the second sample (b). This hints at low levels of the AA film present on the surface, as predicted. The presence of C=O and C-O bonding does however highlight the constituents of a polymerised AA film. The C-C and C-O peaks can mostly be attributed to the organosilicon underlayer ($SiOxC_YH_Z$) as the X-Ray probes to a depth of roughly 7nm. The secondary process appears in this experiment to deliver a more stable carboxylic acid film, removing the soft polyAA growth and therefore the possibility of curing via the previous water based method. This deposition process is therefore chosen as a more appropriate process for surfaces used specifically in high density binding experiments.

4.3.2 – Investigation into the Specific Binding Capacity of TEOS/AA Films

Although the surface wettability is an important factor in the tailoring of the thin film, the original aim was to generate a high density of carboxylic acid groups on the surface for the purpose of biological interaction. An experiment was designed to quantify the density of these groups after deposition. Both hydrophobic and hydrophilic surfaces were tested.

81

Toluidine Blue (Tolonium Chloride) is a cationic dye that shows a high specific affinity for carboxylic acid groups. The experiment was adapted from similar experiments performed in work by Drews et al [142] and Sano et al [146]. By first developing a calibration curve using standard dilution methods, an equation was generated into which all subsequent UV-Vis data could be incorporated. The equation is as follows;

$$molecules\ per\ nm^2 = (1 \times 10^{16}\delta - 1.05 \times 10^{14})/\alpha$$

In this instance α represents the area of the coated flat surface of the substrate (nm^2), and δ represents the absorbance of the solution containing the toluidine blue released from the surface, measured by UV-Vis. The number of molecules per nm^2 was calculated on various surfaces and is shown in Fig 4.21.
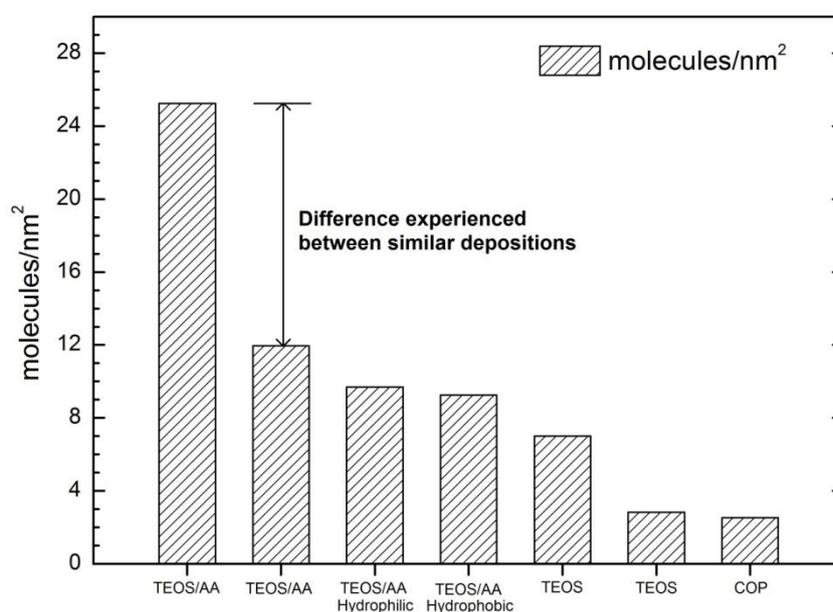
Figure 4.21: Toluidine blue staining results of different TEOS/AA and TEOSsurfaces

Due to the low sensitivity of the scanner used in the work, and the inaccuracy of the equation provided by the calibration curve at low absorbance values, this method of carboxylic acid group quantification was considered not sensitive enough. It did however provide a clear contrast between untreated and treated substrates, displaying the presence of intact carboxylic groups on the surface. Although Zeonor® was employed as a baseline; the plain TEOS sample was used as the true background assessment. The reason for this is that the thin AA layer may well not completely encompass the TEOS matrix, allowing for chemical interaction with the organosilicon layer. The hydrophobic surface shows a lower

concentration of available carboxylic acid groups, this is however a negligible difference considering the limits of the UV-Vis spectrometer. TEOS/AA films created using the secondary process were considered similar, but the results are starkly different further proving the inaccuracy of the toluidine blue method of analysis.

In place of the toluidine blue experiments, direct protein immobilisation was chosen as an accurate method for detection of the presence of carboxylic acid groups. EDC/NHS coupling can be used to create a zero length covalent bond between an amine and a carboxylic acid group (see Fig 2.15). EDC/NHS coupling of single Cy5 labelled proteins, and single Cy5 labelled DNA, was performed on plain TEOS (as a background) and carboxylic acid functionalised surfaces. As fluorescent measurements are highly dependent on the systems used during scanning, and taking into account possible photobleaching of the dyes during experimentation, quantification of the density of carboxylic acid was not possible. It was predicted that due to the lack of carboxylic acid groups on the TEOS deposition the proteins and DNA would not adhere, i.e. low signal received from plain TEOS samples for both protein and DNA with and without EDC. This however was not the case as shown in Fig 4.22.
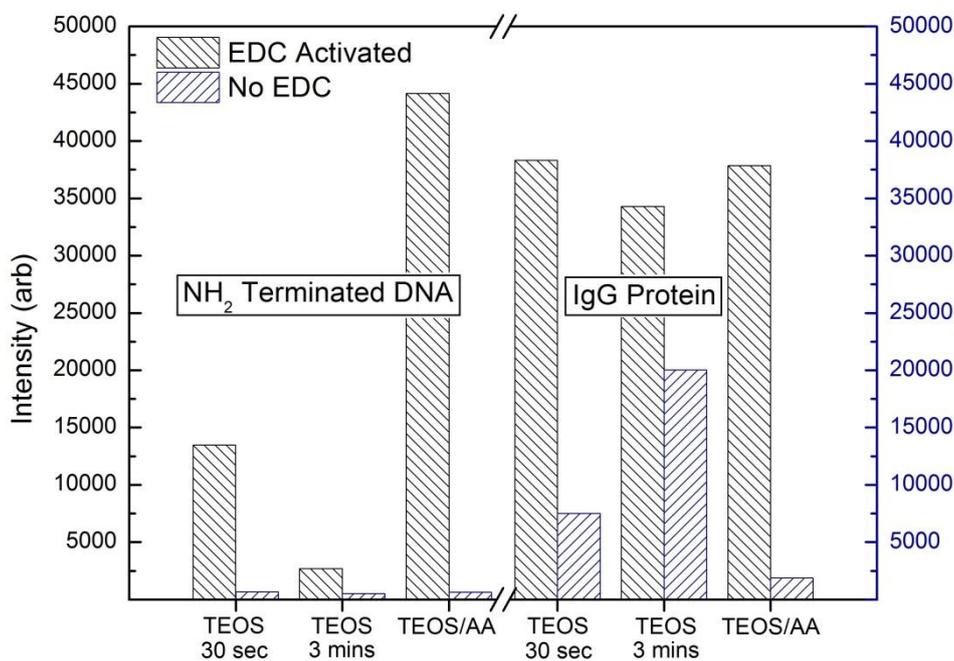
Figure 4.22: Specific and non-specific binding of Cy5 labelled DNA and IgG protein on TEOS and TEOS/AA films

83

IgG protein appears in these experiments to be highly attracted to the plain TEOS surface, more so in the instances where a linker is present. DNA however appears more selective, and shows low signal for the thicker TEOS layer with the linker present. It was discovered that proteins may bind through a secondary mode to an organosilicon surface, specifically between COOH and OH groups interacting. Everaerts et al [147] put forth that carboxylic acid groups can form ester links with hydroxyl groups (-OH groups) in the presence of EDC/NHS. The TEOS surface is also likely within the water CA range that these proteins find attractive, increasing the likelihood of migration to the surface [73], [100].

As the DNA is exempt from these issues, this phenomenon was explored further using only the amine terminated DNA. As the DNA showed moderate adhesion to the thinner TEOS films, it was theorised that coalescence of the film may be an issue, as oxygen plasma treated COPs can generate surface carboxylic acid groups also [128], [145]. Any areas of the slide not completely masked may then provide an area for adhesion. The results of this experiment, shown in Fig 4.23,support this explanation.
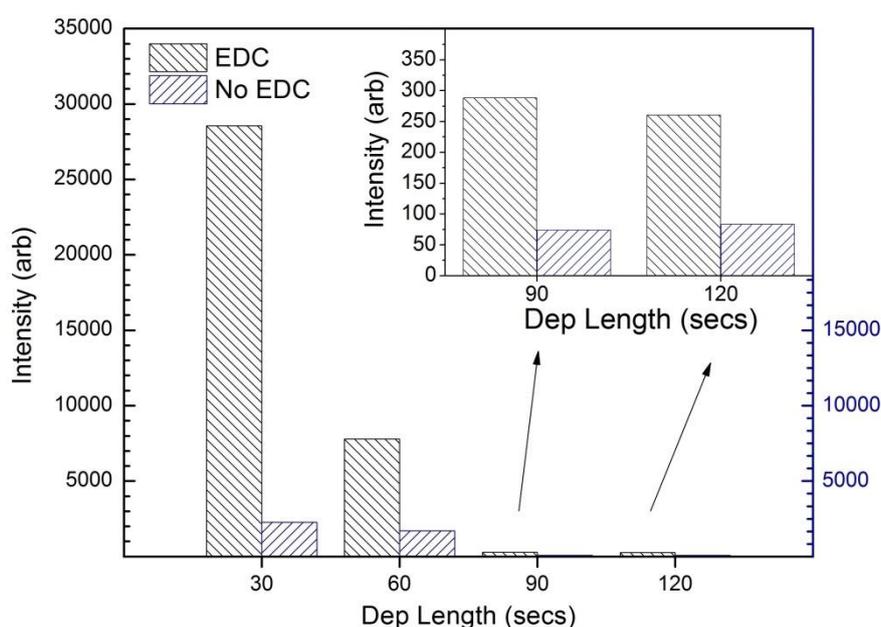
Figure 4.23: Binding of NH$_2$ terminated DNA to plain TEOS film deposited on Zeonor$^{\circledR}$

As can be seen in Fig 4.23, both the EDC and non EDC activated DNA lose their ability to adhere to the surface once a specific thickness is passed (90 seconds relates to ~20nm thickness, see Fig 4.3). This information is important as non-specific adhesion of biomolecules to the surface could ruin the potential of diagnostic systems adapting these surfaces. The TEOS/AA films (see Fig 4.22) however have shown, for both protein and

DNA, to have the lowest non-specific binding and highest specific binding. Experiments carried out early on in this work lend credibility to this result. Hydrophilic TEOS/AA surfaces developed using the standard deposition recipe in the initial stages of the wettability control experimental work often showed high degrees of surface specificity, displaying negligible non-specific surface adsorption. This relates to the primary aim of the TEOS/AA surface, that only through activation does immobilisation of targets take place, as referred to by Coyle et al [144].

It is theorised that the hydrophilic nature of carboxylic acid surfaces contributes to the repulsion of non-specific binding. As proteins dislike surface with low water CA [100]the carboxylic layer protects the underlying organosilicon layer from prolonged contact with the proteins. Only through the use of a linker can proteins then become adhered to the surface in a manner which is not easily washed away afterwards. A secondary hypothesis is also that the AA monomer covalently binds to areas on the TEOS film that are active after the TEOS deposition cycle. Without the AA to passivate these areas, they could possibly retain a certain level of attractiveness to proteins, i.e. hydroxyl group's form as the surfaces takes up hydrogen's.

Coupling this knowledge of the attraction of DNA and proteins by TEOS, a final recipe for the TEOS/AA surfaces was developed specifically for use in biomolecular adhesion studies and applications. It is acknowledged that the TEOS/AA film shown in Fig 4.23 shows little non-specific binding despite being created with a 30 second TEOS deposition, but to ensure as little non-specific adhesion as possible a new recipe is needed. This recipe is as follows;

	Argon (sccm)	Oxygen (sccm)	TEOS	AA	Pressure (mTorr)	Time (sec)	Power (Watts)
Pretreatment 1	50				200	30	50
Pretreatment 2	50	50			200	150	150
Venting						10	
TEOS Stabilisation	0.1		Open		200	60	
TEOS Deposition	0.1		Open		200	90 (30)	25
Venting						10	
AA Stabilisation	0.1			Open	150	30	
AA Deposition	0.1			Open	150	15	50 (10)
Venting						10	

Table 4.2: Second TEOS/AA PECVD process specific to robust and carboxylic acid dense surfaces for adhesion of target biomolecules (changes to standard recipe shown in orange)

Using the new recipe another set of experiments were performed and are shown in Fig 4.24. This graph shows the difference in the binding potential of the new film, compared to the previous recipe.
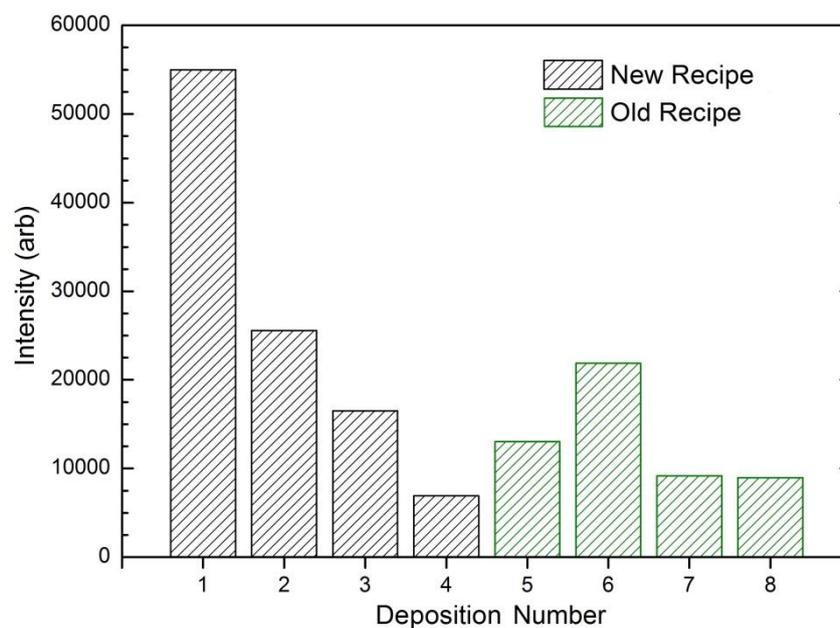
Figure 4.24: DNA and protein spotting using EDC (and EDC/NHS) linkage on TEOS/AA films

Although some of the inconsistencies in the experimentation results may be contributed to the fluorescent scanner (which has become unstable) the new recipe shows large variation across several slides. Although promising, and for the most part matching if not beating the previous recipe, this process will require some fine tuning to generate reproducible results and replace the previous process. Coupling the increased resilience to non-specific adsorption with these results however show the new recipe to be an improvement over the previous iteration.

4.4 - Application of Surfaces to Practical Devices

The TEOS/AA surface has previously been published as a surface that retains high levels of specificity[144], i.e. biomolecules do not adhere in the absence of a linker.An experiment was performed to quantify the level of non-specificprotein adhesion (no chemical linker) to the surface of the TEOS/AA films under development. In unison with this experiment a physical blocking agent, bovine serum albumin (BSA), was used to determine the need, if any, for physical blocking of the PECVD surface to reduce non-specific adsorption. This data is shown in Fig 4.25. For this experiment Cy5 labelled α-hIgG was spotted on the surfaces of the carboxylic acid substrates, with no EDC/NHS linker present.
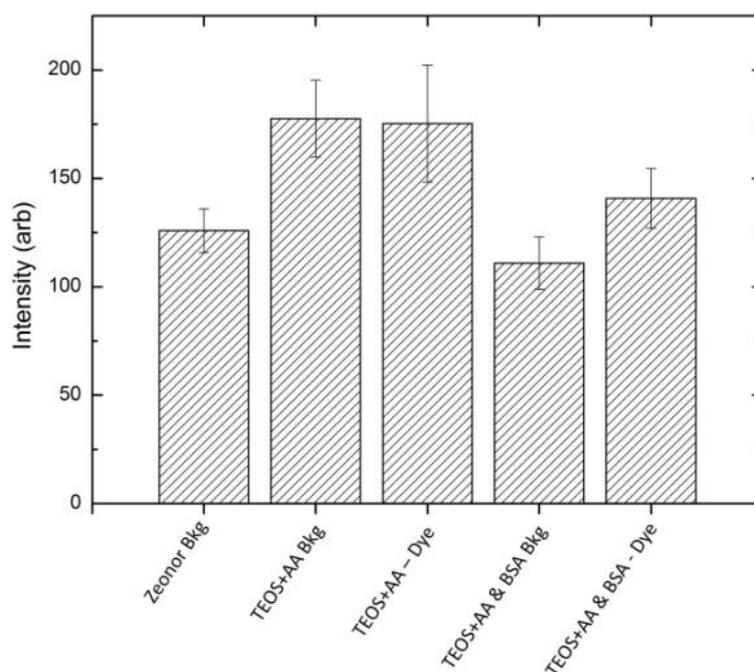
Figure 4.25: Fluorescent analysis of surfaces spotted with Cy5 labelled α-hIgG, compared to the background (Bkg) levels

From Fig 4.25we can safely assume that proteins do not typically adhere to TEOS/AA films. The BSA coated TEOS/AA films however show an increased intensity from the non-protein treated slide. This is negligible however, and the physical blocking of the BSA is seen as unnecessary while performing an immunoassay experiment on TEOS/AA surfaces.

Continuing on from this work, a protocol was developed to perform a complete sandwich immunoassay on the surface, which is to be compared to a standardised plate assay. The details of the assay experiment are described in section 2.3.5. A set of sealant gaskets similar in dimension to the wells of an assay plate were employed to perform the experiments, the idea being that the same scanner can be applied to both platforms, reducing the potential discrepancies. With the gaskets, microscope slides can therefore have several independent areas (wells of 150μL) assessing varying concentrations of antigen (in this case hIgG). Using the 96 well plate as a standard a set of calibration curves were created. These results are shown in Fig 4.26.
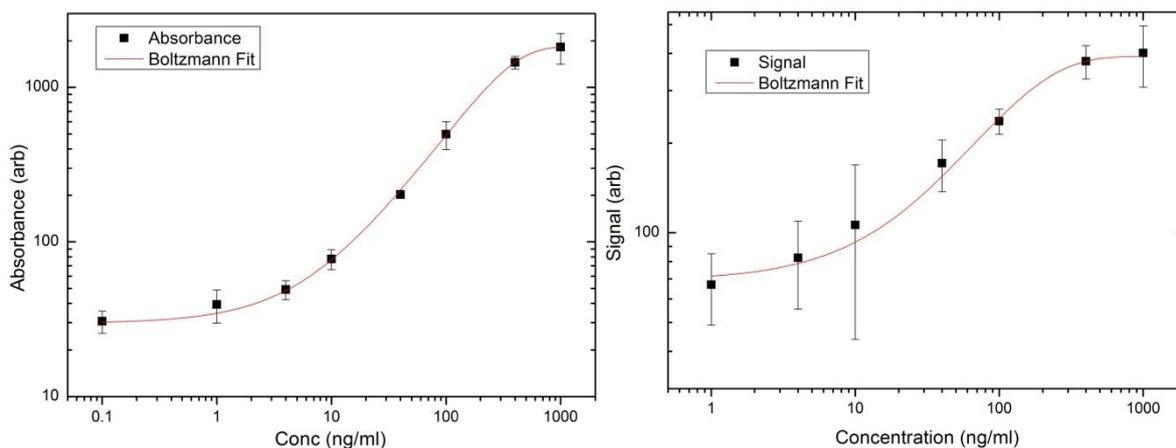
Figure 4.26: (Left) Assay performed on a 96 well plate and (Right) assay performed on a collection of PECVD treated surfaces

As can be seen from Fig 4.26, both the PECVD surfaces and 96 well plate show good S shaped calibration curves. This shape of the PECVD treated assay calibration curve shows that the surfaces are more than capable of being used in assay experiments. The PECVD surfaces however appear to possess larger error bars. There are a number of contributing factors to this problem; the 2 most important of these being slide to slide comparability and the limited size of the gaskets used leading to limited space on each slide for triplicate procedures (only 16 wells per slide using gaskets). In effect the gasket system was seen to be insufficient to provide a set of data as refined as that received from the plate experiment. Only 3 gaskets are available for experimentation, contributing a max of 48 wells per experiment.

Surfaces deposited and cured to exhibit hydrophilic properties were employed in the development of a novel assay. The project involves the combination of a platelet based analysis of human blood samples, and soft lithography of a specific array of binding sites onto a Zeonor® sheet. Soft lithography refers to a process of 'stamping' a set of polymeric structures on a surface. These structures are typically in the low micrometer scale, and allow for repeatable structure placement on a range of surfaces thanks to a singular master being employed.

A surface intended for use in soft lithography however must display satisfactory surface characteristics. It was initially assumed that the hydrophilic nature of our surface would allow for good adhesion of the stamp. Initial experimentation compared the stability of the surface wettability compared to a commercially available hydrophilic coating. The hydrophilic

chemical coating in this experiment was purchased from Hydromer Inc. The exact surface composition of the coating is unknown as the information is proprietary. The coating (referred to as 7-TS-13) is described as a '*thin film of hydrophilic polymer that reduces the contact angle and prevents formation of water beads*'. The hydromer coating however was found to be easily removed during a mild wash phase (3 x 10 minute stirring in H_2O/PBS), and was therefore unsuitable to the assay development. The TEOS/AA film however remains hydrophilic despite several washing phases. Data showing the change from the initial wettability of the hydromer coating to a more COP like water CA is shown in Table 4.3.

Hydromer Film

	CA (degrees)	Err (degrees)
wCA pre wash	11.9	1.5
wCA post PBS wash	76	3.7
wCA post H_2O wash	75	2.9

Table 4.3: Hydromer coating stability post washing phase

A defining characteristic of a suitably adhesive surface is the Surface Energy (SE). Surfaces with high SE are attributed with allowing for stronger bonding of adhesives. Typically hydrophilic surfaces display a high SE as it is closely related to the surfaces wettability. The SE of the TEOS/AA films is shown in Fig 4.27.
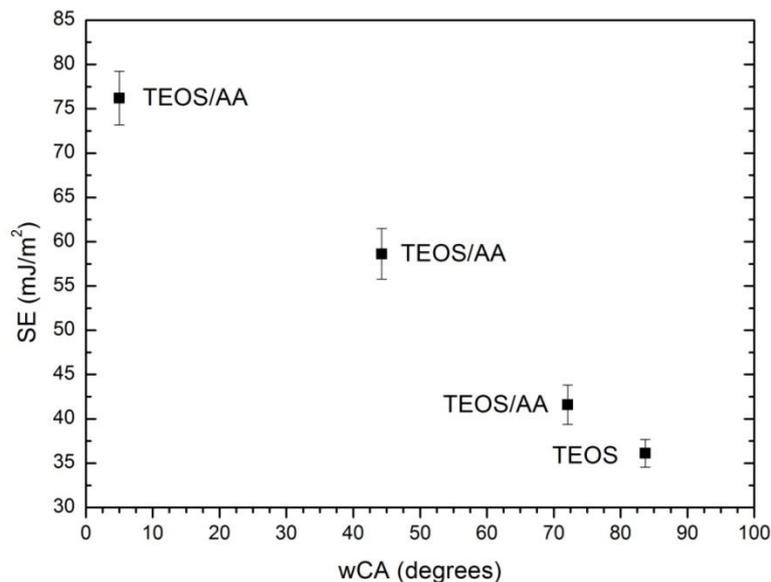
Figure 4.27: Surface Energy versus water contact angle, hydrophilic cured surfaces display the highest surface energy

89

The hydrophilic surfaces display the highest SE, and are therefore considered the appropriate surface for soft lithography. The stability of the surface and lack of hydrophobic recovery allow for extended storage of deposited samples for use in this assay. For these reasons, the TEOS/AA films were employed for use in a novel platelet detection assay device being developed in house. For this experiment 6μm diameter spots of fibrinogen/BSA-Cy3 were microcontact printed using PDMS stamps ontoAPTES (silanised through vapour deposition on an oxidised substrate) treated Zeonor® and hydrophilicTEOS/AA treated Zeonor®.Assay printed array is shown in Fig 4.28.
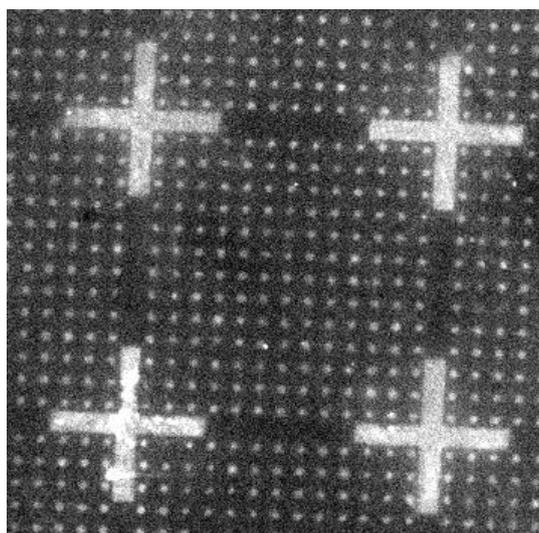
Figure 4.28: Assay array printed onto TEOS/AA film

All surfaces were blocked with 1% BSA for 30 minutes at room temperature and rinsed with PBS prior to incubation with blood. To calculate platelet adhesion, whole blood (1 mL/slide) was added to the protein array in a petri dish and placed on a rocking platform at 35oscillations/min for 30 minutesat room temperature. The slides were washed with PBS and the platelets were fixed with 3.7% paraformaldehyde. The platelets were stained using a primary mouse anti-human CD41 (a heterodimeric integral membrane protein) antibody (1 μg/mL) for 1 hour at room temperature. The slides were washed with PBS and stained using a secondary Alexa Fluor 488-labelled goat anti-mouse IgG antibody (1μg/mL) for 30 minutes at room temperature. The slides were washed with PBS and distilled water for imaging. Platelet adhesion was calculated using a custom-designed computer program, which enables protein dot quantification by colour coding.

TEOS/AA hydrophilic surfaces and APTES (deposited via vapour silanisation) were compared for their binding and specificity. This data is shown in Fig 4.29.
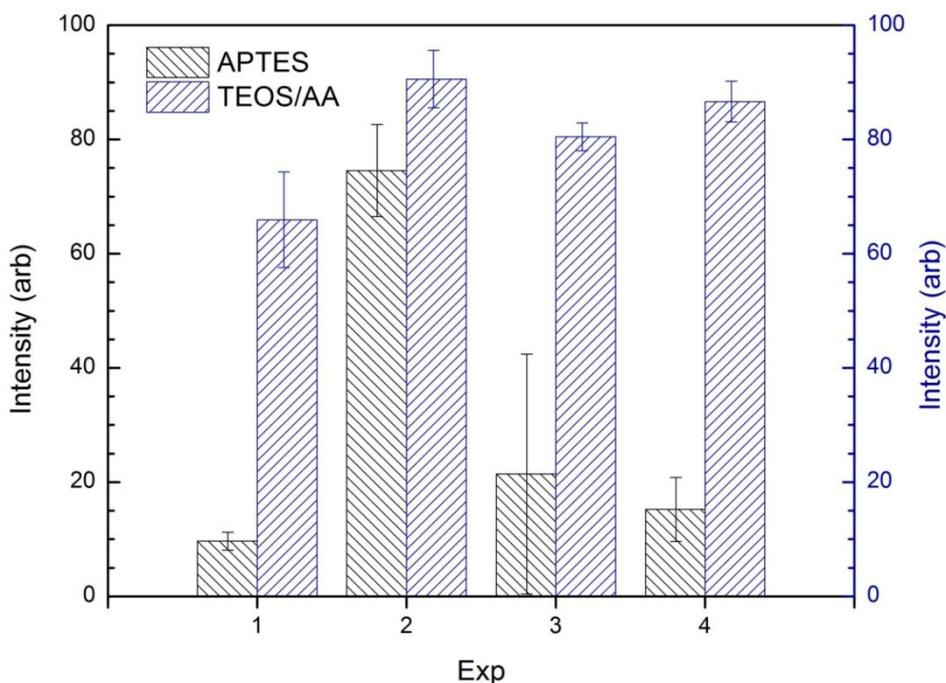
Figure 4.29: Intensity readings from platelet assay using both TEOS/AA and silanised APTES films

As can be seen from Fig 4.29, the TEOS/AA film in every instance generates improved detection of platelets. Adhesion of the patterned fibrinogen/Cy3 printed layer was also found to be improved, creating a more reliable method of micropatterning. Overall the TEOS/AA has shown to be a perfect match for assays based on micropatterning of immobilising agents.

4.5 – Conclusions

TEOS/AA films have been shown to be efficiently processed in a manufacture worthy plasma deposition system. Novel control over the surface wettability has been shown. By effectively treating the TEOS/AA surfaces post deposition a specific range of water CAs has been displayed. Influencing factors have been investigated, but further study is required to assess the physical processes and final surface composition. These films, unlike some chemical coatings available for purchase, show robust retention of surface characteristics. Alterations to the plasma recipe have also been shown to increase surface density of carboxylic acid groups, essential in the use of biomolecular adhesion via chemical linkage.

Chapter 5

Results Section 2 – Dual and Single Layer Amine Coated Surfaces

5.1 – Introduction

In tandem to the development of carboxylic acid based surface chemistries, work has been aimed at developing surfaces based on the amine functional group, NH_2. Like the carboxyl groups, amine groups can be used to immobilise detection elements such as DNA or proteins. Specifically in this work, two separate processes have been developed and characterised.

Firstly, a single stage deposition employing the chemical aminopropyltriethoxysilane (APTES), an amine functionalised organosilicon. Although naturally stable and highly suitable for chemical deposition, it does possess a negative attribute for PECVD processing, namely the low VP. Although still applicable through methods detailed further in this chapter, a secondary process was developed to alleviate the negative qualities of the APTES precursor. This process involves a sequential deposition employing TEOS and a small organic compound, allylamine (AL). The favourable VP and similarity to the process previously developed using the AA monomer made this a suitable choice. Both the APTES and TEOS/AL films will be contrasted and assessed in this work, and a simplified example of the films and the process of film growth are shown in Fig 5.1 and Fig 5.2.
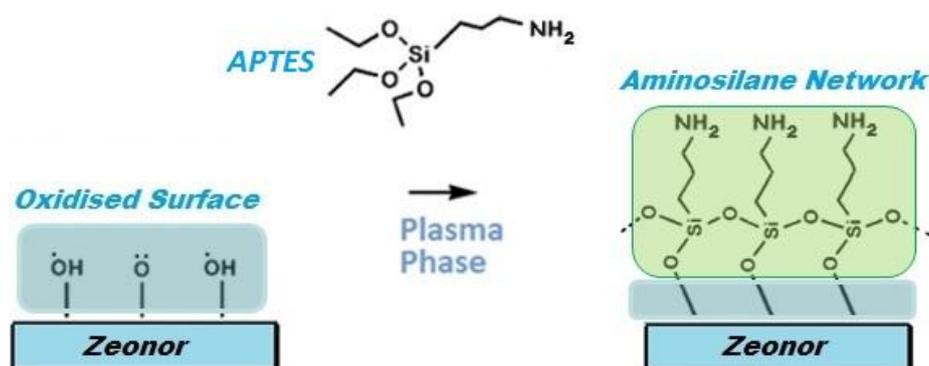
Figure 5.1: Diagram depicting a single monomer (APTES) deposition of an amine rich organosilicon film
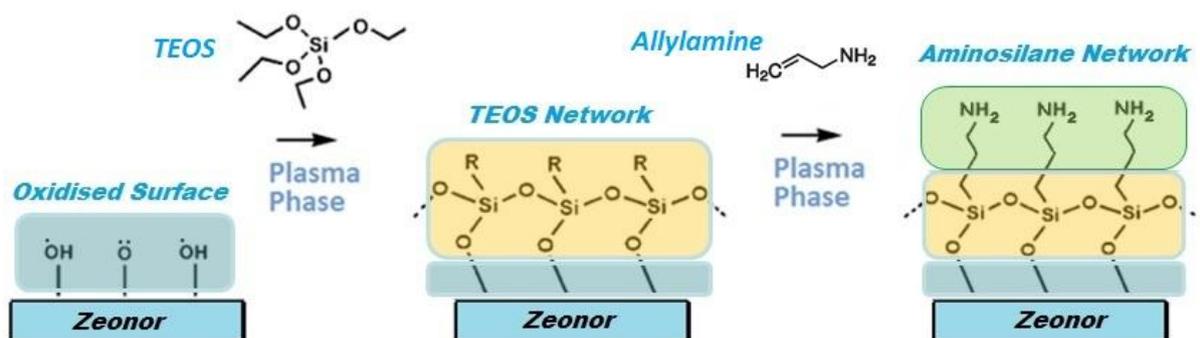
Figure 5.2: Diagram depicting a sequential TEOS/AL deposition designed to closely relate the composition of a single monomer APTES deposition

The results presented in this chapter relates to data published in several papers[9], [107], with several more publications submitted awaiting peer review. Specifically this research follows on from work shown in previous publications from our research group [102], [103], [106]. The key scientific findings are as follows;

- APTES can be deposited via a manufacture worthy plasma deposition system
- TEOS/AL films offer a more applicable PECVD alternative to APTES due to the differences in chemical properties (i.e. VP)
- APTES and TEOS/AL films offer improvement over the CLD of APTES via silanisation on an oxidised surface

5.2 - Process Control and Development

The APTES precursor is shown in Fig 2.3 to have the lowest VP of the chemicals used in this work. Using the data gained from the Clausius-Clapeyron equation it was estimated that the precursor must be heated to a minimum of 52°C before the vaporisation threshold is reached. As shown in Fig 3.8 however, higher temperatures must be employed to counteract the influence exerted by the accompanying input gas. A temperature of 95°C was chosen as the initial heating point, matching the apparent VP of AA at room temperature, i.e. VP ≈ 4000mTorr. VP of AA was chosen as it was the only other functional monomer used in the PECVD at the time of experimentation, and the hope was that similar functional densities would be attained. A secondary temperature of 115°C was chosen, matching again the higher VP displayed by AA previous (@ 40°C), i.e. VP ≈ 15000mTorr. The subsequent thickness of films deposited by these temperatures is shown in Fig 5.3;
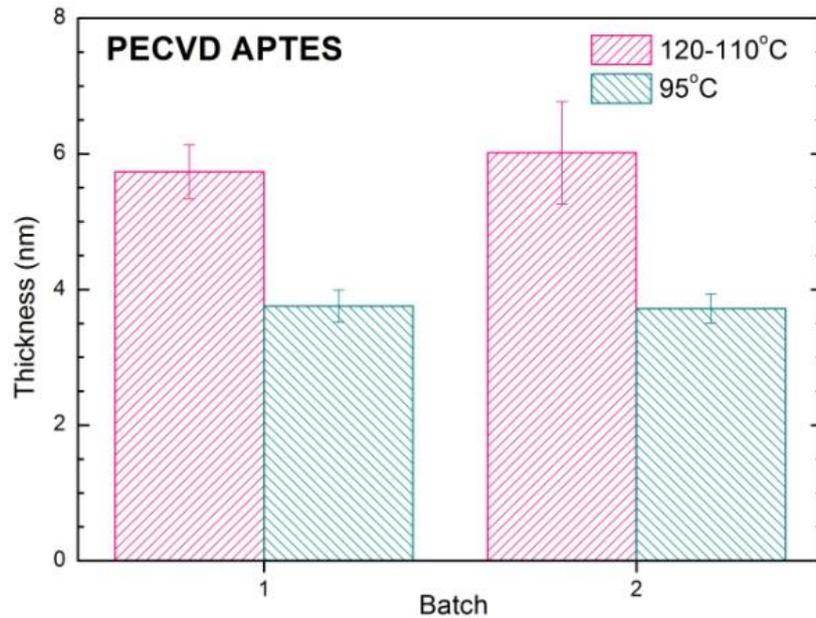
Figure 5.3: Temperature influence on film thickness (directly related to vapour flow)

Assuming depositions below 4nm to be negligible, as per Fig 4.2, the $95^{o}C$ temperature point was deemed ineffective. Therefore all subsequent depositions of APTES in this work, unless otherwise stated, were ran at a temperature of $120^{o}C$ to encourage sufficient vaporisation. APTES depositions, unlike TEOS, AA and AL depositions, are run alongside argon gas. The reason for the difference in processing parameters is the quenching effect of the singular APTES monomer at the low powers chosen for film deposition. Argon is required to both lower the density of the gaseous medium of the chamber to allow for plasma ignition, as well as supply extra electrons to maintain a steady dissociation process.

Using the standard APTES PECVD recipe described in section 3.3, three samples were prepared to test the resistance of the films to aqueous solution. Both thickness and water CA were measured before and after 15 minutes of washing in water. Slides were dried with nitrogen before testing to ensure minimal interference from absorbed water in the film. These results are shown in Fig 5.4;
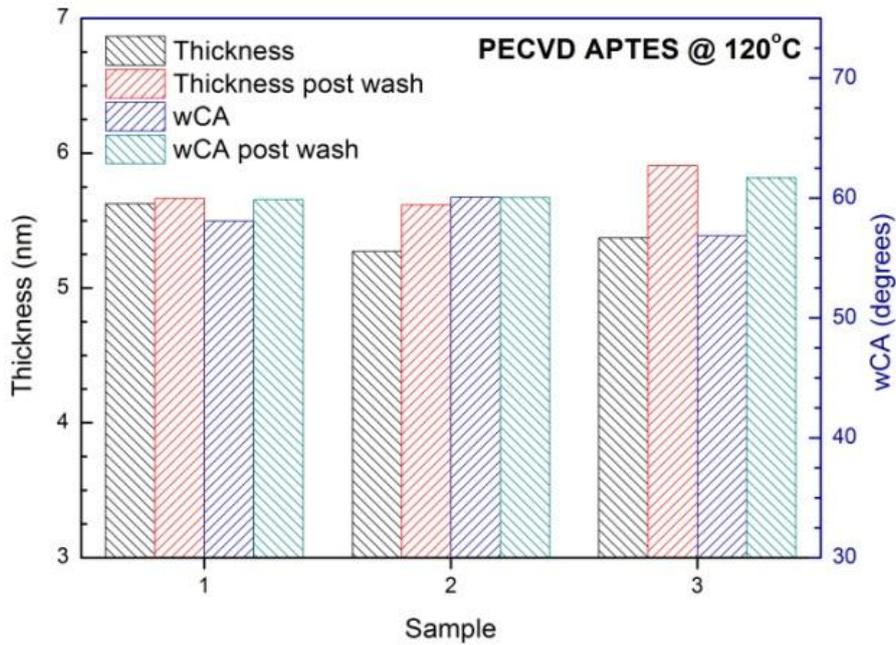
Figure 5.4: Robustness assessment of PECVD APTES films washed in water for 15 minutes

Using the standard APTES deposition recipe once more, but with varying deposition timescales, a linear plot is shown to be produced, showing how the film grows linearly depending on the exposure time. This data is shown in Fig 5.5, and the following equation can be used to predict film thickness should a thicker layer be necessary;

$$Thickness = 0.044(Time) + 3.54 \qquad \text{(Eq 5.1)}$$
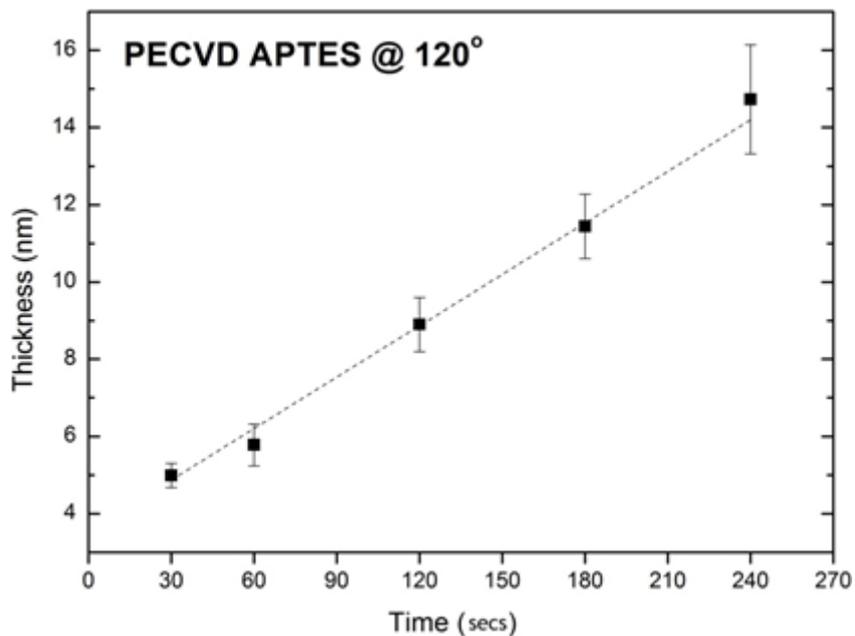
Figure 5.5: Thickness versus time of PECVD APTES

Compared to the TEOS monomer, APTES films deposit at a slower rate. This is most likely due to the reduced concentration present in the chamber, and the added reverse etching caused by the argon heavy process. The thickness of the film is important as there is an increase in binding potential associated with thicker layers, shown in Fig 5.6.
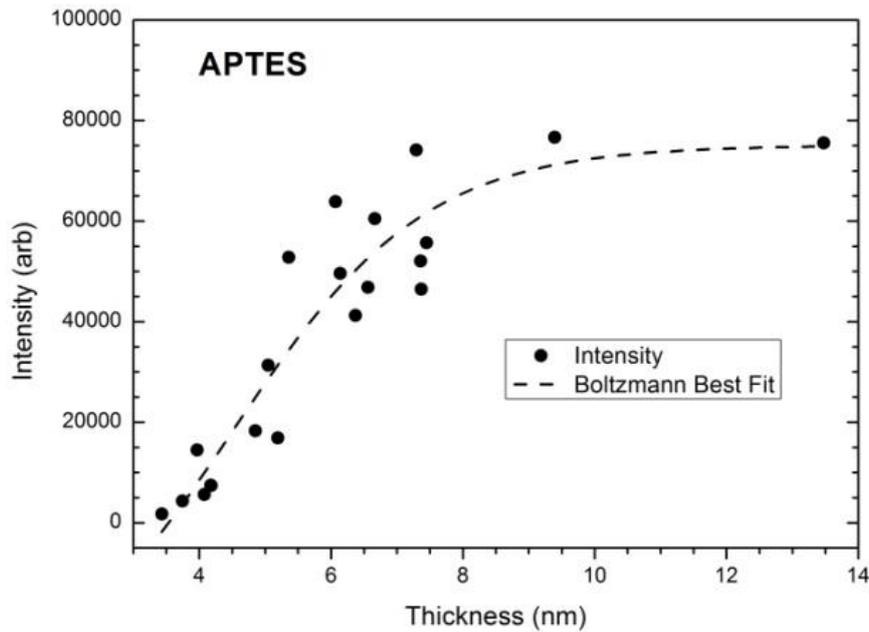
Figure 5.6: Fluorescent intensity versus film thickness

Films exhibiting thicknesses close to or below 4nm are shown to have an inadequate protein binding potential (directly linked to amine density).In this case, as the film is singular in composition, the layer is considered partial and nucleation leads to the growth of islands. Thicker films are shown to display satisfactory protein binding potential, as islands coalesce into a coherent isotropic film. From the results in Fig 5.4, all films will be deposited at a thickness of >6nm. The reason for the increased adhesion is an increased amine concentration as the bulk film reaches surface amine saturation. Increase of film thickness beyond a certain point (6-10nm) does not serve to further increase binding potential of the surface. As the optimal amine density of the process has been reached the subsequent plasma species migrating to the surface cover existing amine groups.

Although a circular shower head is used to disperse the monomer vapour during plasma deposition, the position of the substrate with respect to the central area of the chamber may have an impact on the characteristics. To this end an experiment was performed using multiple samples in 2 separate positions on the slide holder; a central position (position

96

1)andan outer position (position 2) relative to the centre of the slide holder. These results are shown in Fig 5.7.
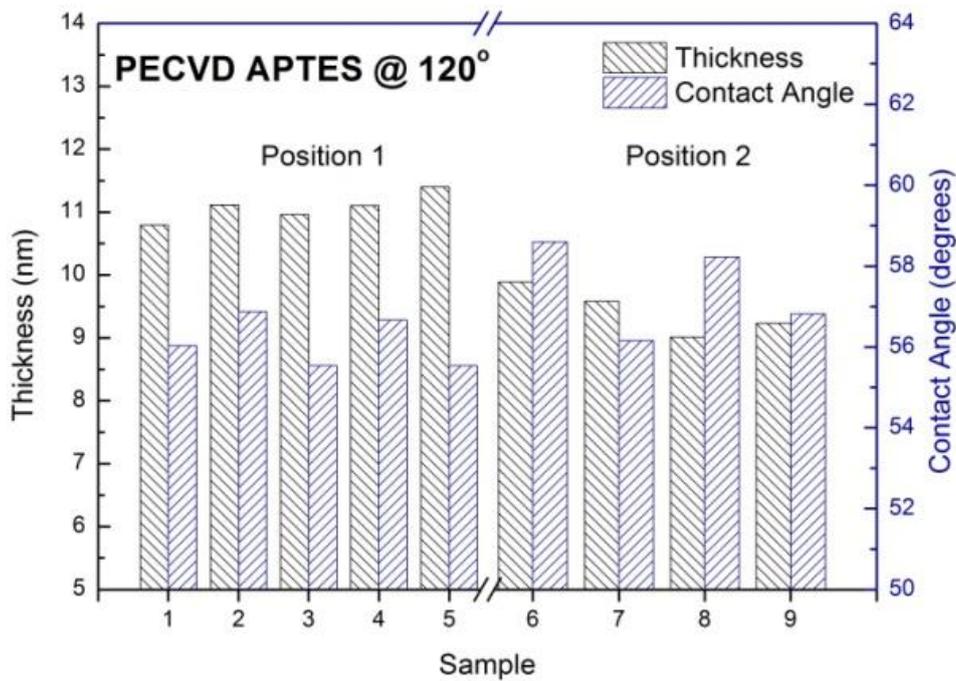
Figure 5.7: Thickness and wettability of samples placed in separate locations relative to the central chamber position

Although a difference in sample thickness is apparent, it relates to an average difference of below 2nm. Both positions generate films thicker than that of the predetermined appropriate thickness, detailing a completely functional film regardless of position. Similar water CA values are also recorded on each sample, showing the reproducibility of the surface composition from each batch. The discrepancy is likely caused by the low levels of the monomer in the chamber, and non-uniformities in the plasma (plasma edge effect).

5.3 – PECVD vs CLD APTES

APTES can be deposited in a variety of processes, but in this work CLD of APTES was chosen as the baseline to compare the PECVD films, as this was the primary method used by my collaborative research groups. PECVD deposition improves upon the CLD method in a variety of ways, from deposition time to chemical waste, making the process more manufacture capable. However the more important aspects of the filmare the physical properties and reactivity. If PECVD surfaces cannot match the biological compatibility of the silanised methods there is limited use for the process in medical device design.

Fig 5.5 was previously employed to show the controllability of the PECVD deposition thickness, using error bars to show the possible slide variation. Fig 5.8 is used to show the difference in thickness experienced across the length of a microscope slide used in silanisation. For this experiment two different deposition solutions were mixed with the intension of creating two thickness profiles.
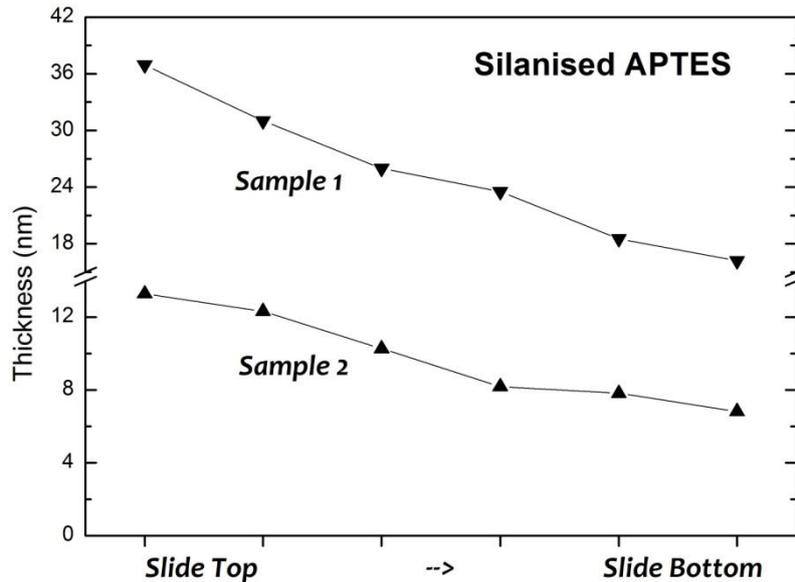
Figure 5.8: Non uniformity of single slide thickness from top of the slide to the bottom (slides stored in upright containers during CLD) – slides measure 75 mm in length top to bottom

As can be seen from the data in Fig 5.6, the silanisation method employed generates films with a large thickness profile when examining the length of the substrate. Although most likely a by-product of the specific manner in which the substrates are housed during deposition, upright in slide container, it shows a fundamental flaw in the deposition method. This flaw is assumed to bedue to the density of the APTES differing from the water/isopropanol mixture. As APTES has a density less than that of water ($0.95g/cm^3$) over time the chemicals may begin to separate, creating an uneven distribution throughout the deposition solution. This process of separation is exacerbated by the length of the deposition phase (typically >1 hour).

As shown previously, water CA and ellipsometric analysis allow for a general approximation of the quality of a coating. By employing these characterising experiments, the films can be assumed to be of an appropriate quality before more intricate biological assessments are performed. A direct comparison was performed between several PECVD and silanised (CLD) APTES films generated using different processes. This data is put forth in Fig 5.9.
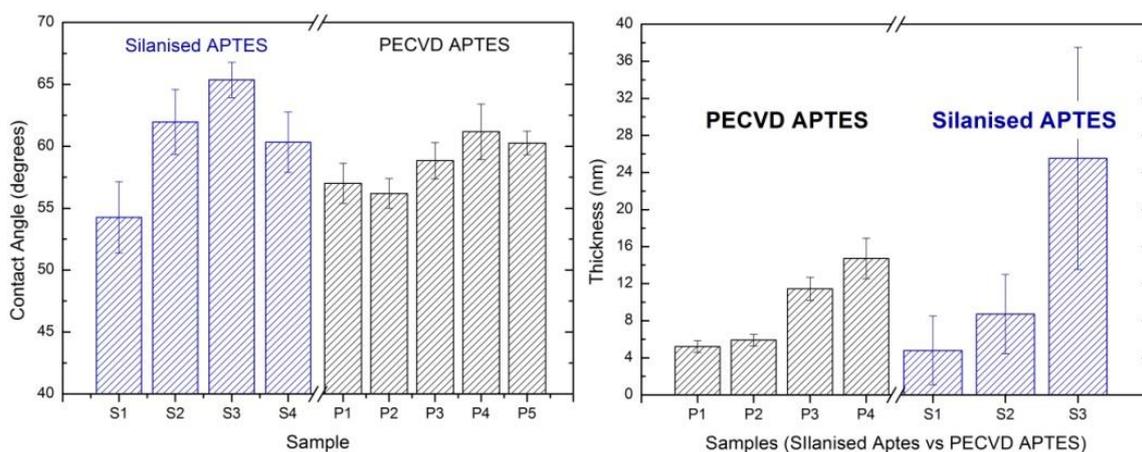
Figure 5.9: (Left) Range of water CA measured across the length of both PECVD and silanised APTES and (Right) thickness measurements of both PECVD and silanised APTES focussing on the standard error experienced by both

As can be seenin Fig 5.9, silanised APTES creates coatings with less control when directly compared to those of the PECVD process. The water CA measurements are important as although the silanised process in this work possess few advantages when compared to PECVD, systems using APTES coatings previously would have been optimised to a very specific wettability. This characteristic must be retained if ease of adaptation of the process to new devices is to be maintained.

Biological assessment of the surfaces was performed via protein adsorption studies. These studies quantify the primary amine concentration on the surfaces by means of analysis of the intensity of fluorescence post adhesion (a direct correlation to the density of immobilised proteins). An equation was created to allow for an estimation of the overall quality of a batch of APTES depositions, taking into account both the surface uniformity and fluorescent intensity. The equation is as follows;

$$Quality = ID \qquad \text{(Eq 5.2)}$$

In this case I is the average intensity of the spotted slide, and D is a correction factor generated by dividing the average slide intensity by the difference between the max and min spot intensities on the slide. Therefore the larger the spot intensity discrepancy measured (indicating non-uniformity), the lower the overall quality of the deposition. This equation was used to compare a batch of PECVD and silanised APTES films. Each batch contains nine slides, each of which were created in sets of three on differing days to remove uncertainty about the batch to batch uniformity. The results are shown in Fig 5.10.

99
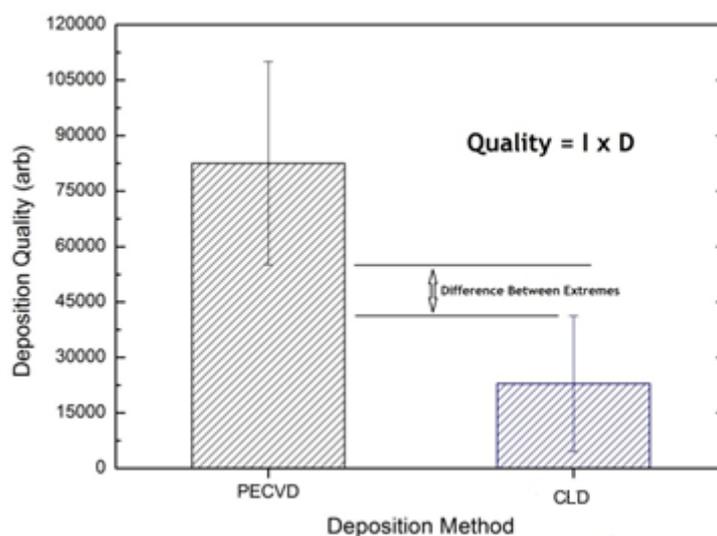
Figure 5.10: Slide quality calculations comparing PECVD and silanised APTES

Fig 5.10 shows how the PECVD depositions appear superior when compared to the in house silanisation method, with the lowermost quality of PECVD films trumping the highest quality silanised films. The reason for this relates mainly to the surface non-uniformity of the silanised slides, and the increased density of amines present on the PECVD films.

5.4 – Application of PECVD APTES Films

The PECVD films optimised in this work were used to replace silanised APTES films in the development of novel immunoassay based microfluidic devices. To this end a paper was published which showed the ability of APTES to rapidly adsorb proteins and single strand DNA (ssDNA) from solution[107]. To this end a small microfluidic device was created in which to test our coatings. The device design is shown in Fig 5.11.
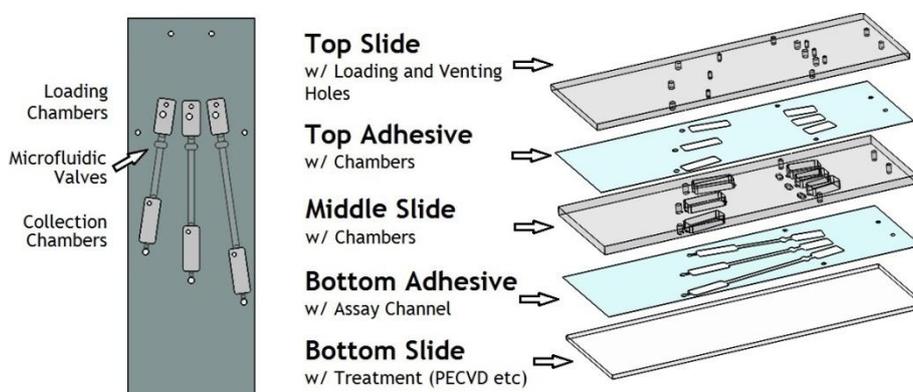
Figure 5.11: Schematic for an assessment microfluidic device used in measuring the protein adsorption of APTES films

100

Using this device and a spin stand to encourage movement of the protein and ssDNA solution through the valves, the APTES film was examined for its adsorption properties. Polyethylene glycol (PEG) and BSA coatings, alongside untreated COPs, are used as comparisons to show the lack of binding by the untreated surfaces that come in contact with the solutions. Fluid was passed through the cells at an average rate of $0.3\mu Ls^{-1}$. Experimentation involved contrasting the concentrations from the original solution and the collection chamber. This allowed for an accurate measurement of the level of biomolecular loss from the solution. The percentage of protein and ssDNA adsorption is shown in Fig 5.12. The channels A, B and C measured 13, 18 and 23mm in length respectively. Channel width remained constant for A, B and C at 1.25mm, with a height of 50μm, creating a treated surface area of 16.25, 22.5 and $28.75mm^2$ respectively.
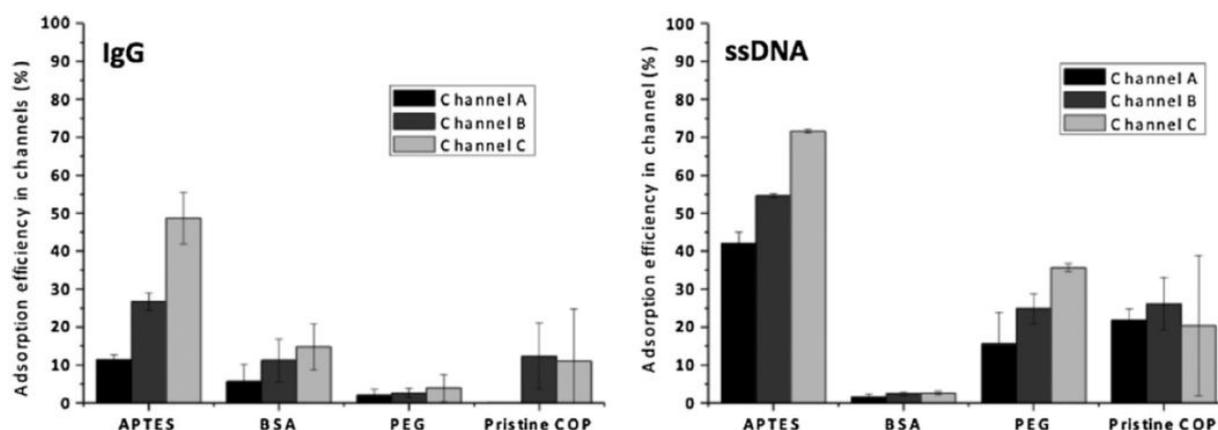
Figure 5.12: (Left) Data showing the adsorption of protein using the novel microfluidic device, and (Right) data showing duplicate experiments using ssDNA [107]

As can be seen from Fig 5.12, the APTES films attract a higher percentage of the biomolecules suspended in solution than the other surfaces, especially in the case of the longer channel with 50% and 70% adsorption of the protein and ssDNA respectively. This work helped to showcase the applicability of the APTES PECVD films compatibility with microfluidic assay devices.

Continuing on from this work the PECVD film was introduced into a novel microfluidic disc design. The disc was used as a stage for testing the applicability of a newly developed assay in conjunction with novel microfluidic components. As this technology is to be used as a point-of-care (POC) device stability and adhesive properties of the film are crucial for successful implementation. POC devices are designed to be fast and accurate diagnostic systems that are simple to use. POC devices therefore relieve some of the burden from

hospitals as they can be used by local healthcare professionals or by the user themselves. Using this disc design a set of experiments were performed and a calibration curve was created, which is shown in Fig 5.13.

These experiments involved a novel fluorescent linked immunosorbent assay (FLISA), specifically tailored to detect hIgG. The first step involves protein A adsorption on the surface. Protein A is used as an immobilising factor for the hIgG, as it naturally immobilises antibodies in a preferential orientation. Once the hIgG antibody is adhered, a biotinylated α-hIgG protein is used to bind to the hIgG. Dye linked neutravidin is then used to combine with the biotinylated protein, creating fluorescent signals where hIgG is present.
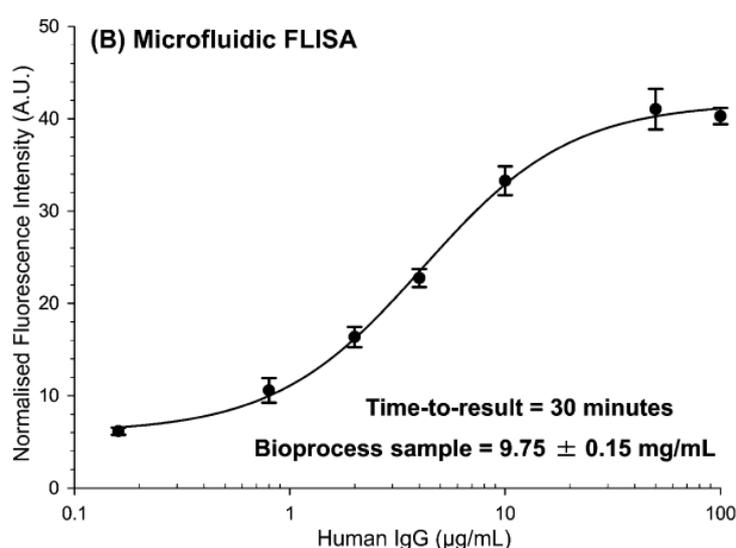
Figure 5.13: Calibration curve of novel microfluidic device with incorporated PECVD APTES film [9]

This work on PECVD deposition of APTES has proven the applicability for use in assay development, as well as the ability to be incorporated into a fluidic system (that had previously exclusively employed silanisation methods). The deposition process has proven robust and reproducible. The only detracting factor for this process is the VP of the precursor, and the need for elevated temperatures to generate appropriate vapour flow. Therefore a secondary process was developed to eliminate the workability issues of the PECVD APTES process while retaining the base characteristics that have proven valuable.

5.5 – Dual TEOS/AL Deposition

To overcome the processing downfalls of working with APTES in a low pressure system (i.e. VP issues, condensation etc.), an alternative process was developed. This process employs an organic compound called allylamine (AL) as the primary amine source for the film. Used in conjunction with TEOS, in a sequential deposition process similar to that described in section 4, the film generated is tailored to be characteristically similar to that of the APTES films. Using the standard deposition process described previously the AL film was characterised in similar fashion to previous chemicals.
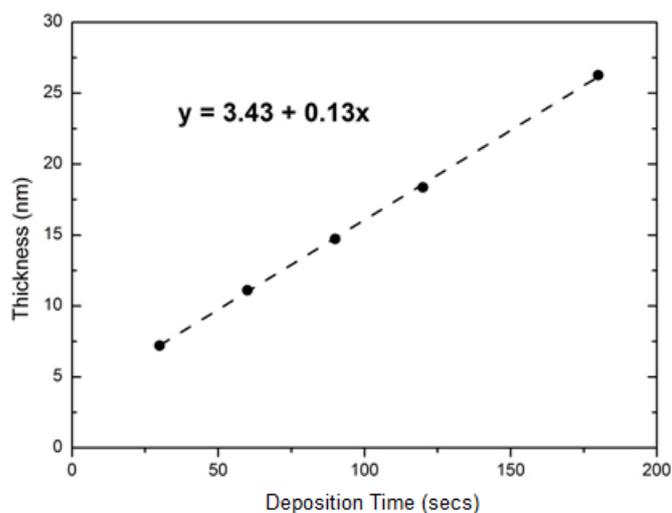
Figure 5.14: Linear thickness increase of AL thin films with respect to deposition time
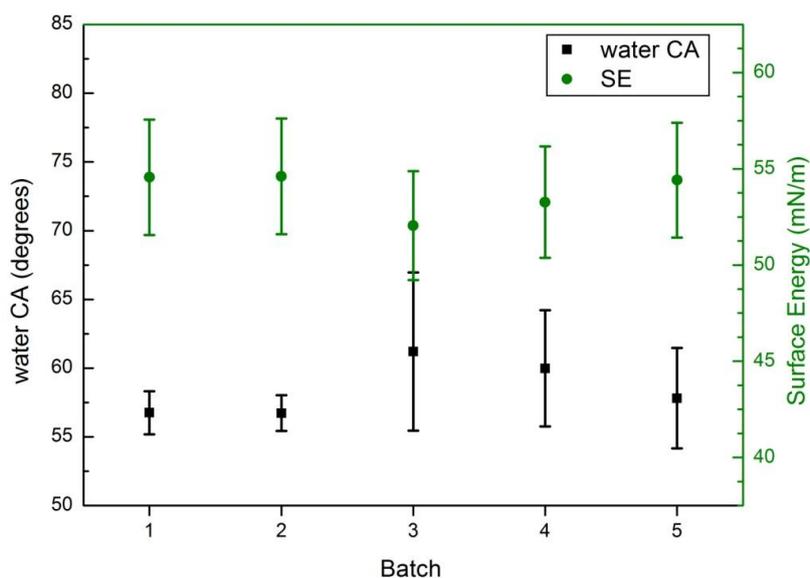
Figure 5.15: Water CA and SE of TEOS/AL dual layers; batches 1 & 2 were allowed a day to settle whereas batches 3, 4 & 5 were washed immediately post deposition

From Fig 5.15 we can see that the process of allowing the films to stabilise over 24 hours helps establish a more uniform surface, as shown by the difference in water CA deviation. Overall however the film appears to generate a surface similar in wettability to that of the APTES films. This is likely due to the predominantly carbon/nitrogen rich surfaces of both depositions.

To more directly compare the elemental composition of the two amine based films an XPS study was conducted. It is assumed that the TEOS/AL films will not present peaks specific to the organosilicon underlayer due to the AL layer developing its own polymeric layer atop the underlying silicon matrix. Like the AA monomer, two power settings were chosen for this experiment, 25 and 100 W. The reason for this is to assess if the increased power leads to inferior or superior levels of surface amines. The APTES monomer however creates an amine-organosilicon film throughout. Both XPS scans were washed and dried before scanning to ensure removal of contaminants. The APTES PECVD deposition was deposited on spin coated Zeonor® on a silicon wafer to better assess the final film state on the COP substrate.
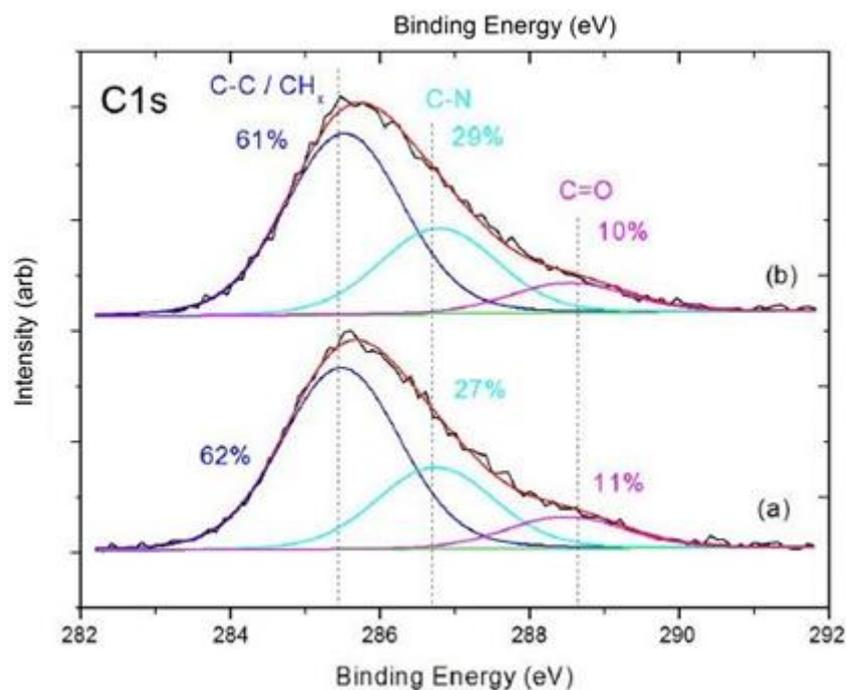
Figure 5.16: XPS spectra of PECVD TEOS/AL coatings with (a) low power AL deposition phase and (b) high power AL deposition phase
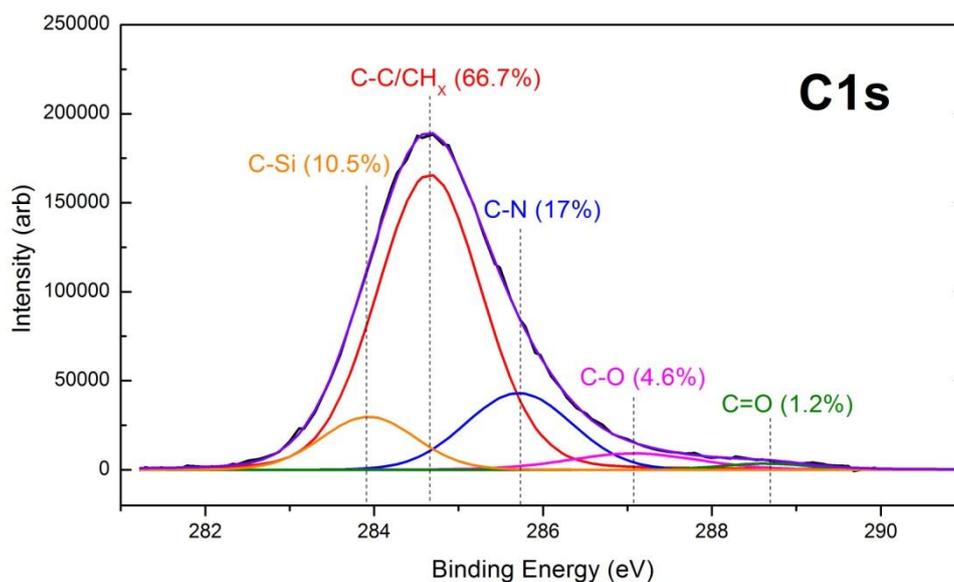
Figure 5.17: XPS spectra of PECVD APTES

One of the primary differences between both depositions is the presence of C-Si bonds throughout the APTES film. The TEOS/AL films do not possess a similar peak due to the polymerisation of the AL monomer atop the organosilicon matrix, which in turn contributes negligibly to the XPS spectra in these films. The APTES films however have the organosilicon running throughout the entire film, allowing for the prevalence of C-O peaks and C-Si peaks. These peaks correlate to the silicon bound ethoxyl and silicon-nitrogen bridging propyl groups respectively, both of which are found on the complete APTES monomer. AL therefore is responsible for generating a robust individual amine rich film atop the organosilicon, which is employed as an anchoring matrix. It is worth noting that the stability of the APTES film allows for little amide formation (C=O bonds), whereas AL films are prone to reactions with oxygen for a period after deposition.

The 2 AL films were shown to have little difference in surface composition, unlike the AA monomer shown in section 4.3.1 (Fig 4.21). This is likely due to the electronegativity difference between the carbon and nitrogen (C-N) compared to that of the carbon and oxygen in the carboxylic group, 0.49 and 0.89 respectively. This makes the bond stronger andhelps to partially negate the extensive breakdown and crosslinking experienced by the AA chemical. AL films will therefore likely retain high levels of primary amines throughout varying deposition processes.

Due to the removal of APTES from the PECVD system, owed to the improvement in processing with the new TEOS/AL combination (and difficulties in heating the APTES etc.),

a direct comparison of the binding intensity was not available. Instead the processes are compared for their uniformity of adhesion, i.e. the average intensity of the slide divided by the difference between the max and min intensity of the protein spots.
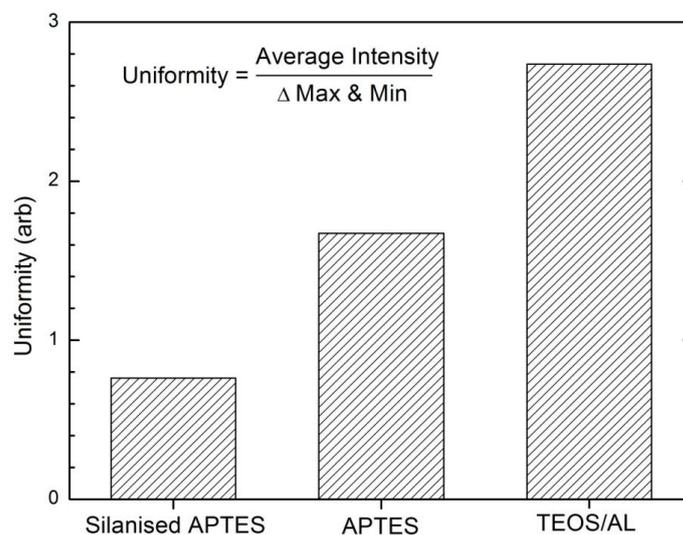
Figure 5.18: Uniformity of protein adhesion across Silanised APTES, PECVD APTES and PECVD TEOS/AL films

Fig 5.18 shows how the TEOS/AL deposition displays a better overall uniformity of amine dispersal than the previous methods. This is attributed to the volatility (high VP) of the AL precursor and the comparatively low vapour density compared to APTES, allowing for more AL monomer to be present at once in the chamber for matching pressures. APTES (somewhat like TEOS) often deposits with a slight non-uniformity of thickness across a full slide (see Fig 4.3 and Fig 5.7) due to the manner in which the gas is delivered to the chamber and the dispersal of monomer within the chamber (related to vapour density). AL is typically immune to this negative processing affect.

5.6 – Conclusions

APTES and TEOS/AL films have been shown to be efficiently processed in a manufacture worthy plasma deposition system. APTES has shown to be applicable to PECVD processes, generating robust and functionalised amine films. TEOS/AL has been shown to be an improvement over APTES PECVD depositions, basing this on both processing parameters and uniformity of coatings. These films, unlike CLD silanised APTES, generate little waste products and greatly increased throughput speeds and control of surface variables.

Chapter 6

Results and Discussion Part 3 - Ideas and Future Work

6.1 – Development of Process Strategies Involving Mixtures of Precursor Chemicals

As described in section 2.1, APTES has a VP that requires external energy to encourage adequate vaporisation. To this affect if possible, alteration of this characteristic could serve to extend the applicability of APTES as a PECVD precursor without the use of a bubbler or nebuliser. Raoult's Law states that the VP of a solution relies on the VP of all chemical components, and the mole fraction of each component, present in the solution [148]. This law applies directly to ideal solutions, i.e. intermolecular forces between unlike chemicals are similar to those of like chemicals, yet the principle idea behind it may be applied to a mixture of chemicals to improve the overall VP of the target precursor. This is based on the assumption that corresponding liquids are non-reactive and acceptably miscible, i.e. liquid separation is a slow process. The more similar the two components, the more their behaviour approaches that described by the theoretical Raoult's Law [148], [149].

Taking APTES as an example of a chemical that requires external heating to encourage vaporisation, a chemical with a sufficiently high VP may be introduced to increase the overall VP. The addition of a secondary chemical however could prove problematic if the deposition surface characteristics and composition are to be maintained. To this effect a chemical such as ethanol may be employed. Ethanol is a by-product of the silanisation process, and also a by-product of the plasma dissociation of the oxysilane compounds used in this work. With respect to this an assumption must be validated that ethanol will not become embedded into the films, and will instead be continually removed from the chamber much like the cleaved oxysilane terminals. With an appropriate mixture ratio of chemicals, the new precursor combo could serve to create a single phase amine deposition not requiring external heating apparatus, simplifying the procedure while removing a source of possible process instability (condensation of chemical in pipe ways, non-uniform heating of precursor etc.).

There is also scope for a combination of amine containing precursors to increase VP, i.e. AL and APTES. A study performed previously by our group (Gandhiraman et al) [102] shows a similar experiment with respect to using two separate amine containing chemicals in a single deposition cycle. The aim of this work however was infusing two singular precursors into the deposition chamber with the intension of increasing the overall amine concentration of the surface. In these experiments ethylenediamine (EDA) was used to augment the deposition process of APTES. The work showed how EDA was insufficient by its self, as the silicon backbone supplied by the APTES monomer was required for robust adhesion to the polymer. Collectively however the film showed good stability with an increased amine density.

Compared to AL however, EDA shows a much lower VP (13 hPA @ 20°C), likely due to the level of hydrogen bonding attributed with a chemical containing multiple amine groups. Due to the design of the vapour delivery system on the Oxford system however, running simultaneous vapour from two separate sources may cause a problem considering APTES is heated. The mixture of vapours could cause excessive vapour condensation in the lines over time. Therefore a physically mixed solution is considered the only plausible combination of AL and APTES in a deposition.

6.2 – Extension of Chemical Portfolio for PECVD Processes

A study by Wang and Jin [150] details the use of another secondary chemical using during silanisation deposition of APTES. The chemical is methyltriethoxysilane (MTES), a stable organosilane similar in composition to TEOS. The report details how MTES is employed to create an APTES/MTES mixture which is then deposited through traditional silanisation methods. This leads to the creation of amine film with unreactive methyl components. The report details how the addition of methyl groups to the surface creates functional films that exhibit higher specificity than that of regular APTES coatings. By creating a mixture of these 2 chemicals, assuming they are in fact miscible (following the same principles as Raoult's Law theory), the plan is to replicate the effect observed by Wang and Jin but through a plasma deposition process as opposed to a wet chemistry procedure.

MTES is bought in powder form, as opposed to liquid, and will therefore need to be diluted into the APTES precursor. Due to the difference of the mass and reactivity of each chemical this may serve to decrease the overall VP from that of pure APTES, but likely heating will be

required unless success is attained through the previously detailed plan of altering the APTES precursors overall vaporisation rate.

Another proposal for furthering the portfolio of plasma recipes is to build upon the research aimed at the control of surface wettability using the TEOS/AA process. By extending the range of the surface wettability into the $>100^o$ hydrophobic range, the plasma deposited coatings will find new use in a variety of projects, from microfluidic valvesto non-stick surfaces[22], [151], [152]. Increases in hydrophobicity relate directly to a decrease in SE. MTES can be used to this end, as methyl groups on a surface are typically non polar and have very low SE. Another chemical of particular interest with respect to the increase of surface water CA is tetramethylcyclotetrasiloxane (TMCTS). TMCTS is used for superhydrophobic surfaces (water CA $>150^o$)[153], and has a VP (~9.5hPa) considered within the favourable range for passive evaporation in the low pressure system when comparing to the other chemicals used in this work.

In work by Nwankire et al [153] TMCTS is used to develop superhydrophobic surfaces. The final wettability is however also influenced by the surface roughness, which will also need to be addressed.Whereas the work performed herein has shown the PECVD to create films of low roughness, there are methods to change this. Nanosphere lithography for example allows for the creation of specific surface structures[154], [155]. By selectively etching away specific areas of a thin film, using nanosphere lithography, a combination of layer characteristics can be combined. This could allow for more advanced control over the surface wettability, by allowing for two surfaces with different water CA to exert influence on the surface interface. This process may perform more robustly than the previously researched H_2O based curing method, and allow for a greater range of possible surface wettability depending on the chemicals combined. The lithography process may also allow for controlled manipulation of the surface roughness, aiding in the manipulation of surface wettability.
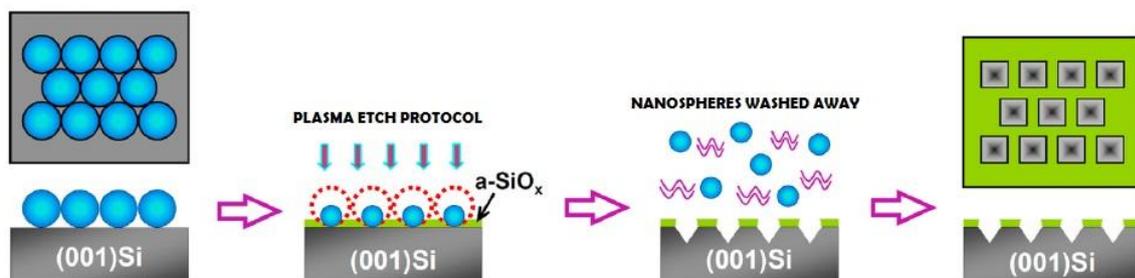
Figure 6.1: Example of a nanosphere lithography process [155]

The use of TMCTS as a precursor will likely not negatively impact on any other processes (build up on chamber walls etc.) as it is an organosilicon, like TEOS and HMDSO. The combination of TMCTS and AA may also allow for a process of wettability manipulation similar to that of the TEOS/AA film, as the underlying organosilicon layers are elementally similar and the same process of surface alteration may apply.

Another addition to the possible plasma portfolio for biomedical devices could be the introduction of dimethoxyethane (DME) or diethylene glycol dimethyl ether (DEGDME). DME and DEGDME have previously been employed in the Europlasma system with the intension of creating PEG layers to improve the specificity of the TEOS/AA films[104]. PEG layers would be developed with the expressed intension of limiting nonspecific adhesion of biomolecules. PEG films have been attributed with these protein repellent properties in a variety of literature [156]–[160]. Some of the determining factors behind this are the films repulsive steric affect, electrically neutral state, and the hydrophilic wettability.

By developing a more effective repulsive film, compared to plain TEOS (which as shown rejects protein adhesion of IgG), a combination of film properties can be deposited onto a specific device. Repulsion of a variety of biomolecules and proteins will be required by devices which will be used to test blood samples, and this type of film may therefore lend much needed characteristics to prototype devices.

Other functional groups that may be advantageous for biomedical devices are epoxy and thiol groups. Epoxy groups are highly reactive compared to carboxylic acids, and do not require the same linker chemistries to bind biomolecules. Difficulties may arise however due to the reactivity of the chemicals functional group, making epoxy surfaces less specific and allowing for immobilisation of a range of proteins etc.[118]. Protein adsorption from solution however is a possible application of epoxy surfaces, similar to the use of APTES in immobilisation without linkers. Typically epoxy surfaces are silanised, much like the CLD of APTES. 3-(Glycidyloxypropyl) triethoxysilane (GPTES) is a chemical similar in structure to APTES and is traditionally used to silanise epoxy surface. It however has a VP lower than that of APTES (~0.01hPa), so is considered impractical for non-heated evaporation in a low pressure system. A differing approach would be to combine TEOS with a smaller epoxy containing chemical called allyl glycidyl ether (AGE). This chemical contains a vinyl group (a double carbon bond similar to that of AA) that could be targeted for dissociation, allowing

the film to grow up epoxy groups orientated in a position that would allow for biomolecular adhesion.

Thiol groups on the other hand typically show an affinity to soft metals, like gold. Gold surfaces are used for a range of applications, from surface plasmon resonance (SPR) analysis to scanning electron microscopes (SEM).A paper by Olkhov et al [161] details how gold nanoparticles are printed and grown on a substrate. These gold nanoparticles are then functionalised to allow for the capture of a target analyte. The gold nanoparticles provide a means for employing SPR to analyse the capture of the analytes on the surface. Nanoparticle arrays of gold differ from a continuous gold layer (typically used in SPR) because each individual particle exhibits localised plasmon. Therefore it is possible that single nanoparticles can act as a biosensor [162]. More likely however, small arrays of nanoparticles could be used in a lab-on-a-chip design, where particles functionalised for different analytes are blocked together in specific areas of a chip, similar to the design shown in Fig 4.28.

A thiol containing chemical similar in nature to those researched in this thesis is Mercaptopropyltrimethoxysilane (MPTMS). It is almost identical to the APTES precursor in structure, but in place of the amine (NH_2) there is a thiol group (SH). The VP of MPTMS is ~7hPA, placing it above TEOS and AA on the VP graph. This is within acceptable limits for heat free vaporisation at low pressure. MPTMS has been used previously in the surface group, as shown in this paper by Gandhiraman et al [104].

6.3 - Limit of Detection Analysis of TEOS/AA Films

Development of a calibration curve using the slide holding gaskets with TEOS/AA was found to be unsuitable in generating reliably reproducible data from slide to slide. It was apparent however that an assay can in fact be performed in its entirety on a TEOS/AA surface. Therefore as a method of assessing the applicability of TEOS/AA as a surface for assay development, a secondary comparative experiment was planned. The basis behind this experiment is to show that the TEOS/AA slides can be used in a more specific manner than the plate, i.e. the lowest dilution produces a higher signal on the TEOS/AA films compared to the 96 well plate.

The Limit of Detection (LoD) is a measure of the lowest distinguishable amount of an analyte likely to be detected reliably, although not necessarily quantified. LoD experiments can be

used in this instance to assess to an extent the level of specificity each device possesses with respect to low dilutions of analyte. The Limit of Blank (LoB) relates to the highest likely analyte signal received from blank (no analyte) replicate samples. The LoD can use the LoB to generate a more accurate measurement. The equations are shown below [163], [164];

$$LoB = mean_{Blank} + 1.645(SD_{Blank})$$

$$LoD = LoB + 1.645(SD_{Lowest\ Concentraion})$$

By applying these equations to the data received from specially designed experiments using the gaskets (or other well forming apparatus), we hope to find the LoD of the TEOS/AA samples, which has already shown signal similar to the 96 well plates for low concentrations previously (Fig 4.26). Limit of Quantification (LoQ) is another method for analysing the lowest measureable concentration of analyte. LoD and LoQ are related, in that the only difference between both is typically a change to the multiple of the SD in the equation. In many instance the LoD and LoQ may be equivalent. Generally the LoQ is considered more accurate as it accounts for assay bias and imprecision's. For these experiments however, as the surface is under investigation as opposed to the assay and procedure, the LoD experiment will suffice [163], [164].

To attempt to remove some of the problems associated with using the gasket devices for testing the TEOS/AA surfaces (see section 4.4), and to develop a means of testing the surfaces under typical device conditions, a small fluidic chip design was created. The idea behind this was to allow for continuous flow during the assay cycle, removing the chance of wells drying between steps. This would also allow for experimentation on the stability of the film after several hours' worth of fluidic interaction, a timescale much larger than that likely experience on microfluidic devices. The design is simple and made from Zeonor® and pressure sensitive adhesive (PSA). This is shown in Fig 6.2.
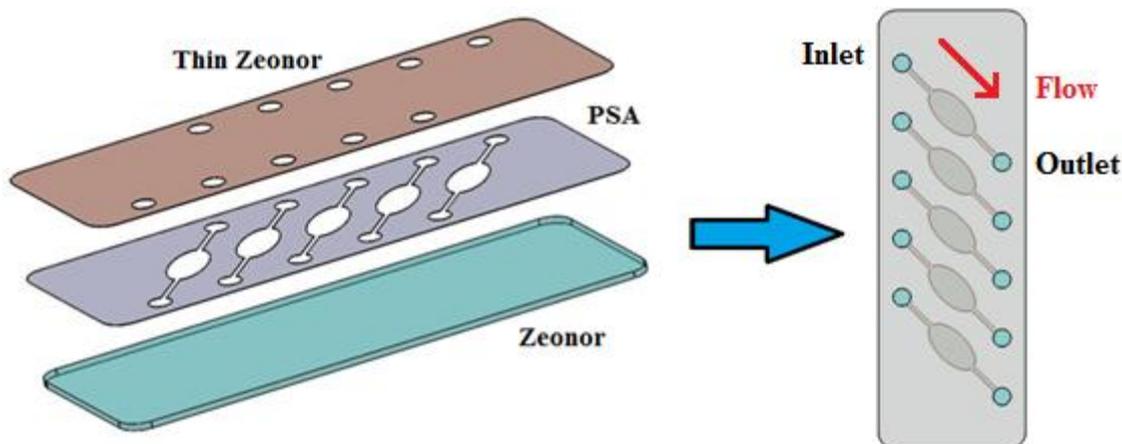
Figure 6.2: Fluidic device planned for use in assay studies of TEOS/AA films
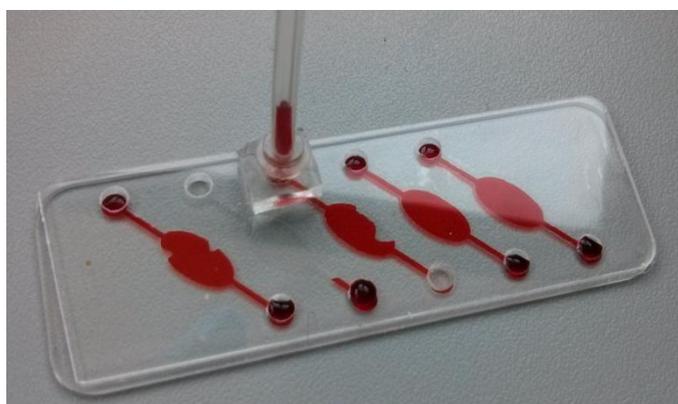
Figure 6.3: Fluidic device being used in suction mode

The optical properties of the thin Zeonor® top layer should allow for fluorescent analysis without the need for disassembly of the fluidic chip. A syringe pump will be employed to suck liquid through the chamber from the outlet position. By suctioning the liquid, as opposed to injecting it, the solutions being passed through can be easily changed without interruption to the flow. This method of fluidic driving process was also employed previously by our group in similarly designed fluidic chips [165]. With this device, or a similarly designed chip depending on the outcome, assays will be able to be performed and studied in greater and more accurate detail using the TEOS/AA films.

6.4 – Novel Applications of Wettability Controlled TEOS/AA films – Mask Free Masking of a Surface

TEOS/AA films have been shown in this work to be applicable in robust surface modification. In reference to the ability to control surface wettability a novel processing

function may apply to devices intended for use with these films. The soft polyAA layers have been shown to be the primary factor in the changes in wettability experienced by the films. It has also been shown to be loosely bound and easily removed through physical interaction. It is therefore assumed that it is possible to selectively remove areas of the soft polyAA film without damaging neighbouring areas. For example, a felt tip pen (replacing ink with water) could be used to remove very specific and small areas of the polyAA layer, removing the ability for the wettability to shift drastically. Typically creating areas of differing surface characteristics involves the use of a mask to protect specific sites from plasma interaction. In this case however, the polyAA soft layer acts as its own mask, where areas can be easily removed during the curing process to create a surface with a variety of water CAs.

Take for an applied example a microfluidic disc. The polyAA film may be selectively removed at specific areas on a surface where hydrophobic valves are required. These valves may also be allowed varying times to cure, creating valves of specific water CA. This allows for a cascading valve system, where specific valves allow flow at specific rotational speeds. Therefore the assay process can be step controlled, as opposed to occasional increases in rotational velocity to pass a specific valve before returning to normal operating speed. As the hydrophilic surface will allow for adequate migration of solutions, and provide low non-specific binding (see Fig 4.25) with good specific binding (see Fig 4.22), the combination of wettability's made possible from this process on a single disc is an attractive prospect.

It is worth noting that the combination of TMCTS and AA (as described in section 6.2), if similar curing processes are effective, would improve upon this plan as hydrophobic valves of higher water CA may be more applicable to certain microfluidic designs.

References

[1] A. P. F. Turner, "Biosensors: sense and sensibility.," *Chem. Soc. Rev.*, vol. 42, no. 8, pp. 3184–96, Apr. 2013.

[2] B. Wang, X. Ji, H. Zhao, N. Wang, X. Li, R. Ni, and Y. Liu, "An amperometric β-glucan biosensor based on the immobilization of bi-enzyme on Prussian blue-chitosan and gold nanoparticles-chitosan nanocomposite films.," *Biosens. Bioelectron.*, vol. 55, pp. 113–9, May 2014.

[3] O. O. Soldatkin, I. S. Kucherenko, V. M. Pyeshkova, a L. Kukla, N. Jaffrezic-Renault, a V El'skaya, S. V Dzyadevych, and a P. Soldatkin, "Novel conductometric biosensor based on three-enzyme system for selective determination of heavy metal ions.," *Bioelectrochemistry*, vol. 83, pp. 25–30, Feb. 2012.

[4] H. Yang, "Enzyme-based ultrasensitive electrochemical biosensors.," *Curr. Opin. Chem. Biol.*, vol. 16, no. 3–4, pp. 422–8, Aug. 2012.

[5] Z. Zhao and H. Jiang, "Enzyme-based Electrochemical Biosensors," in *Biosensors*, vol. Current Op, no. February, 2010, pp. 1–23.

[6] L. S. Bachan Upadhyay and N. Verma, "Enzyme Inhibition Based Biosensors: A Review," *Anal. Lett.*, vol. 46, no. 2, pp. 225–241, Jan. 2013.

[7] V. V. R. Sai, T. Kundu, C. Deshmukh, S. Titus, P. Kumar, and S. Mukherji, "Label-free fiber optic biosensor based on evanescent wave absorbance at 280nm," *Sensors Actuators B Chem.*, vol. 143, no. 2, pp. 724–730, Jan. 2010.

[8] B. B. Kim, W. J. Im, J. Y. Byun, H. M. Kim, M.-G. Kim, and Y.-B. Shin, "Label-free CRP detection using optical biosensor with one-step immobilization of antibody on nitrocellulose membrane," *Sensors Actuators B Chem.*, vol. 190, pp. 243–248, Jan. 2014.

[9] C. E. Nwankire, G. G. Donohoe, X. Zhang, J. Siegrist, M. Somers, D. Kurzbuch, R. Monaghan, M. Kitsara, R. Burger, S. Hearty, J. Murrell, C. Martin, M. Rook, L. Barrett, S. Daniels, C. McDonagh, R. O'Kennedy, and J. Ducrée, "At-line bioprocess monitoring by immunoassay with rotationally controlled serial siphoning and integrated supercritical angle fluorescence optics.," *Anal. Chim. Acta*, vol. 781, pp. 54–62, Jun. 2013.

[10] R. B. Queirós, N. de-los-Santos-Álvarez, J. P. Noronha, and M. G. F. Sales, "A label-free DNA aptamer-based impedance biosensor for the detection of E. coli outer membrane proteins," *Sensors Actuators B Chem.*, vol. 181, pp. 766–772, May 2013.

[11] H.-P. Peng, Y. Hu, P. Liu, Y.-N. Deng, P. Wang, W. Chen, A.-L. Liu, Y.-Z. Chen, and X.-H. Lin, "Label-free electrochemical DNA biosensor for rapid detection of mutidrug resistance gene based on Au nanoparticles/toluidine blue–graphene oxide nanocomposites," *Sensors Actuators B Chem.*, vol. 207, pp. 269–276, Oct. 2014.

[12]   H.-B. Wang, H.-D. Zhang, S.-P. Xu, T. Gan, K.-J. Huang, and Y.-M. Liu, "A sensitive and label-free electrochemical impedance biosensor for protein detection based on terminal protection of small molecule-linked DNA," *Sensors Actuators B Chem.*, vol. 194, pp. 478–483, Apr. 2014.

[13]   X. Y. Zhang, L. Y. Zhou, H. Q. Luo, and N. B. Li, "A sensitive and label-free impedimetric biosensor based on an adjunct probe.," *Anal. Chim. Acta*, vol. 776, pp. 11–6, May 2013.

[14]   C. S. Kim, B.-H. Choi, J. H. Seo, G. Lim, and H. J. Cha, "Mussel adhesive protein-based whole cell array biosensor for detection of organophosphorus compounds.," *Biosens. Bioelectron.*, vol. 41, pp. 199–204, Mar. 2013.

[15]   G. Wen, X. Wen, S. Shuang, and M. M. F. Choi, "Whole-cell biosensor for determination of methanol," *Sensors Actuators B Chem.*, vol. 201, pp. 586–591, Oct. 2014.

[16]   A. Schenkmayerová, A. Bertóková, J. Sefčovičová, V. Stefuca, M. Bučko, A. Vikartovská, P. Gemeiner, J. Tkáč, and J. Katrlík, "Whole-cell Gluconobacter oxydans biosensor for 2-phenylethanol biooxidation monitoring.," *Anal. Chim. Acta*, vol. 854, no. 1334, pp. 140–4, Jan. 2015.

[17]   Y. Lei, W. Chen, and A. Mulchandani, "Microbial biosensors.," *Anal. Chim. Acta*, vol. 568, no. 1–2, pp. 200–10, May 2006.

[18]   H. Nakamura and I. Karube, "Current research activity in biosensors," *Anal. Bioanal. Chem.*, vol. 377, no. 3, pp. 446–68, 2003.

[19]   S. D'Souza, "Microbial biosensors," *Biosens. Bioelectron.*, vol. 16, no. 6, pp. 337–53, 2001.

[20]   M. Byfield and R. Abuknesha, "Biochemical aspects of biosensors," *Biosens. Bioelectron.*, vol. 9, no. 4–5, pp. 373–400, 1994.

[21]   J. E. Childerhose and M. E. Macdonald, "Health consumption as work: the home pregnancy test as a domesticated health tool.," *Soc. Sci. Med.*, vol. 86, pp. 1–8, Jun. 2013.

[22]   Y. Feng, Z. Zhou, X. Ye, and J. Xiong, "Passive valves based on hydrophobic microfluidics," *Sensors Actuators A Phys.*, vol. 108, no. 1–3, pp. 138–143, Nov. 2003.

[23]   W. Wu, L. Yu, Z. Fang, P. Lie, and L. Zeng, "A lateral flow biosensor for the detection of human pluripotent stem cells.," *Anal. Biochem.*, vol. 436, no. 2, pp. 160–4, May 2013.

[24]   Z. Fang, C. Ge, W. Zhang, P. Lie, and L. Zeng, "A lateral flow biosensor for rapid detection of DNA-binding protein c-jun.," *Biosens. Bioelectron.*, vol. 27, no. 1, pp. 192–6, Sep. 2011.

[25] F. Liu and C. Zhang, "A novel paper-based microfluidic enhanced chemiluminescence biosensor for facile, reliable and highly-sensitive gene detection of Listeria monocytogenes," *Sensors Actuators B Chem.*, vol. 209, pp. 399–406, Nov. 2014.

[26] J. Wang, M. Aki, D. Onoshima, K. Arinaga, N. Kaji, M. Tokeshi, S. Fujita, N. Yokoyama, and Y. Baba, "Microfluidic biosensor for the detection of DNA by fluorescence enhancement and the following streptavidin detection by fluorescence quenching.," *Biosens. Bioelectron.*, vol. 51, pp. 280–5, Jan. 2014.

[27] A. R. Abate, J. Thiele, M. Weinhart, and D. a Weitz, "Patterning microfluidic device wettability using flow confinement.," *Lab Chip*, vol. 10, no. 14, pp. 1774–6, Jul. 2010.

[28] R. . Weber, K. . Möller, M. Unger, and C. . O'Connor, "The chemical vapour and liquid deposition of tetraethoxysilane on the external surface of ZSM-5," *Microporous Mesoporous Mater.*, vol. 23, no. 3–4, pp. 179–187, Aug. 1998.

[29] T. Kasputis, M. Koenig, D. Schmidt, D. Sekora, K. B. Rodenhausen, K.-J. Eichhorn, P. Uhlmann, E. Schubert, A. K. Pannier, M. Schubert, and M. Stamm, "Slanted Columnar Thin Films Prepared by Glancing Angle Deposition Functionalized with Polyacrylic Acid Polymer Brushes," *J. Phys. Chem. C*, vol. 117, no. 27, pp. 13971–13980, Jul. 2013.

[30] K. Yoshida, R. Hashide, T. Ishii, S. Takahashi, K. Sato, and J. Anzai, "Layer-by-layer films composed of poly(allylamine) and insulin for pH-triggered release of insulin.," *Colloids Surf. B. Biointerfaces*, vol. 91, pp. 274–9, Mar. 2012.

[31] I. a. Rahman, M. Jafarzadeh, and C. S. Sipaut, "Synthesis of organo-functionalized nanosilica via a co-condensation modification using γ-aminopropyltriethoxysilane (APTES)," *Ceram. Int.*, vol. 35, no. 5, pp. 1883–1888, Jul. 2009.

[32] J. Raj, G. Herzog, M. Manning, C. Volcke, B. D. MacCraith, S. Ballantyne, M. Thompson, and D. W. M. Arrigan, "Surface immobilisation of antibody on cyclic olefin copolymer for sandwich immunoassay.," *Biosens. Bioelectron.*, vol. 24, no. 8, pp. 2654–8, Apr. 2009.

[33] C. Voulgaris, E. Amanatides, D. Mataras, S. Grassini, E. Angelini, and F. Rosalbino, "RF power and SiOxCyHz deposition efficiency in TEOS/O2 discharges for the corrosion protection of magnesium alloys," *Surf. Coatings Technol.*, vol. 200, no. 22–23, pp. 6618–6622, Jun. 2006.

[34] A. Abbas, D. Vercaigne-Marko, P. Supiot, B. Bocquet, C. Vivien, and D. Guillochon, "Covalent attachment of trypsin on plasma polymerized allylamine.," *Colloids Surf. B. Biointerfaces*, vol. 73, no. 2, pp. 315–324, Oct. 2009.

[35] R. Jafari, M. Tatoulian, W. Morscheidt, and F. Arefi-Khonsari, "Stable plasma polymerized acrylic acid coating deposited on polyethylene (PE) films in a low frequency discharge (70kHz)," *React. Funct. Polym.*, vol. 66, no. 12, pp. 1757–1765, Dec. 2006.

[36] M. Pykönen, H. Silvaani, J. Preston, P. Fardim, and M. Toivakka, "Plasma activation induced changes in surface chemistry of pigment coating components," *Colloids Surfaces A Physicochem. Eng. Asp.*, vol. 352, no. 1–3, pp. 103–112, Dec. 2009.

[37] P. Alves, R. Cardoso, T. R. Correia, B. P. Antunes, I. J. Correia, and P. Ferreira, "Surface modification of polyurethane films by plasma and ultraviolet light to improve haemocompatibility for artificial heart valves.," *Colloids surfaces B Biointerfaces*, vol. 113, no. 1, pp. 25–32, Sep. 2014.

[38] K. Miyauchi and M. Yuasa, "A study of adhesive improvement of a Cr–Ni alloy layer on a polyimide surface by low pressure gas plasma modification," *Prog. Org. Coatings*, vol. 76, no. 11, pp. 1536–1542, Nov. 2013.

[39] O. Mrad, S. Saloum, and a. Al-Mariri, "Effect of a new low pressure SF6 plasma sterilization system on polymeric devices," *Vacuum*, vol. 88, pp. 11–16, Feb. 2013.

[40] H. Miao and G. Yun, "The sterilization of Escherichia coli by dielectric-barrier discharge plasma at atmospheric pressure," *Appl. Surf. Sci.*, vol. 257, no. 16, pp. 7065–7070, Jun. 2011.

[41] A. Bogaerts, E. Neyts, R. Gijbels, and J. van der Mullen, "Gas discharge plasmas and their applications," *Spectrochim. Acta Part B At. Spectrosc.*, vol. 57, no. 4, pp. 609–658, Apr. 2002.

[42] M. A. Lieberman and A. J. Lichtenberg, *Principles of Plasma Discharges and Materials Processing - Second Edition*. John Wiley & Sons, 2005.

[43] N. S. J. Braithwaite, "Introduction to gas discharges," *Plasma Sources Sci. Technol.*, vol. 9, no. 4, pp. 517–527, 2000.

[44] W. Simmler, "Silicon Compounds, Inorganic," *Ullmann's Encyclopedia of Industrial Chemistry*. Wiley-VCH, 2000.

[45] M. C. Vasudev, K. D. Anderson, T. J. Bunning, V. V Tsukruk, and R. R. Naik, "Exploration of plasma-enhanced chemical vapor deposition as a method for thin-film fabrication with biological applications.," *ACS Appl. Mater. Interfaces*, vol. 5, no. 10, pp. 3983–94, May 2013.

[46] Y. Chang, D. Peng, H. Wu, C. Tsaur, C. Shen, H. Tsai, J. Chen, E. Yuan, and S. City, "Revisiting of a Silane Explosion in a Photovoltaic Fabrication," *Process Saf. Prog.*, vol. 26, no. 2, pp. 155–158, 2007.

[47] J. Chen, H. Tsai, S. Chen, H. Pan, S. Hu, and C. Shen, "Analysis of a Silane Explosion in a Photovoltaic Fabrication Plant," *Process Saf. Prog.*, vol. 25, no. 3, pp. 237–244, 2006.

[48] S. Kondo, K. Tokuhashi, H. Nagai, M. Iwasaka, and M. Kaise, "Spontaneous ignition limits of silane and phosphine," *Combust. Flame*, vol. 101, no. 1–2, pp. 170–174, Apr. 1995.

[49]   A. M. Mahajan, L. S. Patil, J. P. Bange, and D. K. Gautam, "Growth of SiO2 films by TEOS-PECVD system for microelectronics applications," *Surf. Coatings Technol.*, vol. 183, no. 2–3, pp. 295–300, May 2004.

[50]   D. A. DeCrosta, J. J. Hackenberg, and J. H. Linn, "Characterization of High Oxygen:Tetraethylorthosilicate Ratio Plasma-Enhanced Chemical Vapor Deposited Films," *J. Electrochem. Soc.*, vol. 143, no. 3, pp. 1079–1084, 1996.

[51]   K. Sano, S. Hayashi, S. Wickramanayaka, and Y. Hatanaka, "High quality SiO2 depositions from TEOS by ECR plasma," *Thin Solid Films*, vol. 281–282, pp. 397–400, Aug. 1996.

[52]   S. K. Ray, C. K. Maiti, S. K. Lahiri, and N. B. Chakrabarti, "Properties of silicon dioxide films deposited at low temperatures by microwave plasma enhanced decomposition of tetraethylorthosilicate," *J. Vac. Sci. Technol. B Microelectron. Nanom. Struct.*, vol. 10, no. 3, p. 1139, May 1992.

[53]   N. T. K. Thanh and L. a. W. Green, "Functionalisation of nanoparticles for biomedical applications," *Nano Today*, vol. 5, no. 3, pp. 213–230, Jun. 2010.

[54]   N. . Chaudhury, R. Bhardwaj, and B. . Murari, "Fluorescence spectroscopic study to characterize and monitor TEOS based sol–gel process for development of optical biosensors," *Curr. Appl. Phys.*, vol. 3, no. 2–3, pp. 177–184, Apr. 2003.

[55]   R. a. M. Carvalho, R. R. Lima, a. P. Nascimento Filho, M. L. P. Silva, and N. R. Demarquette, "Plasma polymerized TEOS films for nanochannels formation and sensor development," *Sensors Actuators B Chem.*, vol. 108, no. 1–2, pp. 955–963, Jul. 2005.

[56]   J. H. Lee, C. H. Jeong, J. T. Lim, N. G. Jo, S. J. Kyung, and G. Y. Yeom, "Properties of SiOxNy thin film deposited by low temperature plasma enhanced chemical vapor deposition using TEOS–NH3–O2–N2 gas mixtures," *Surf. Coatings Technol.*, vol. 200, no. 1–4, pp. 680–685, Oct. 2005.

[57]   S. P. Mukherjee and P. E. Evans, "The Deposition of Thin Films by the Decomposition of Tetra-Ethoxy Silane in a Radio Frequency Glow Discharge," *Thin Solid Films*, vol. 14, no. 1, pp. 105–118, 1972.

[58]   A. M. Mahajan, L. S. Patil, and D. K. Gautam, "Influence of process parameters on the properties of TEOS–PECVD-grown SiO2 films," *Surf. Coatings Technol.*, vol. 188–189, pp. 314–318, Nov. 2004.

[59]   Y. T. Zhang, J. Lou, Q. Li, and Q. Li, "Electrode-Gap Effects on the Electron Density and Electron Temperature in Atmospheric Radio-Frequency Discharges," *IEEE Trans. Plasma Sci.*, vol. 41, no. 3, pp. 414–420, Mar. 2013.

[60]   C. Voulgaris, a. Panou, E. Amanatides, and D. Mataras, "RF power effect on TEOS/O2 PECVD of silicon oxide thin films," *Surf. Coatings Technol.*, vol. 200, no. 1–4, pp. 351–354, Oct. 2005.

[61] J. Zeng, J. Lin, and X. Zhang, "Deposition of silicon oxide films by non-equilibrium, atmospheric-pressure plasma jet," *Surf. Coatings Technol.*, vol. 1, pp. 5–7, May 2012.

[62] F. Nicolazo, a. Goullet, a. Granier, C. Vallée, G. Turban, and B. Grolleau, "Study of oxygen/TEOS plasmas and thin SiOx films obtained in an helicon diffusion reactor," *Surf. Coatings Technol.*, vol. 98, no. 1–3, pp. 1578–1583, Jan. 1998.

[63] C. Vallée, A. Goullet, A. Granier, A. Van Der Lee, and J. Durand, "Inorganic to organic crossover in thin films deposited from O 2 / TEOS plasmas," *J. Non. Cryst. Solids*, vol. 272, no. 2–3, pp. 163–173, 2000.

[64] R. W. Weber, K. P. Moller, and C. T. O'Connor, "The chemical vapour and liquid deposition of tetraethoxysilane on ZSM-5 , mordenite and beta," *Microporous Mesoporous Mater.*, vol. 35–36, pp. 533–543, 2000.

[65] H. S. Park, G. Dodbiba, L. F. Cao, and T. Fujita, "Synthesis of silica-coated ferromagnetic fine powder by heterocoagulation.," *J. Phys. Condens. Matter*, vol. 20, no. 20, p. 204105, May 2008.

[66] F. L. Buchholz and A. T. Graham, *Modern superabsorbent polymer technology*. 1998.

[67] C. A. Scotchford, C. P. Gilmore, E. Cooper, G. J. Leggett, and S. Downes, "Protein adsorption and human osteoblast-like cell attachment and growth on alkylthiol on gold self-assembled monolayers.," *J. Biomed. Mater. Res.*, vol. 59, no. 1, pp. 84–99, Jan. 2002.

[68] M. J. E. Fischer, *Surface Plasmon Resonance*, vol. 627. Totowa, NJ: Humana Press, 2010.

[69] L. Detomaso, R. Gristina, R. d'Agostino, G. S. Senesi, and P. Favia, "Plasma deposited acrylic acid coatings: Surface characterization and attachment of 3T3 murine fibroblast cell lines," *Surf. Coatings Technol.*, vol. 200, no. 1–4, pp. 1022–1025, Oct. 2005.

[70] L. Detomaso, R. Gristina, G. S. Senesi, R. d'Agostino, and P. Favia, "Stable plasma-deposited acrylic acid surfaces for cell culture applications.," *Biomaterials*, vol. 26, no. 18, pp. 3831–41, Jun. 2005.

[71] D. L. Cho, P. M. Claesson, C.-G. Golander, and K. Johansson, "Structure and Surface Properties of Plasma Polymerized Acrylic Acid Layers," *J. Appl. Polym. Sci.*, vol. 41, no. 4, pp. 1373–1390, 1990.

[72] M. R. Alexander and T. M. Duc, "The chemistry of deposits formed from acrylic acid plasmas," *J. Mater. Chem.*, vol. 8, no. 4, pp. 937–943, 1998.

[73] S. Dominguez-Medina, J. Blankenburg, J. Olson, C. F. Landes, and S. Link, "Adsorption of a Protein Monolayer via Hydrophobic Interactions Prevents Nanoparticle Aggregation under Harsh Environmental Conditions.," *ACS Sustain. Chem. Eng.*, vol. 1, no. 7, pp. 833–842, Jul. 2013.

[74]   M. R. Alexander and T. M. Duc, "A study of the interaction of acrylic acid/1,7-octadiene plasma deposits with water and other solvents," *Polymer (Guildf).*, vol. 40, no. 20, pp. 5479–5488, Sep. 1999.

[75]   C. Vilani, D. E. Weibel, R. R. M. Zamora, a. C. Habert, and C. a. Achete, "Study of the influence of the acrylic acid plasma parameters on silicon and polyurethane substrates using XPS and AFM," *Appl. Surf. Sci.*, vol. 254, no. 1, pp. 131–134, Oct. 2007.

[76]   R. Morent, N. De Geyter, S. Van Vlierberghe, a. Beaurain, P. Dubruel, and E. Payen, "Influence of operating parameters on plasma polymerization of acrylic acid in a mesh-to-plate dielectric barrier discharge," *Prog. Org. Coatings*, vol. 70, no. 4, pp. 336–341, Apr. 2011.

[77]   S. J. Hutton, J. M. Crowther, and J. P. S. Badyal, "Complexation of Fluorosurfactants to Functionalized Solid Surfaces : Smart Behavior," *Chem. Mater.*, vol. 12, no. 23, pp. 2282–2286, 2000.

[78]   S. Ricciardi, R. Castagna, S. M. Severino, I. Ferrante, F. Frascella, E. Celasco, P. Mandracci, I. Vallini, G. Mantero, C. F. Pirri, and P. Rivolo, "Surface functionalization by poly-acrylic acid plasma-polymerized films for microarray DNA diagnostics," *Surf. Coatings Technol.*, vol. 207, pp. 389–399, Aug. 2012.

[79]   H. Aizawa, S. Kurosawa, K. Kobayashi, K. Kashima, T. Hirokawa, Y. Yoshimi, M. Yoshimoto, T. Hirotsu, J. Miyake, and H. Tanaka, "Turning of contact angle on glass plates coated with plasma-polymerized styrene, allylamine and acrylic acid," *Mater. Sci. Eng. C*, vol. 12, no. 1–2, pp. 49–54, Aug. 2000.

[80]   C. G. Spanos, J. P. S. Badyal, a. J. Goodwin, and P. J. Merlin, "Pulsed plasmachemical deposition of polymeric salt networks," *Polymer (Guildf).*, vol. 46, no. 21, pp. 8908–8912, Oct. 2005.

[81]   S. a. Voronin, M. R. Alexander, and J. W. Bradley, "Time-resolved mass and energy spectral investigation of a pulsed polymerising plasma struck in acrylic acid," *Surf. Coatings Technol.*, vol. 201, no. 3–4, pp. 768–775, Oct. 2006.

[82]   M. Dhayal and J. W. Bradley, "Time-resolved electric probe measurements in the pulsed-plasma polymerisation of acrylic acid," *Surf. Coatings Technol.*, vol. 194, no. 1, pp. 167–174, Apr. 2005.

[83]   D. Mangindaan, W.-H. Kuo, C.-C. Chang, S.-L. Wang, H.-C. Liu, and M.-J. Wang, "Plasma polymerization of amine-containing thin films and the studies on the deposition kinetics," *Surf. Coatings Technol.*, vol. 206, no. 6, pp. 1299–1306, Dec. 2011.

[84]   E. Punzón-Quijorna, V. Sánchez-Vaquero, a. Muñoz Noval, D. Gallach Pérez, a. Climent Font, G. Ceccone, R. Gago, J. P. García Ruiz, and M. Manso Silván, "Optimized allylamine deposition for improved pluripotential cell culture," *Vacuum*, vol. 85, no. 12, pp. 1071–1075, Jun. 2011.

[85]   N. Moreau, O. Feron, B. Gallez, B. Masereel, C. Michiels, T. Vander Borght, F. Rossi, and S. Lucas, "Chemical reactivity of plasma polymerized allylamine (PPAA) thin films on Au and Si: Study of the thickness influence and aging of the films," *Surf. Coatings Technol.*, vol. 205, no. S2, pp. S462–S465, Jul. 2011.

[86]   K. L. Jarvis and P. Majewski, "Plasma polymerized allylamine coated quartz particles for humic acid removal.," *J. Colloid Interface Sci.*, vol. 380, no. 1, pp. 150–8, Aug. 2012.

[87]   a Harsch, J. Calderon, R. B. Timmons, and G. W. Gross, "Pulsed plasma deposition of allylamine on polysiloxane: a stable surface for neuronal cell adhesion.," *J. Neurosci. Methods*, vol. 98, no. 2, pp. 135–44, Jun. 2000.

[88]   S. Massey, A. Duboin, D. Mantovani, P. Tabeling, and M. Tatoulian, "Stable modification of PDMS surface properties by plasma polymerization: Innovative process of allylamine PECVD deposition and microfluidic devices sealing," *Surf. Coatings Technol.*, vol. 206, no. 19–20, pp. 4303–4309, May 2012.

[89]   A. J. Beck, F. R. Jones, and R. D. Short, "Plasma copolymerization . Allyl amine (alam), acrylic," *Polymer (Guildf).*, vol. 37, no. 24, pp. 5537–5539, 1996.

[90]   Z. Zhang, Q. Chen, W. Knoll, R. Foerch, R. Holcomb, and D. Roitman, "Plasma Polymer Film Structure and DNA Probe Immobilization," *Macromolecules*, vol. 36, no. 20, pp. 7689–7694, Oct. 2003.

[91]   E. Gallino, S. Massey, M. Tatoulian, and D. Mantovani, "Plasma polymerized allylamine films deposited on 316L stainless steel for cardiovascular stent coatings," *Surf. Coatings Technol.*, vol. 205, no. 7, pp. 2461–2468, Dec. 2010.

[92]   X. Wang, J. Wang, Z. Yang, Y. Leng, H. Sun, and N. Huang, "Structural characterization and mechanical properties of functionalized pulsed-plasma polymerized allylamine film," *Surf. Coatings Technol.*, vol. 204, no. 18–19, pp. 3047–3052, Jun. 2010.

[93]   Z. Yang, J. Wang, R. Luo, M. F. Maitz, F. Jing, H. Sun, and N. Huang, "The covalent immobilization of heparin to pulsed-plasma polymeric allylamine films on 316L stainless steel and the resulting effects on hemocompatibility.," *Biomaterials*, vol. 31, no. 8, pp. 2072–83, Mar. 2010.

[94]   E. D. Cranston and D. G. Gray, "Morphological and optical characterization of polyelectrolyte multilayers incorporating nanocrystalline cellulose.," *Biomacromolecules*, vol. 7, no. 9, pp. 2522–30, Sep. 2006.

[95]   W. Chen and T. J. Mccarthy, "Layer-by-Layer Deposition : A Tool for Polymer Surface Modification," *Macromolecules*, vol. 9297, no. 96, pp. 78–86, 1997.

[96]   M. Olek, M. Hilgendorff, and M. Giersig, "A simple route for the attachment of colloidal nanocrystals to noncovalently modified multiwalled carbon nanotubes," *Colloids Surfaces A Physicochem. Eng. Asp.*, vol. 292, no. 1, pp. 83–85, Jan. 2007.

[97] A. Choukourov, H. Biederman, D. Slavinska, L. Hanley, A. Grinevich, H. Boldyryeva, and A. Mackova, "Mechanistic studies of plasma polymerization of allylamine.," *J. Phys. Chem. B*, vol. 109, no. 48, pp. 23086–95, Dec. 2005.

[98] W. Song and J. F. Mano, "Interactions between cells or proteins and surfaces exhibiting extreme wettabilities," *Soft Matter*, vol. 9, no. 11, p. 2985, 2013.

[99] N. V Churaev, "Contact Angles and Surface Forces," *Adv. Colloid. Interface Sci.*, vol. 58, no. 1, pp. 87–118, 1995.

[100] Y. Arima and H. Iwata, "Effect of wettability and surface functional groups on protein adsorption and cell adhesion using well-defined mixed self-assembled monolayers.," *Biomaterials*, vol. 28, no. 20, pp. 3074–82, Jul. 2007.

[101] A. Abbas, C. Vivien, B. Bocquet, D. Guillochon, and P. Supiot, "Preparation and Multi-Characterization of Plasma Polymerized Allylamine Films," *Plasma Process. Polym.*, vol. 6, no. 9, pp. 593–604, Sep. 2009.

[102] R. P. Gandhiraman*, C. Volcke, V. Gubala, C. Doyle, L. Basabe-Desmonts, C. Dotzler, M. F. Toney, M. Iacono, R. I. Nooney, S. Daniels, B. James, and D. E. Williams, "High efficiency amine functionalization of cycloolefin polymer surfaces for biodiagnostics," *J. Mater. Chem.*, vol. 20, no. 20, p. 4116, 2010.

[103] C. Volcke, R. P. Gandhiraman, V. Gubala, C. Doyle, G. Fonder, P. a Thiry, A. a Cafolla, B. James, and D. E. Williams, "Plasma functionalization of AFM tips for measurement of chemical interactions.," *J. Colloid Interface Sci.*, vol. 348, no. 2, pp. 322–8, Aug. 2010.

[104] R. P. Gandhiraman, V. Gubala, C. C. O'Mahony, T. Cummins, J. Raj, A. Eltayeb, C. Doyle, B. James, S. Daniels, and D. E. Williams, "PECVD coatings for functionalization of point-of-care biosensor surfaces," *Vacuum*, vol. 86, no. 5, pp. 547–555, Jan. 2012.

[105] V. Gubala, R. P. Gandhiraman, C. Volcke, C. Doyle, C. Coyle, B. James, S. Daniels, and D. E. Williams, "Functionalization of cycloolefin polymer surfaces by plasma-enhanced chemical vapour deposition: comprehensive characterization and analysis of the contact surface and the bulk of aminosiloxane coatings.," *Analyst*, vol. 135, no. 6, pp. 1375–81, Jun. 2010.

[106] R. P. Gandhiraman, V. Gubala, N. C. H. Le, L. C. H. Nam, C. Volcke, C. Doyle, B. James, S. Daniels, and D. E. Williams, "Deposition of chemically reactive and repellent sites on biosensor chips for reduced non-specific binding.," *Colloids Surf. B. Biointerfaces*, vol. 79, no. 1, pp. 270–5, Aug. 2010.

[107] V. Gubala, J. Siegrist, R. Monaghan, B. O'Reilly, R. P. Gandhiraman, S. Daniels, D. E. Williams, and J. Ducrée, "Simple approach to study biomolecule adsorption in polymeric microfluidic channels.," *Anal. Chim. Acta*, vol. 760, no. 1, pp. 75–82, Jan. 2013.

[108] A. Nanci, J. D. Wuest, L. Peru, P. Brunet, V. Sharma, S. Zalzal, and M. D. McKee, "Chemical modification of titanium surfaces for covalent attachment of biological molecules.," *J. Biomed. Mater. Res.*, vol. 40, no. 2, pp. 324–35, May 1998.

[109] E. J. Szili, S. Kumar, R. S. C. Smart, and N. H. Voelcker, "Generation of a stable surface concentration of amino groups on silica coated onto titanium substrates by the plasma enhanced chemical vapour deposition method," *Appl. Surf. Sci.*, vol. 255, no. 15, pp. 6846–6850, May 2009.

[110] A. Puleo, "Activity of enzyme immobilized on silanised Co-Cr-Mo," *J. Biomed. Mater. Res.*, vol. 29, no. 8, pp. 951–957, 1995.

[111] W. M. Weaver, S. Dharmaraja, V. Milisavljevic, and D. Di Carlo, "The effects of shear stress on isolated receptor-ligand interactions of Staphylococcus epidermidis and human plasma fibrinogen using molecularly patterned microfluidics.," *Lab Chip*, vol. 11, no. 5, pp. 883–9, Mar. 2011.

[112] C. Jönsson, M. Aronsson, G. Rundström, C. Pettersson, I. Mendel-Hartvig, J. Bakker, E. Martinsson, B. Liedberg, B. MacCraith, O. Ohman, and J. Melin, "Silane-dextran chemistry on lateral flow polymer chips for immunoassays.," *Lab Chip*, vol. 8, no. 7, pp. 1191–7, Jul. 2008.

[113] K. K. Sharma and T. Asefa, "Efficient bifunctional nanocatalysts by simple postgrafting of spatially isolated catalytic groups on mesoporous materials.," *Angew. Chem. Int. Ed. Engl.*, vol. 46, no. 16, pp. 2879–82, Jan. 2007.

[114] K. K. Sharma, A. Anan, R. P. Buckley, W. Ouellette, and T. Asefa, "Toward efficient nanoporous catalysts: controlling site-isolation and concentration of grafted catalytic sites on nanoporous materials with solvents and colorimetric elucidation of their site-isolation.," *J. Am. Chem. Soc.*, vol. 130, no. 1, pp. 218–28, Jan. 2008.

[115] G. Longo, L. Alonso-Sarduy, L. M. Rio, a Bizzini, a Trampuz, J. Notz, G. Dietler, and S. Kasas, "Rapid detection of bacterial resistance to antibiotics using AFM cantilevers as nanomechanical sensors.," *Nat. Nanotechnol.*, vol. 8, no. 7, pp. 522–6, Jul. 2013.

[116] A. R. Yadav, R. Sriram, J. a. Carter, and B. L. Miller, "Comparative study of solution-phase and vapor-phase deposition of aminosilanes on silicon dioxide surfaces," *Mater. Sci. Eng. C*, vol. 35, no. 1, pp. 283–290, 2014.

[117] Y. Liang, J. Huang, P. Zang, J. Kim, and W. Hu, "Molecular layer deposition of APTES on silicon nanowire biosensors: Surface characterization, stability and pH response," *Appl. Surf. Sci.*, vol. 322, pp. 202–208, 2014.

[118] K. Awsiuk, a. Psarouli, P. Petrou, a. Budkowski, S. Kakabakos, a. Bernasik, J. Rysz, and I. Raptis, "Spectroscopic and microscopic examination of protein adsorption and blocking of non-specific binding to silicon surfaces modified with APTES and GOPS," *Procedia Eng.*, vol. 25, pp. 334–337, Jan. 2011.

[119] H. Mansur, R. Oréfice, M. Pereira, Z. Lobato, W. Vasconcelos, and L. Machado, "FTIR and UV–vis study of chemically engineered biomaterial surfaces for protein immobilization," *Spectroscopy*, vol. 16, no. 3–4, pp. 351–360, 2002.

[120] Z.-H. Wang and G. Jin, "Covalent immobilization of proteins for the biosensor based on imaging ellipsometry.," *J. Immunol. Methods*, vol. 285, no. 2, pp. 237–43, Feb. 2004.

[121] U. Jonsson, B. Ivarsson, I. Lundstrom, and L. Berghem, "Adsorption behaviour of fibronectin on well-characterized silica surfaces," *J. Colloid Interface Sci.*, vol. 90, no. 1, pp. 148–163, 1982.

[122] P. Shah, N. Sridevi, A. Prabhune, and V. Ramaswamy, "Structural features of Penicillin acylase adsorption on APTES functionalized SBA-15," *Microporous Mesoporous Mater.*, vol. 116, no. 1–3, pp. 157–165, Dec. 2008.

[123] D. S. Mishra and S. H. Yalkowsky, "Estimation of vapor pressure of some organic compounds," *Ind. Eng. Chem. Res.*, vol. 30, no. 7, pp. 1609–1612, Jul. 1991.

[124] D. G. Miller, "Estimating vapor pressures - A comparison of equations," *Ind. Eng. Chem. Res.*, vol. 56, no. 3, pp. 46–57, 2002.

[125] P. J. Brucat, "CHM2041 - Phases and Equilibrium." [Online]. Available: http://www.chem.ufl.edu/~itl/2041_u98/lectures/lec_f.html. [Accessed: 17-Dec-2013].

[126] J. Y. Shin, J. Y. Park, C. Liu, J. He, and S. C. Kim, "Chemical structure and physical properties of cyclic olefin copolymers (IUPAC Technical Report)," *Pure Appl. Chem.*, vol. 77, no. 5, pp. 801–814, 2005.

[127] M. Yamazaki, "Industrialization and application development of cyclo-olefin polymer," *J. Mol. Catal. A Chem.*, vol. 213, no. 1, pp. 81–87, Apr. 2004.

[128] I. Beaulieu, M. Geissler, and J. Mauzeroll, "Oxygen plasma treatment of polystyrene and Zeonor: substrates for adhesion of patterned cells.," *Langmuir*, vol. 25, no. 12, pp. 7169–7176, Jun. 2009.

[129] H. G. Tompkins and E. A. Irene, *Handbook of Ellipsometry*. 2005.

[130] H. Arwin, "Spectroscopic ellipsometry and biology: recent developments and challenges," *Thin Solid Films*, vol. 313–314, pp. 764–774, Feb. 1998.

[131] H. Arwin, "Ellipsometry on thin organic layers of biological interest: characterization and applications," *Thin Solid Films*, vol. 377–378, pp. 48–56, Dec. 2000.

[132] R. H. Yoon, D. H. Flinn, and Y. I. Rabinovich, "Hydrophobic Interactions between Dissimilar Surfaces," *J. Colloid Interface Sci.*, vol. 185, no. 2, pp. 363–370, 1997.

[133] L.-C. Xu and C. a Siedlecki, "Effects of surface wettability and contact time on protein adhesion to biomaterial surfaces.," *Biomaterials*, vol. 28, no. 22, pp. 3273–83, Aug. 2007.

[134] R. Tadmor, "Line energy and the relation between advancing, receding, and young contact angles.," *Langmuir*, vol. 20, no. 18, pp. 7659–64, Aug. 2004.

[135] E. Chibowski and K. Terpilowski, "Surface free energy of sulfur--revisited I. Yellow and orange samples solidified against glass surface.," *J. Colloid Interface Sci.*, vol. 319, no. 2, pp. 505–13, Mar. 2008.

[136] G. Wolansky and A. Marmur, "Apparent contact angles on rough surfaces: the Wenzel equation revisited," *Colloids Surfaces A Physicochem. Eng. Asp.*, vol. 156, no. 1–3, pp. 381–388, Oct. 1999.

[137] G. Whyman, E. Bormashenko, and T. Stein, "The rigorous derivation of Young, Cassie–Baxter and Wenzel equations and the analysis of the contact angle hysteresis phenomenon," *Chem. Phys. Lett.*, vol. 450, no. 4–6, pp. 355–359, Jan. 2008.

[138] J. F. Watts and J. Wolstenholme, *An Introduction to Surface Analysis by XPS and AES*. 2003.

[139] L. C. d Carvalho, "Basic Components of a Monochromatic XPS System," *Wikipedia*, 2009. [Online]. Available: http://en.wikipedia.org/wiki/File:System2.gif. [Accessed: 12-Dec-2013].

[140] A. Gibaud and S. Hazra, "X-ray reflectivity and diffuse scattering," *Curr. Sci.*, vol. 78, no. 12, pp. 1467–1477, 2000.

[141] A. Larsson, T. Ekblad, O. Andersson, and B. Liedberg, "Photografted poly(ethylene glycol) matrix for affinity interaction studies.," *Biomacromolecules*, vol. 8, no. 1, pp. 287–95, Jan. 2007.

[142] J. Drews, H. Launay, C. M. Hansen, K. West, S. Hvilsted, P. Kingshott, and K. Almdal, "Hydrolysis and stability of thin pulsed plasma polymerised maleic anhydride coatings," *Appl. Surf. Sci.*, vol. 254, no. 15, pp. 4720–4725, May 2008.

[143] R. P. Gandhiraman, N. C. H. Le, C. K. Dixit, C. Volcke, C. Doyle, V. Gubala, S. Uppal, R. Monaghan, B. James, R. O'Kennedy, S. Daniels, and D. E. Williams, "Multi-layered plasma-polymerized chips for SPR-based detection.," *ACS Appl. Mater. Interfaces*, vol. 3, no. 12, pp. 4640–8, Dec. 2011.

[144] C. Coyle, R. P. Gandiraman, V. Gubala, N. C. H. Le, C. C. O'Mahony, C. Doyle, B. James, P. Swift, S. Daniels, and D. E. Williams, "Tetraethyl Orthosilicate and Acrylic Acid Forming Robust Carboxylic Functionalities on Plastic Surfaces for Biodiagnostics," *Plasma Process. Polym.*, vol. 9, no. 1, pp. 28–36, Jan. 2012.

[145] V. Gubala, N. C. H. Le, R. P. Gandhiraman, C. Coyle, S. Daniels, and D. E. Williams, "Functionalization of cyclo-olefin polymer substrates by plasma oxidation: stable film containing carboxylic acid groups for capturing biorecognition elements.," *Colloids Surf. B. Biointerfaces*, vol. 81, no. 2, pp. 544–8, Dec. 2010.

[146] S. Sano, K. Kato, and Y. Ikada, "Introduction of functional groups onto the surface of polyethylene for protein immobilization," *Biomaterials*, vol. 14, no. 11, pp. 817–822, 1993.

[147] F. Everaerts, M. Torrianni, M. Hendriks, and J. Feijen, "Biomechanical properties of carbodiimide crosslinked collagen: influence of the formation of ester crosslinks.," *J. Biomed. Mater. Res. A*, vol. 85, no. 2, pp. 547–55, May 2008.

[148] P. Perrot, *A to Z of Thermodynamics*. Oxford University Press, 1998.

[149] J. Clark, "Raoult's Law and Ideal Mixtures of Liquids," 2005. [Online]. Available: http://www.chemguide.co.uk/physical/phaseeqia/idealpd.html. [Accessed: 14-Aug-2012].

[150] Z.-H. Wang and G. Jin, "Silicon surface modification with a mixed silanes layer to immobilize proteins for biosensor with imaging ellipsometry.," *Colloids Surf. B. Biointerfaces*, vol. 34, no. 3, pp. 173–7, Apr. 2004.

[151] G. Londe, A. Wesser, H. J. Cho, L. Zhai, A. Chunder, and S. Subbarao, "A Passive Microfluidic Valve using Superhydrophobic/Hydrophilic Nanostructures for Lab-on-A-Chip (LOC) Systems," in *Transducers '07*, 2007, pp. 1801–1804.

[152] H. Andersson, W. Van Der Wijngaart, P. Griss, F. Niklaus, and G. Stemme, "Hydrophobic valves of plasma deposited octafluorocyclobutane in DRIE channels," *Sensors Actuators B Chem.*, vol. 75, no. 1–2, pp. 136–141, 2001.

[153] C. E. Nwankire, G. Favaro, Q.-H. Duong, and D. P. Dowling, "Enhancing the Mechanical Properties of Superhydrophobic Atmospheric Pressure Plasma Deposited Siloxane Coatings," *Plasma Process. Polym.*, vol. 8, no. 4, pp. 305–315, Apr. 2011.

[154] C. K. Dixit, A. Kumar, and A. Kaushik, "Nanosphere lithography-based platform for developing rapid and high sensitivity microarray systems.," *Biochem. Biophys. Res. Commun.*, vol. 423, no. 3, pp. 473–7, Jul. 2012.

[155] S. L. Cheng, Y. H. Lin, S. W. Lee, T. Lee, H. Chen, J. C. Hu, and L. T. Chen, "Fabrication of size-tunable, periodic Si nanohole arrays by plasma modified nanosphere lithography and anisotropic wet etching," *Appl. Surf. Sci.*, vol. 263, pp. 430–435, Dec. 2012.

[156] J. Blümmel, N. Perschmann, D. Aydin, J. Drinjakovic, T. Surrey, M. Lopez-Garcia, H. Kessler, and J. P. Spatz, "Protein repellent properties of covalently attached PEG coatings on nanostructured SiO(2)-based interfaces.," *Biomaterials*, vol. 28, no. 32, pp. 4739–47, Nov. 2007.

[157] N. Shirahata and A. Hozumi, "Ultrathin Poly(ethylene glycol) Monolayers Formed by Chemical Vapor Deposition on Silicon Substrates," *J. Nanosci. Nanotechnol.*, vol. 6, no. 6, pp. 1695–1700, Jun. 2006.

[158] H. Bi, S. Meng, Y. Li, K. Guo, Y. Chen, J. Kong, P. Yang, W. Zhong, and B. Liu, "Deposition of PEG onto PMMA microchannel surface to minimize nonspecific adsorption.," *Lab Chip*, vol. 6, no. 6, pp. 769–75, Jun. 2006.

[159] B. W. Muir, A. Tarasova, T. R. Gengenbach, D. J. Menzies, L. Meagher, F. Rovere, A. Fairbrother, K. M. McLean, and P. G. Hartley, "Characterization of low-fouling ethylene glycol containing plasma polymer films.," *Langmuir*, vol. 24, no. 8, pp. 3828–35, Apr. 2008.

[160] Y. Nagasaki, T. Ishii, K. Uchida, H. Otsuka, and K. Kataoka, "PEG-MODIFIED NANOPARTICLES FOR NEW MOLECULAR RECOGNITION," *Eur. Cells Mater.*, vol. 6, no. S1, p. S23, 2003.

[161] R. V Olkhov, J. D. Fowke, and A. M. Shaw, "Whole serum BSA antibody screening using a label-free biophotonic nanoparticle array.," *Anal. Biochem.*, vol. 385, no. 2, pp. 234–41, Feb. 2009.

[162] A. Haes, D. Stuart, S. Nie, and R. Van Duyne, "Using solution-phase nanoparticles, surface-confined nanoparticle arrays and single nanoparticles as biological sensing platforms.," *J. Fluoresc.*, vol. 14, no. 4, pp. 355–67, 2004.

[163] D. A. Armbruster and T. Pry, "Limit of blank, limit of detection and limit of quantitation.," *Clin. Biochem. Rev.*, vol. 29 Suppl 1, no. August, pp. S49–52, Aug. 2008.

[164] A. Shrivastava and V. Gupta, "Methods for the determination of limit of detection and limit of quantitation of the analytical methods," *Chronicles Young Sci.*, vol. 2, no. 1, p. 21, 2011.

[165] N. C. H. Le, V. Gubala, R. P. Gandhiraman, C. Coyle, S. Daniels, and D. E. Williams, "Total internal reflection ellipsometry as a label-free assessment method for optimization of the reactive surface of bioassay devices based on a functionalized cycloolefin polymer.," *Anal. Bioanal. Chem.*, vol. 398, no. 5, pp. 1927–36, Nov. 2010.